https://ntrs.nasa.gov/search.jsp?R=19680028241 2020-03-12T05:39:10+00:00Z

General Disclaimer

One or more of the Following Statements may affect this Document

- This document has been reproduced from the best copy furnished by the organizational source. It is being released in the interest of making available as much information as possible.

- This document may contain data, which exceeds the sheet parameters. It was furnished in this condition by the organizational source and is the best copy available.

- This document may contain tone-on-tone or color graphs, charts and/or pictures, which have been reproduced in black and white.

- This document is paginated as submitted by the original source.

- Portions of this document are not fully legible due to the historical nature of some of the material. However, it is the best reproduction available from the original submission.

Produced by the NASA Center for Aerospace Information (CASI)

[redacted]

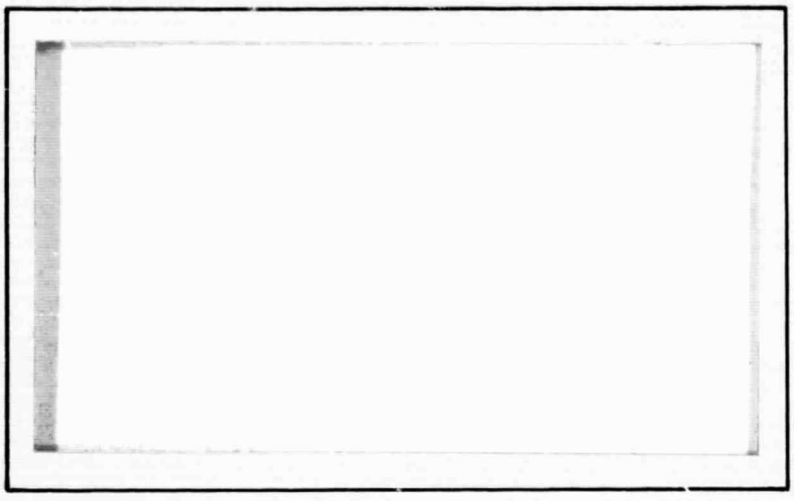

FACILITY FORM 602

N68-37713 (ACCESSION NUMBER)		1 (THRU)
124 (PAGES)		1 (CODE)
CR 98043 (NASA CR OR TMX OR AD NUMBER)		03 (CATEGORY)

FAIRCHILD HILLER

REPUBLIC AVIATION DIVISION

FARMINGDALE, LONG ISLAND, NEW YORK

GPO PRICE $ _____

CFSTI PRICE(S) $ _____

Hard copy (HC) 3.00

Microfiche (MF) _____

ff 653 July 65

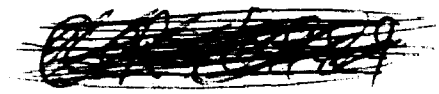

PCD-TR-67-9A
FHR 3287-2
PC090R0002
September, 1967

FINAL REPORT

Volume II - Technical Report

Measurement of Electric Fields In The Ionosphere

For Period: August, 1966 - September, 1967

Contract NAS 8-20663

September, 1967

by

Gerald Levy
Herbert Jacobs
Edgar Bendor

Prepared For:

George C. Marshall Space Flight Center
National Aeronautics and Space Administration
Huntsville, Alabama 35812

FAIRCHILD HILLER CORPORATION
REPUBLIC AVIATION DIVISION
Power Conversion Department
Farmingdale, New York 11735

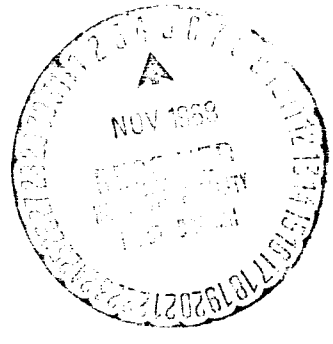

CONTENTS

NOTATIONS

c	Velocity of light
d	Body dimension
e	Electronic charge
$\underline{E}$, E	Electric field
f	Distribution function
$\underline{H}$	Magnetic field
j	Current density
k	Boltzmann's constant
l	Larmor radius
m	Particle mass
$\underline{r}$	Position vector
n	Particle density
R	Reflection factor
S_∞	"Speed ratio" $(m_e V^2/2kT)^{1/2}$
T	Temperature
u	Random velocity
$\underline{V}$, V	Vehicle velocity
δ_∞	Debye length based on n_∞ as $(kT/4\pi e^2 n_\infty)^{1/2}$
ξ, η	Distances, parallel and normal to the beam path
θ, φ	Angles
λ	Mean free path
ν	Collision frequency
Φ	Electric potential
t	Time

O ( ) of the order of

SUFFIXES

s	Surface
∞	At infinity
e	Electrons
i	Ions
r	After reflection
b	Satellite body
f	Field meter components
th	Thermal
coll	Collisions

FOREWORD

This report describes the development of an experimental laboratory model of an electric field meter using the electron beam deflection technique and the system considerations for its use. This meter is designed to operate within the ionosphere in the vicinity of spacecrafts.

The effort was supported by the Space Science Laboratory of George C. Marshall Space Flight Center under the technical management of Mr. E. L. Shriver with the consultation of Dr. A. H. Weber, Chairman of the Physics Department of St. Louis University.

The facilities of Republic Aviation Division of Fairchild Hiller Corporation, Power Conversion Department which is under the direction of Mr. A. E. Kunen, were made available for this work.

The project investigator was Mr. G. Levy. The chief instrument engineer was Mr. H. Jacobs and principal physicist was Dr. E. Bendor. Major contributions to the program were made by Dr. L. Zadoff, Mr. S. Cohen, and Mr. E. Kuhn. The assistance of Mr. P. Forsyth and Mr. E. Vogel in establishing the framework of the problem is gratefully acknowledged. Messrs: G. Steward, C. Hausman, and L. Brown very capably provided the technical support in the laboratory.

This work was performed under contract number NAS 8-20663. The Final Report, Volume II, "Technical Report," is Fairchild Hiller Corporation Report No. PCD-TR-67-9A, FHR 3287-1A, dated September , 1967.

ABSTRACT

The development of an experimental laboratory model of an electric field meter using the electron beam deflection techniques and the systems considerations for its use. This meter is designed to operate in the vicinity of a spacecraft within the ionosphere. The use of a weak electron beam (less than 1 microampere) provides a field sensing element which does not disturb the environment or the field it is measuring, while still permitting the association of the measured fields with the orbiting spacecraft at desired locations on, near, or far from its surface.

The meter has a dynamic range from 10 mv/meter to 1000 v/meter with an accuracy of ± 1 mv/meter at 10 mv/meter and ± 1% above 100 mv/meter.

SECTION I
INTRODUCTION

This volume of the final report will involve the presentation of technical data associated with the development of the electron beam deflection electric field meter and its use in the measurements in the vicinity of the spacecraft.

Based upon the results of the laboratory field meter tests and the analytic studies of the ionospheric environment, an experiment configuration has been developed which will have the following capabilities:

- Dynamic Range: ± 10 mv/m to ± 1000 v/m
- Accuracy: ± 1 mv/m at 10 mv/m and ± 1% above 100 mv/m.
- Operation within the ionosphere in the vicinity of spacecraft.
- Two electric field components simultaneous readouts.

A. GENERAL

The measurement of electric fields in the vicinity of spacecraft operating within the ionosphere has presented many problems. The paucity of knowledge of electric fields within the ionosphere is a reflection of the extreme difficulty in obtaining this information without modifying the fields being measured. (1)

In addition to the scientific requirement of understanding the space environment, there are also engineering requirements which necessitate the development of an electric field meter which is compact, can operate within the ionosphere, has a wide dynamic range and is extremely sensitive to small field changes. These engineering requirements include the measurement of:

(1) Electric fields created by charged particulate clouds near the spacecraft.

(2) Electric fields created by the plasma sheath surrounding the spacecraft.

(3) Electrodynamic forces and moments upon the spacecraft caused by this charged body moving through an ambient ionospheric electric field.

A meter that fulfills these requirements must be relatively compact so that it can be moved from point to point within the spacecraft's external environment without elaborate calibration or mechanical requirements. The range of electric fields that this meter encounters will vary from 1000 volts/meter close to the vehicle surface down to 10 millivolts/meter at a distance of 5 body radii from the spacecraft, thus a meter used for housekeeping of the environment needs a wide dynamic range. The meter should not modify the electric field or other environment parameters, in particular, the field sensing element should be a non-participating observer. The physical design of the meter must be compatible with the plasma properties of the ionosphere-magnetosphere in relation to a body moving through it.

This report describes the development of an electron beam electric field meter which has been designed to perform these engineering tasks as well as the survey of the ambient electric field within the ionosphere.

B. ELECTRIC FIELD MEASUREMENTS WITHIN THE IONOSPHERE

The measurement of the electric field in the vicinity of the spacecraft within the ionosphere presents many unique problems in meter design and interpretation of data.

Electric fields in the atmosphere or vacuums are commonly measured by "field mills." These meters measure the charge collected on a metal surface which is intermittently screened from the field to be measured.[2] Another means is by the potential difference of two or more high impedance probes of known geometry.[3] In addition charged particle interaction with the field to be measured has also been used.[4] Two of the most severe problems associated with the measurement of electric fields within the ionosphere are:

1) The ionosphere consists of a highly ionized plasma. A plasma sheath develops about bodies which produce high electric fields near surfaces. The conductivity of the plasma tends to neutralize charges collected by the meters.

2) Vehicle motion relative to the earth's magnetic field produces an apparent electric field which must be known in order to determine the actual electric field being measured.

The "field mill" class of meters are thus faced with the problems that the plasma sheath covering the meter creates electric fields, as high as 1000 volts/meter, at the surfaces used for charge collection. Also electric currents flow from the plasma to the field mill. Since the concept of this meter is the measurement of current flowing to a surface element that is intermittently screened from the outer field, it is noted that the sensing element in a plasma presents extreme difficulties to the measurement of the electric fields.

The electrostatic potential difference probes are faced with similar difficulties. Each probe of the measuring system is surrounded by a plasma sheath and acquires a potential different from the plasma. The voltage drop in a sheath depends upon the geometry and orientation of the probes; thus the potential difference may not be the same for each probe. The orientation of the probes is extremely important since, due to the earth's magnetic field, the plasma is anisotropic. Further, the probes must be far away from each other and all other obstacles that could disturb the symmetry by screening different parts of the incoming charged particle flux. In addition, the probe material and electrical connections must be identical physically and electrically to assure the same photoemission and electrical impedance characteristics. The distance between the probes becomes extremely great when small fields are being measured. For example, Fahleson[5] has performed an excellent design evaluation for the measurement of electric fields in the ionosphere using a probe system; he finds that a 300 km altitude minimum probe distance of 6 meters must be used to assure all the design restraints are met. For higher altitude, the distance becomes significantly greater. This analysis assumed that the meter constituted the spacecraft; if the meter was carried aboard a multipurpose spacecraft, it would have to be placed at an extremely large distance from the craft to assure no screening that would destroy the symmetry.

Another technique that is being used to measure the electric fields in the ionosphere is the motion of an ionized barium cloud. In these experiments barium

vapor is released at altitude in sunlight. The cloud is rapidly photoionized (within 100 seconds) and is diffused in a long straight beam in the earth's magnetic field. The relative motion of this barium cloud and a neutral gas cloud simultaneously released is used to determine the electric field in the ionosphere. The increased ionization caused by the presence of the ionized cloud within the ionosphere modified the ambient electric field, and the diffusion of the magnetic field into the ionized gas cloud creates a time as well as a spatially dependent problem which is still being analyzed.

In summary, the only compact (quasi-point) field measuring device presently being used is the field mill, however, significant problems are associated with its use in the highly ionized ionosphere. The potential probe systems and barium cloud techniques are applicable over large spatially separated points or volumes remote from the spacecraft. None of these concepts meet the requirement for an electric field meter that can measure electric fields in the vicinity of a spacecraft within the ionosphere.

The electron beam electric field meter has been designed to meet this requirement. This meter utilizes the deflection of an electron beam under the influence of an electric field. The sensitivity of the device is enhanced by utilizing a feed-back loop which continually nulls the virtual center of the electron beam and by synchronously detecting chopped electric field deflections. The meter is designed to operate within the ionosphere and has a range from 10 millivolts/meter to 1000 volts/meter. It has a sensitivity of ± 1 millivolt/meter at the 10 mV/meter level. The meter that will be designed for space use will have a physical size of 1 foot long by 9 inches on the sides and weigh under 1 pound, and the auxiliary housekeeping package will be remote from the meter, weighing 2 pounds and occupying a volume of 0.1 cubic feet. These units are shown in Figure 1.

C. HISTORY OF DEVELOPMENT

In 1964, the Marshall Space Flight Center's Space Sciences Laboratory began an in-the-house investigation of the use of electron beam deflection to measure electric field strength. The results of this feasibility study and associated laboratory effort demonstrated that fields of less than 1 volt/meter could easily be measured in the laboratory.[6]

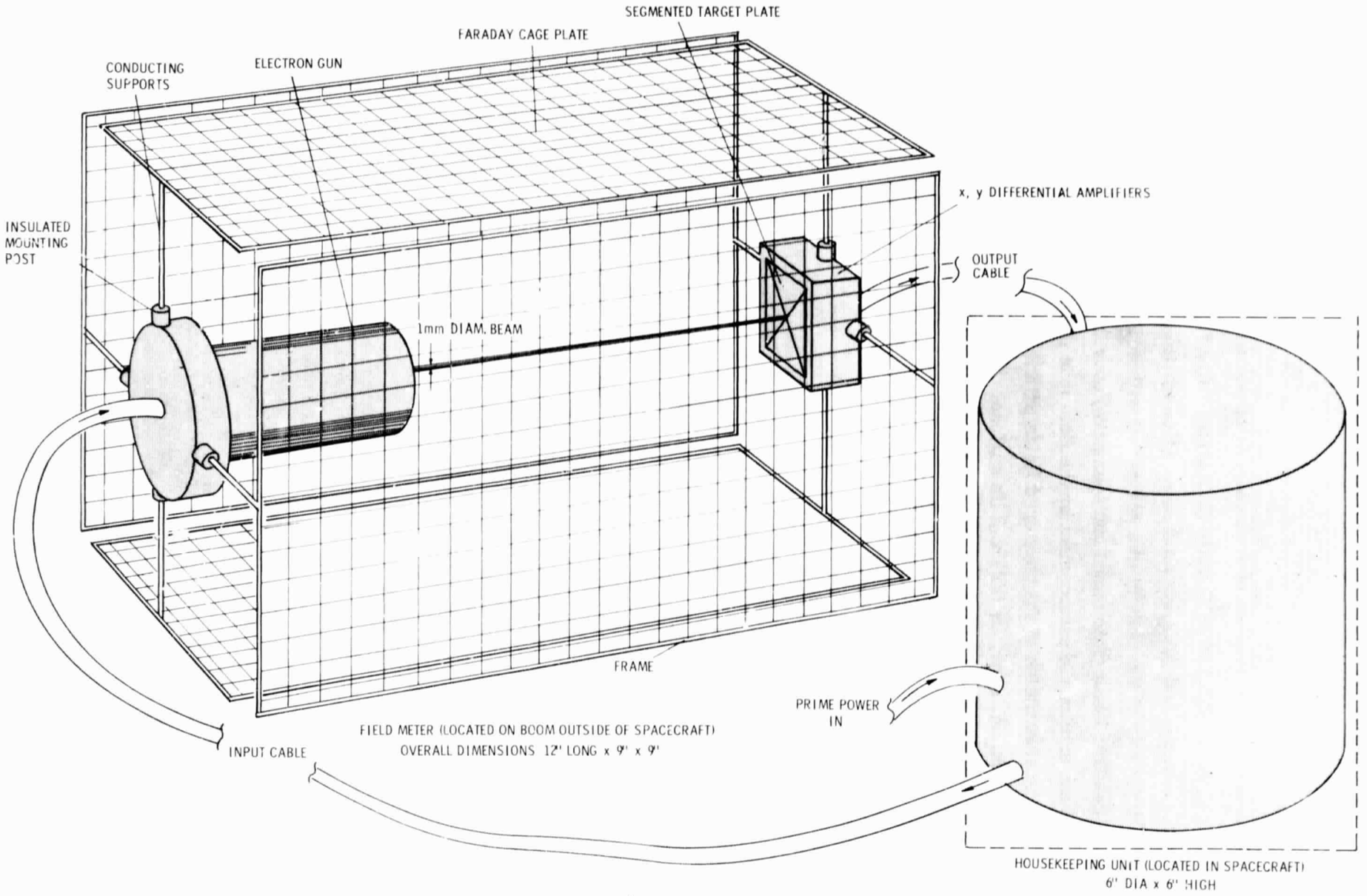

Figure 1: Electron Beam Deflection Electric Field Meter

The present work described in this report is the development of an experimental laboratory model of an electric field meter using the electron beam deflection technique and the system considerations for its use. This meter is designed to operate in the vicinity of a spacecraft within the ionosphere. The use of a weak electron beam (less than 1 microampere) provides a field sensing element which does not disturb the environment or the field it is measuring, while still permitting the association of the measured fields with the orbiting spacecraft at desired locations on, near, or far from its surface.

SECTION II

INTERACTION OF BODIES WITH THE IONOSPHERE

A. INTRODUCTION

When a body moves at high speed through a low density, partially ionized gas, electrically neutral particles are disturbed and exchange momentum and energy with the surface. This gives rise to aerodynamic drag (perhaps lift) and heat transfer. These purely aerodynamic phenomena may be regarded as extensions to low density of the familiar results of aerodynamics, and will receive little attention below. Ionized particles interact not only with the surface of the body, but also with electric and magnetic fields in the vicinity of the body. These fields are present in the ionosphere, and are themselves locally modified by the body and the distributions of charged particles.

We shall be primarily interested in the electric fields induced by the body. As we shall see, these may be of higher order than the fields which it is intended to investigate by means of the electron beam field meter. This last remark has more than one significance in the present context. Thus, if it is intended to use the field meter to measure "ambient" fields in the ionosphere, then care must be taken that fields induced by the vehicle carrying the field meter are either calculated or else reduced to a small "noise" level. On the other hand, if the fields induced by the vehicle are to be investigated, then the incremental field induced by the components of the field meter itself must be taken into account. In either case, it is important to note that since the conditions in which the field meter is to be used are difficult to duplicate in the laboratory, no calibration of the instrument can be carried out which would vitiate the importance of our estimates of these induced fields. We must necessarily carry out a theoretical study which will enable us to correct measured field values, or at least to indicate under what conditions of use the induced electric fields will be small enough to be regarded as negligible. That is the principal purpose of the following sections of this report.

The nature of interaction between free electrons and ions in the ionosphere is described by the usual electromagnetic equations and requires no further comment at this stage. Some remarks must be made, however, on the interaction between particles and the body. Particles striking the surface may be reflected or absorbed. As

regards reflection, particles may be assumed to be reflected specularly, in which case they retain the temperature characteristic of the plasma, or they may be diffusely reflected with the temperature of the surface. Charged particles may be taken to be absorbed or neutralized by the surface. Finally, under certain circumstances (particularly in conditions of very high vacuum), emission of electrons becomes significant. Such emission may be due to photoelectric effects or due to thermionic action. The relative importance of these different types of interactions between the charged species and the surface depends on the properties of the surface, the condition of the plasma, the intensity of incident radiation and so on. The calculation of the potential acquired by the body and the surrounding induced electric field therefore involves the condition of the ambient plasma, the interaction of electrons and ions with the surface and the induced field, and the local geomagnetic field. To obtain useful answers to the problem, it will be necessary to deal with different regimes of interaction, in each of which sufficient assumptions are possible to make the theory tractible.

B. IONOSPHERIC PARAMETERS

Ambient electric fields in the ionosphere arise when neutral plasma flows across the geomagnetic field lines. It is not our purpose here to enter into the details of these ionospheric phenomena. We merely note that the $\underline{E}$ field appears to vary in the range 10^{-2} volts/meter to 10^{-1} volts/meter in a direction perpendicular to the local magnetic field lines. (The field parallel to the geomagnetic force lines is at least two orders of magnitude less).[3, 5] This $\underline{E}$ field has been observed in the F_1 and F_2 regions. Gdalveich and Imyanitov[18] quote results obtained with sounding rockets which show $\underline{E}$ to be about 5×10^{-2} volts/meter through the F region, with a maximum of about 8×10^{-2} volts/meter at 200 km. The field parallel to H was found to be measurable only in the F_2 region. These results, however, are highly variable and should be regarded as qualitative only. We may conclude only that our instruments should function down to 10^{-2} volts/meter, and that the simultaneous use of a vector magnetometer would be helpful in interpreting the results. Induced fields (where these are to be measured) might present a more difficult problem, since they vary from zero far from the body to hundreds of volts per meter at the body surface, and their direction is not in general known (except near the surface) even qualitatively.

C. DIMENSIONLESS PARAMETERS

The altitude range with which we shall deal is from 100 km to about 700 km. Some of the relevant properties of the ionosphere are presented in Figure 2. From these we can see the order of magnitude of the dimensionless groups of the various problems we shall investigate.

The satellite velocity is approximately 10^6 cm/sec. Where we are dealing with the vehicle induced fields, we shall take its typical dimension to be 10^2 cm, denoted by d_b. The typical dimension of the components of the field meter d_f, is taken to be 1 cm. We then have the following approximate values of the dimensionless groups:

$$v_e/V_o \sim 0(10) \qquad l_i/d_f \sim 0(10^2)$$

$$v_i/V_o \approx v_n/V_o \sim 0(10^{-1}) \qquad d_b/\delta_\infty \sim 0(10^2) \text{ to } 0(10^3)$$

$$l_e/d_b \sim 0(10^{-2}) \qquad d_f/\delta_\infty \sim 0(1) \text{ to } 0(10)$$

$$l_e/d_f = l_i/d_b \sim 0(1) \qquad \lambda_e/d_b \sim 0(10^2) = \lambda_i/d_b$$

We note that on the scale of the body, the plasma is essentially collisionless, and that the thermal velocity of electrons is much greater than, and the thermal velocity of ions much less than, the satellite velocity. The quantity $\delta_\infty = (kT/4\pi e^2 n_\infty)^{1/2}$ is the Debye length based on the undisturbed electron density, and is typically small compared with the body, i.e., there exists a thin, well defined, "plasma sheath". This is true however, only when the local electron density n_e is of the same order as the undisturbed value. As we shall see this is not the case in regions downstream of a body, from which electrons are repelled by high negative potentials.

D. REGIONS OF INTERACTION

The various regions in which certain sets of assumptions will be approximately valid are illustrated in Figure 3. In region A far from the body, the plasma is undisturbed by the body, but the effect of ambient electric fields on the particle distribution functions should be taken into account. We shall not consider the presence (or scattering by the body) of magnetohydrodynamic waves. Electrical neutrality is completely preserved far from the body. Regions B and B' are near the body, but outside the Debye region. The local potential and the electron distributions are

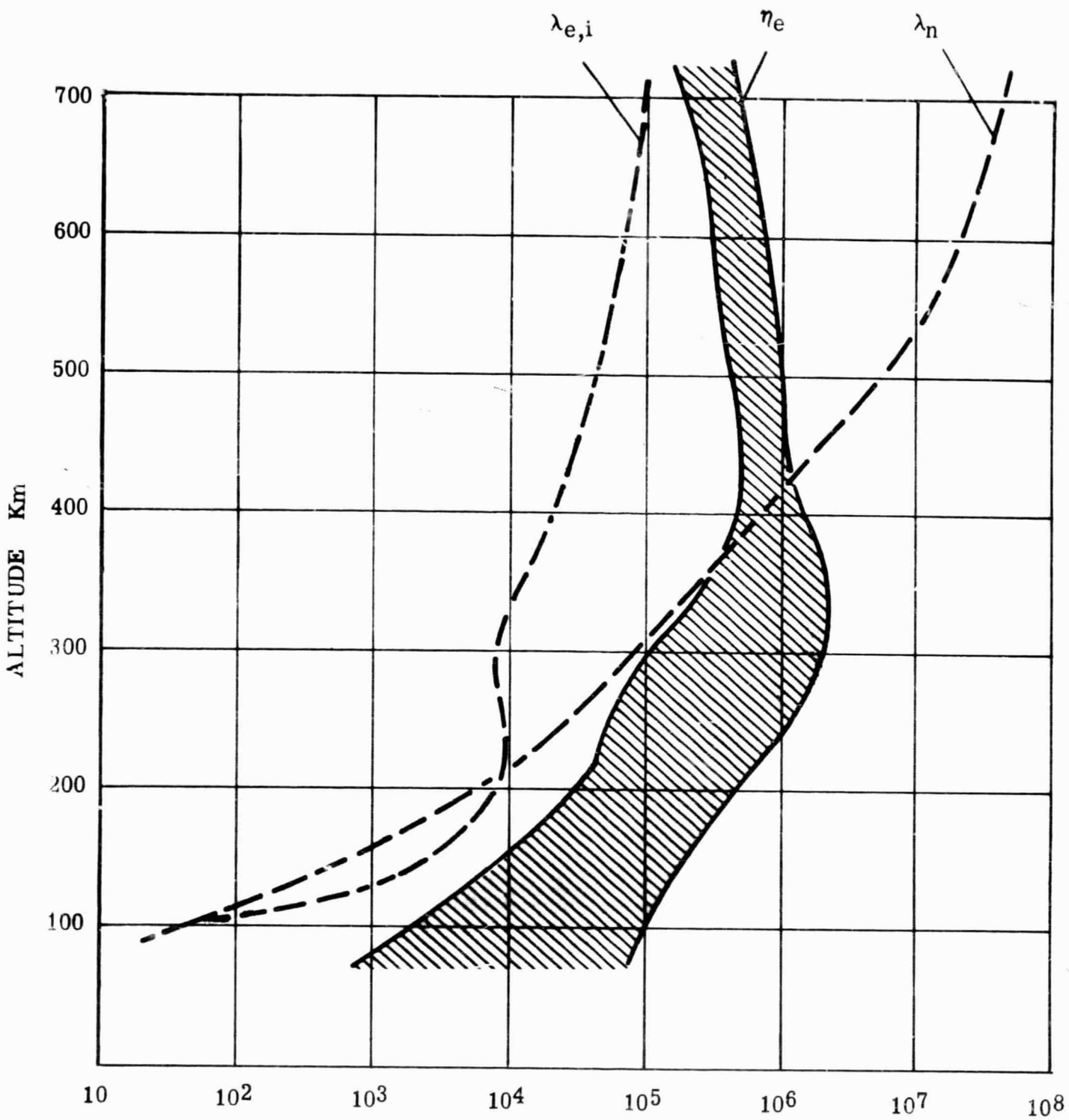

Figure 2 : Electron Density (n_e - cm^{-3}) Neutral Particle Mean Free Path (λ_n - cm.) and Electron and Ion Mean Free Path (λ_e, λ_i - cm.) vs. Altitude

Figure 3: Regions of Interaction

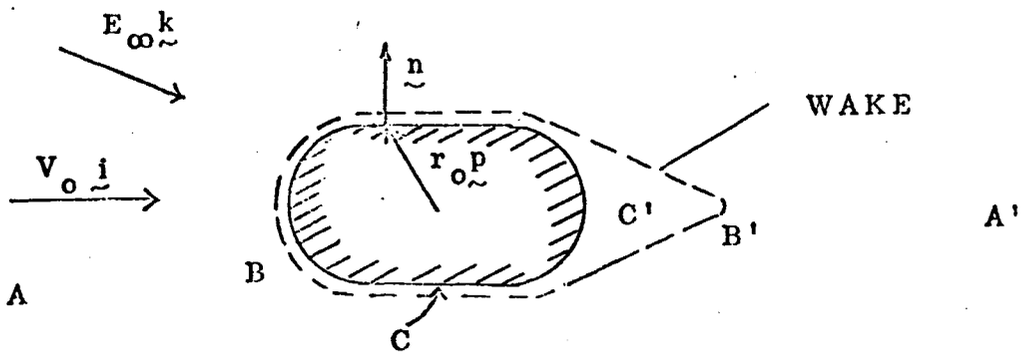

A Undisturbed Ionospheric Plasma, with $\underset{\sim}{E}_\infty$

B Disturbed Region $|r| \gg \delta_\infty$ Upstream

B' Disturbed Region $|r| > d_b$ Downstream

C Debye Region Upstream

C' Debye Region Downstream $\delta_\infty \sim (d_b)$

strongly coupled here. Electrical neutrality is only approximately preserved, but surface interactions have only a weak effect on the state of the plasma. We shall show below that in this region the kinetic energy of ions (in the frame of the body) is much greater than their thermal energy or potential energy. Since, as noted above, $l_i/d_b \sim 0(1)$ or greater, ion trajectories in the neighborhood of the body are nearly straight lines and the ion concentration can therefore be estimated, to a first order, without consideration of the influence of the electric or magnetic fields. (These remarks must be modified somewhat where applied to the wake region B'. Ions are shaded by the body in C' and, to a lesser extent, in B'. Thus the ability of ions to penetrate B' depends on the magnitude and orientation of the magnetic field if $l_i/d_b \sim 0(1)$; for components of the field meter, since $l_i/d_f \sim 0(10^2)$, the curvature of ion paths may be neglected. The effect of electric fields on the ion concentration is more important here than at the front or sides of the body, since the interaction distance is much longer; but it is still of smaller order).

To sum up, we may say that in B and B' electrons behave as in the neighborhood of a body at rest, whereas ions are scattered principally only by the body itself and behave as a high Mach number collisionless stream of neutral particles.

The sheath region C upstream and at the sides of the body extends for a distance of the order of δ_∞. In the wake region C' the "Debye length" can be shown to extend to distances of the order of the body dimension. In both these regimes there is substantial charge density and a high electric field. The absorption, neutralization, reflection (both specular and diffuse) and emission of particles at the surface must be accounted for; the particle distribution functions are therefore highly anisotropic and discontinuous. It is this last fact which is responsible for the difficulty of the theoretical problem presented by these Debye regions. In fact, the cases we shall consider are somewhat similar to the problem of the plasma sheath at an electrode or the analysis of the characteristics of the electrostatic probe in collisionless plasma. Both these problems have been the subject of numerous papers in the last few years.

Our task here is to estimate the potential distribution in the neighborhood of the satellite vehicle and the components of the electric field meter. Since there can obviously be no general solution, even for bodies of simple shape, the analysis must be reduced to a number of separate problems, each for a particular regime, orientation of vehicle velocity, magnetic field, surface condition and so on. In each of these problems, hopefully, sufficient assumptions will be justifiable to reduce the formulation to a tractable form, and to arrive at results from which a picture of the induced field can be built up and its influence on the electric field meter inferred. Many of these cases have been solved before; we shall apply them to our problem and modify them as necessary.

E. BRIEF LITERATURE SURVEY

The most important reference which has been used here is a book by Alpert, Gurevich and Pitoevski[7] which deals with almost all aspects of the satellite ionosphere interaction problem. This volume is in fact a compendium of some 20 or 30 papers published by these authors in the period from 1959 to 1965. They deal with the distributions of neutral and charged particles, the induced electric and magnetic fields, the effect of collisions and the Debye problem in central force fields. No

consideration is given, however, to the effect of ambient fields, and we shall have occasion below to modify their work to take account of such fields. The problem of the Debye region, as dealt with by Alpert, et al, is of little relevance to us and is useful chiefly for the case of a spherical probe in a collisionless plasma. The assumption of spherically symmetric fields is also useful when the Debye region is much larger than the body dimensions; this, however, is nowhere the case in the ionosphere. It is noteworthy that some early work on this problem was based on such assumptions, Kraus and Watson,[14] for example considered a small charge in a plasma both by the magnetohydrodynamic and the Boltzmann equation formulation.

The work of Alpert, Gurevich and Pitaevski appears to contain the only attempt to derive a comprehensive picture of the electric potential distribution around satellites, although for obvious reasons, the examples they give are mostly confined to spherical bodies. Other authors have dealt with portions of the problem only. Thus, Chen[8] considers the particle densities in what we have called region B and derives, on the basis of the assumptions we have stated here for this region, the particle fluxes and hence the potential on the satellite surface. His result is valid only for a conducting sphere in the absence of anisotropies due to external fields. Davis and Harris[10] have carried out numerical calculations of the potential field. Their method was to solve Poisson's equation for an equilibrium distribution of electrons and a constant ion density. This yields a first approximation to the potential distribution; the latter is then inserted into the equation of motion for ions and a second approximation to the ion density obtained. Their method consists of an iterative procedure for potential and ion density, in which the equilibrium electron density is retained at each step, and a conducting spherical body which completely absorbs incident ions is assumed. In this solution, therefore, no attempt is made to separate the treatment of the Debye region from the remaining neighborhood of the body, although a sheath appears in the solution. The results of Davis and Harris are somewhat similar to those of Jastrow and Pearse[12] who carried out one of the earliest investigations of this problem. Their treatment was based on the same assumptions as that of Davis and Harris, but was analytical rather than numerical. In both cases the solution is limited (apart from the lack of generality in the type of surface interaction chosen) by the assumption of an equilibrium (Maxwellian) electron distribution, even in the sheath. In fact, the electron distribution is highly subject

to surface interactions, is anisotropic and discontinuous, and approaches equilibrium only at distances from the surface much greater than the Debye length.

As regards the Debye region itself, or the "double layer" as Alpert, et al refer to it, the problem here is to solve simultaneously the Vlasov and Poisson equations subject to the specified interactions on the surface. The solution must conform to the conditions pertaining in region B at large distances from the surface, which in our case involve an anisotropy in the electron distribution function. This problem, as we have noted earlier, has received a great deal of attention, although not in the present context; it has been studied, rather, in its application to electrodes and electrostatic probes. It should be noted that the electrostatic probe problem has been studied not only in the collisionless case but also in the "continuum" regime for dense plasmas and in the Boltzmann equation formulation with account taken of collisions. Examples of the latter problem are to be found in papers by Chou, Talbot and Willis[9] and by Wasserstrom, Su and Probstein.[17] The former deal with the case of low collision frequency by means of the "Krook model" for the collision term, and find that the effect of collisions is to reduce the charge density in the sheath, and consequently to increase the extent of the Debye region. Since their solution is for a weakly ionized gas, (like the ionosphere in the E and F regions) the collisions are those between charged and neutral particles principally. We may expect that the effect of collisions, which we have neglected, would be similar in our case, at least, upstream of the body. Like all other authors dealing with electronic probes, Chou, et al consider a stationary body and make no distinction between the sheath and the "near field" regions. In our case, however, this distinction is essential if progress is to be made, since the problem is otherwise too difficult.

Previous work most interesting in connection with paragraph I of this report is due to Kiel and Gustafson,[13] Pung and Ziering[11] and Parker.[16] They deal with the collisionless case, respectively, for a spherical probe, a flat electrode and a satellite vehicle presumably of arbitrary shape. The work of Parker is intended to lead to computer solutions of the Vlasov and Poisson equations, and he considers the electron motions in the presence of the local magnetic field. We shall discuss the details of the Debye region problem in paragraph I but for the present it

may be noted that the solution to the Vlasov equation for a given potential depends on the analysis of the motion of a charge in that potential. It is for this reason that previous research on this problem has been confined to spherically or cylindrically symmetric potentials or to the one dimensional case; these are the cases for which integrals of the motion are easily derived. In our case the potential is certainly not spherically symmetric, and the work of Kiel and Gustafson, as well as that of previous authors on the same problem is therefore not directly applicable, although it is certainly of interest in revealing some of the difficulties.

The most useful reference is Pung and Ziering. They deal with a one dimensional problem of an infinite flat electrode, the potential being a function only of the coordinate normal to the surface. They take account of the various possible surface interactions by writing separate electron and ion distribution functions for each type of interaction and by treating separately the "trapped" and "free" particles moving in the potential field. Their solution to the one dimensional Poisson equation yields the potential distribution in terms of the various parameters of the surface interaction. With certain modifications their method is applicable to our problem at the upstream side of the body. We have here, for a conducting body, a Debye region very thin compared with the radius of curvature of the surface, and consequently an electric field in the region which must be nearly normal to the surface. Difficulties arise in attempting to match conditions at the edge of this thin layer with our approximate solution for region B. In the latter there is a small tangential component of field. We have attempted to generalize the method of Pung and Ziering to account for such a component; but the slightest departure from the strictly one dimensional case immediately leads to great difficulties in dealing with the equations of motion of an electron in the field, and we have not succeeded in making progress along these lines. We have confined ourselves, therefore, to suggesting an extension of the work of Pung and Ziering to take account of anisotropic electron distributions at the edge of the sheath upstream of the body.

There appears to have been no previous work on an extensive, highly rarefied Debye region such as arises downstream of a satellite surface. Alpert, Gurevich and Pitaevski have suggested that the plasma charge density here be neglected altogether, so that the field would be due to the electrostatic potential of the surface

only. We have modified this field so as to pass smoothly to the field of region B' and also put forward a scheme whereby the effect of space charge density can be accounted for to a first order.

F. THEORETICAL FOUNDATIONS

We shall write the Boltzmann or Vlasov equations in a coordinate frame fixed in the body. Since we are interested only in stationary phenomena, the distribution function of species j, say, is independent of time. Then

$$\underline{v}\,\frac{\partial f_j}{\partial \underline{r}} + \frac{e}{m_j}\left\{-\frac{\partial \phi}{\partial \underline{r}} + \frac{1}{c}\,(\underline{v} + \underline{V}) \times \underline{H}\right\}\frac{\partial f_j}{\partial \underline{v}} = \left(\frac{\partial f_j}{\partial t}\right)_{coll.} + A_j(\underline{r}, \underline{v})\,\delta(\underline{r} - \underline{r}_s) \qquad (1)$$

The second term on the right hand side is given in this form by Alpert, Gurevich and Pitaevski. It signifies the rate of change of number density of particles at $\underline{r}$ with velocity $\underline{v}$, $\underline{v} + \underline{dv}$ due to interactions at the surface $\underline{r} = \underline{r}_s$. $\delta\ (\underline{r} - \underline{r}_s)$ is the delta function. The boundary conditions at the surface may be given in terms of the probability $w_j\ (\underline{v}, \underline{v}', \underline{r}_s)$ that a particle of species j, impinging with velocity $\underline{v}$ on point $\underline{r}_s$ of the surface will be reflected with velocity $\underline{v}'$. Thus, for specular reflection, for example:

$$w\ (\underline{v}, \underline{v}', \underline{r}_s) = \delta\ (\underline{v}' - \underline{v} + 2\,(\underline{v} \cdot \underline{n})\ \underline{n}\ )$$

which expresses the condition that the probability is unity if the normal component of $\underline{v}'$ is minus the normal component of $\underline{v}$, and zero otherwise. Other cases of this type are tabulated by Alpert, et al, who also derive the corresponding functions A $(\underline{r}, \underline{v})$ from these surface interaction probabilities. We shall, however, not pursue this formulation of the boundary conditions further, since they play little part in our analysis. A further condition which has to be satisfied, for steady conditions is that the net current flowing into the surface shall be zero. Then,

$$\sum_j e_j \int_{\underline{v}\cdot\underline{n} < 0} f_j(\underline{r}_s, \underline{v})\,(\underline{v} \cdot \underline{n})\,d\underline{v} = \sum_j e_j \int_{\underline{v}\cdot\underline{n} > 0} f_j(\underline{v}, \underline{r}_s)(\underline{v} \cdot \underline{n})\,d\underline{v} \qquad (2)$$

When there is thermionic or photoelectric emission from the surface suitable terms must be added. But we shall not take these into account, since they are not very significant at the altitudes we shall consider.

The potential distribution is given by the Poisson equation:

$$\nabla^2 \Phi = -4\pi e (n_i - n_e) \tag{3}$$

where

$$n_j (\underline{r}) = \int_{-\infty}^{\infty} f_j (\underline{r}, \underline{v}) \, d\underline{v}$$

Equations (1) and (3), with the surface conditions at the body and the (given) functions f_i, f_e and Φ far from the body are theoretically sufficient for the solution of the problem. Equation (2) is the condition which yields the value of the surface potentials. Physically, what this means is that a neutral surface has different affinities for electrons and ions, so that a surface potential (usually negative) is built up until the net current falls to zero. This latter equation is written here for a dielectric surface. When the surface is a conductor it is not necessary that the current density at the surface be zero; the proper condition then is that the total current flowing into the vehicle be zero, i.e., the above relation has to be integrated over the surface.

Finally, we note that in the absence of an ambient electric field the undisturbed distribution functions are Maxwellian:

$$f_j = n_j \left(\frac{m_j}{2\pi k T_j} \right)^{3/2} \exp \left\{ - \frac{m_j}{2kT_j} (\underline{v} + \underline{V})^2 \right\}$$

This condition has to be modified somewhat when an ambient field is present, as we shall see.

G. THE UNDISTURBED IONOSPHERE AND THE SURFACE POTENTIAL

1. The Far Field - Region A

If the undisturbed plasma far from the body supports an electric as well as a magnetic field, it is clear that collisions cannot be altogether neglected.*

---

* The energy imparted to electrons must be dissipated in collisions and the momentum randomized.

Otherwise electrons would be accelerated indefinitely and the only steady state would be that where sufficient electrons have been attracted to the high potential region to cancel out the field. This is clear when we write down the (exact) solution to the Vlasov equation for a uniform field, viz:

$$f = \exp\left(\frac{e\Phi}{kT_e}\right) f_m(\underline{v}) \quad ; \text{where} \quad f_m = n_\infty \left(\frac{m_e}{2\pi kT_e}\right)^{3/2} \exp\left\{-\frac{m_e \underline{v}^2}{2kT_e}\right\}$$

is the Maxwellian and $n_e = n_\infty \exp(e\Phi/kT_e)$ is the local electron density. Since $\Phi = -E_\infty \underset{\sim}{k} \cdot \underline{r}$ for a uniform field, we get infinite electron densities as $\underline{r} \rightarrow \infty$.

To take collisions into account, we write the Boltzmann equation (in the frame in which the satellite is at rest):

$$L(f) = \underline{v} \frac{\partial f}{\partial \underline{r}} + \frac{e}{m_e}\left\{\frac{\partial \Phi}{\partial \underline{r}} - \frac{1}{c}(\underline{v} + \underline{V}) \times \underline{H}\right\} \frac{\partial f}{\partial \underline{v}} = -\nu\left\{f - \frac{f_o'}{n_e'} \int f \, d\underline{v}\right\} \tag{4}$$

(see Bhatnager, Gross and Krook,[19] where ν is the mean electron collision frequency, and

$$f_o' = n_e' f_m = \exp\left\{\frac{e}{kT_e}(\Phi + E_\infty \underline{k} \cdot \underline{r})\right\} f_m \tag{5}$$

Here

$$f_m = n_\infty \left(\frac{m_e}{2\pi kT_e}\right)^{3/2} \exp\left\{-\frac{m_e}{2kT_e}(\underline{v} + \underline{V})^2\right\}$$

is the Maxwellian with respect to our moving frame. Note that when $f = f_o'$ then $\int f \, d\underline{v} = \int f_o' \, d\underline{v} = n_o'$ and the collision term in Equation (4) is zero. We now write:

$$f = f_o' + f_1 \tag{6}$$

whereupon Equation (4) becomes:

$$\left[\underline{v}\cdot\frac{\partial f_1}{\partial \underline{r}} + \frac{e}{m_e}\left\{\frac{\partial \bar{\Phi}}{\partial \underline{r}} - \frac{1}{c}(\underline{v}+\underline{V})\times \underline{H}\right\}\frac{\partial f_1}{\partial \underline{v}}\right] + \frac{e}{kT_e} f_m' \left[E_\infty \underline{k}\cdot\underline{v} - \frac{\partial \bar{\Phi}}{\partial \underline{r}}\cdot\underline{V}\right]$$
$$= -\nu\left[f_1 - \frac{f_m'}{n_e}\int f_1 \, d\underline{v}\right] \qquad (7)$$

The first term contains terms in f_1 which are of smaller order; and since we anticipate that f_1 is not only small but also anisotropic in $\underline{v}$, we have that $\int f_1 \, d\underline{v} = 0$. Since the mean electron velocity is much greater than $\underline{V}$, the term $\underline{V}\cdot\partial\bar{\Phi}/\partial\underline{r} \ll E_\infty \underline{k}\cdot\underline{v}$ in the mean, except near the body where the induced electric fields are large. We are not concerned here with this region so that the term in $\underline{V}$ may be neglected. We then have:

$$f = \exp\left\{\frac{e}{kT_e}(\bar{\Phi} + E_\infty \underline{r}\cdot\underline{k})\right\} f_m\left[1 - \frac{eE_\infty}{kT_e\nu}\underline{k}\cdot\underline{v}\right] \qquad (8)$$

This distribution function requires some explanation. We note that:

$$f \to \exp(e\bar{\Phi}/kT_e)\, f_m \quad \text{as} \quad E_\infty \to 0$$

$$\text{and} \quad f \to f_m\left[1 - \frac{eE_\infty}{kT_e\nu}\underline{k}\cdot\underline{v}\right] \quad \text{as} \quad \underline{r} \to \infty$$

The latter limit arises since the undisturbed potential is that of a uniform ambient field $\bar{\Phi} = -E_\infty \underline{k}\cdot\underline{r}$. It is clear now why we have chose the particular form of the distribution function given by Equations (5) and (6). When E_∞ disappears we recover the equilibirum distribution function corresponding to the "barometric density" formula $n_e \sim \exp(e\bar{\Phi}/kT_e)$. Thus f is simply a function of the total energy (Hamiltonian) of the electron, viz. $\left\{e\bar{\Phi} - 1/2\, m_e(\underline{v}+\underline{V})^2\right\}$. On the other hand, when the influence of the body is removed as we pass to $\underline{r} \to \infty$, we have a Maxwellian with an anisotropy in the direction of the ambient field. This is the usual solution for a spatially homogeneous plasma supporting a weak field.

In the absence of the influence of a surface, the electron density would be simply:

$$n_e = \exp\left\{\frac{e}{kT_e}\left(\Phi + E_\infty \underline{k}\cdot\underline{r}\right)\right\}$$

i.e., it is a function only of the "induced potential".

2. Potential of the Surface

Using the distribution function (Equation 7), we can arrive at an approximate value for the potential. Consider an element of surface, with normal $\underline{n}$ in our coordinate system, and of properties such that the mean reflection factors (averaged over all velocities and directions of impact) are R_i and R_e for ions and electrons respectively. Let:

$$\bar{R} = (1 - R_i) / (1 - R_e) \tag{9}$$

be the ratio of absorptivity of ions and electrons by the surface. We have to satisfy the condition:

$$\underline{j}_e \cdot \underline{n} = \bar{R}\,(\underline{j}_i \cdot \underline{n}) \tag{10}$$

The ion current may be computed without reference to the electric field, and retains a Maxwellian distribution function. In such circumstances the ion current is given by the same expression as that for neutral particles with the same reflection factor. This can be shown to be:

$$\underline{j}_i \cdot \underline{n} = \frac{1}{2} n_\infty (\underline{V}\cdot\underline{n})\left[1 + \mathrm{erf}\,\gamma_n + \frac{1}{\sqrt{\pi}\gamma_n} e^{-\gamma_n^2}\right] \tag{11}$$

where

$$\gamma_n = \left(\frac{m_i}{2kT_i}\right)^{1/2} \underline{V}\cdot\underline{n} = \left(\frac{m_i}{m_e}\right)^{1/2} \beta_n \quad (\text{when } T_i = T_e) \tag{12}$$

The electron current to the surface is given by

$$\underline{n} \cdot \underline{j}_e = \int_{\underline{v} \cdot \underline{n}} f (\underline{v} \cdot \underline{n}) \, d\underline{v}$$

where f is given by Equation (8) but with $E_\infty(\underline{k} \cdot \underline{v})$ replaced by:

$$E_\infty \, \underline{k} \cdot \underline{v} - \frac{\partial \Phi}{\partial \underline{r}} \cdot \underline{V}$$

i.e., we revert to the step before the assumption $(\underline{V} \cdot \partial\Phi / \partial \underline{r}) \ll E_\infty(\underline{k} \cdot \underline{v})$ was made. We shall later reintroduce this assumption, at a point where its consequences become clearer. In using Equation (8) we have neglected any influence of the surface on f; the distribution function for $\underline{n} \cdot \underline{v} < 0$ is taken to persist right up to the surface. On the other hand, for receding particles ($\underline{n} \cdot \underline{v} > 0$) the distribution function must obviously be truncated, and may even be zero at the surface if total absorption takes place. However, we are not dealing with this part of the distribution function. Our assumption is equivalent to neglecting the term $A_e(\underline{r}, \underline{v}) \, \delta(\underline{r} - \underline{r}_s)$ in Equation (1) for the half phase-space $\underline{v} \cdot \underline{n} < 0$.

The electron current is then:

$$\underline{j}_e \cdot \underline{n} = \exp\left\{\frac{e(\Phi + E_\infty \, \underline{r} \cdot \underline{k})}{kT_e}\right\}\left[\left(1 + \frac{e}{kT_e \nu} \frac{\partial \Phi}{\partial \underline{r}} \cdot \underline{V}\right) \int_{\underline{v} \cdot \underline{n} < c} f_m (\underline{v} \cdot \underline{n}) \, d\underline{v} - \frac{e E_\infty}{kT_e \nu} \int_{\underline{v} \cdot \underline{n} < c} f_m (\underline{v} \cdot \underline{n})(\underline{v} \cdot \underline{k}) \, d\underline{v}\right] \quad (13)$$

After performing the required integrations, we find the condition giving the surface potential Φ_s,

$$\exp\left\{\frac{e(\Phi_s + E_\infty \, \underline{r} \cdot \underline{k})}{kT_e}\right\}\left[\left(1 + \frac{e}{kT_e \nu}\left(\frac{\partial \Phi}{\partial \underline{r}}\right)_s \underline{V} + \frac{e E_\infty}{kT_e \nu} \underline{V} \cdot \underline{k}\right)\left(\frac{1}{\sqrt{\pi}\,\beta_n} e^{-\beta_n^2} + \operatorname{erf} \beta_n + 1\right)\right.$$

$$\left. + \frac{e E_\infty}{kT_e \nu} \frac{1}{2\beta_n^2} (\operatorname{erf} \beta_n + 1)(\underline{V} \cdot \underline{n})(\underline{n} \cdot \underline{k})\right] = \bar{R}\left[\frac{1}{\sqrt{\pi}\,\gamma_n} e^{-\gamma_n^2} + \operatorname{erf} \gamma_n + 1\right]$$

Note that we have assumed that the electron and ion temperatures are equal ($T_i = T_e = T$). This expression is valid locally for a satellite body which is dielectric. For conductors the electron and ion currents must be integrated over the surface.

Our method here has been based on the assumptions that in the region of the ionosphere in which we are interested the mean thermal velocity of electrons is much greater than, and the mean thermal velocity of ions much less than, the satellite velocity. Thus $\gamma_n \gg 1 \gg \beta_n$, unless the vector $\underline{V}$ lies nearly in the body surface tangent plane ($\underline{V} \cdot \underline{n} = V \cos\theta$ say). The above expression now becomes:

$$\exp\left\{\frac{e(\bar{\Phi}_s + E_\infty \underline{r}_s \cdot \underline{k})}{kT}\right\}\left(1 + \frac{e}{kTV}\left(\frac{\partial \bar{\Phi}}{\partial \underline{r}_s}\right)\cdot \underline{V}\right)\left[1 + \frac{eE_\infty}{kTV}\left(\underline{V}\cdot\underline{k} + \frac{\sqrt{\pi}}{2\beta_n}(\underline{V}\cdot\underline{n})(\underline{n}\cdot\underline{k})\right)\cdot\right.$$

$$\left.\cdot\left(1 - \frac{e}{kTV}\left(\frac{\partial \bar{\Phi}}{\partial \underline{r}_s}\right)\cdot \underline{V}\right)\right] = 2\sqrt{\pi}\,\bar{R}\,\beta_n$$

or to a first order in E_∞ or $(\partial \bar{\Phi} / \partial \underline{r})_s$:

$$\frac{e\bar{\Phi}_s}{kT} = \ln(2\sqrt{\pi}\,\bar{R}\,\beta_n) - \frac{e}{kTV}\left(\frac{\partial \bar{\Phi}}{\partial \underline{r}_s}\right)\cdot \underline{V} - \frac{eE_\infty}{kTV}\left\{V(\underline{r}_s\cdot\underline{k}) + \underline{V}\cdot\underline{k} + \frac{\sqrt{\pi}}{2\beta_n}(\underline{V}\cdot\underline{n})(\underline{n}\cdot\underline{k})\right\}$$

The term $\ln(2\pi\bar{R}\beta_n)$ here is precisely that given by Alpert, Gurevich and Pitaevski for the case without ambient electric field. The second term can be seen to be a correction which arises since the solution to the Boltzmann equation in the limit $\underline{E}_\infty \to 0$ is $\exp(e\bar{\Phi}/kT) f_m$ only to order $|\underline{V}| / v_{e\ mean}$. We have already discussed this approximation above. The third term gives the effect, to a first order, of the ambient field $\underline{E}_\infty$ on the surface potential. The term containing $(\partial \bar{\Phi} / \partial \underline{r})_s$ (which is the field at the body surface) may be of the same order as the third term or larger; it is certainly larger than the first and second items in the third term. We neglect it nonetheless, however, because the logarithmic term predominates, and we are interested only in the increment in potential due specifically to $\underline{E}_\infty$, and not in increments due to other effects or corrections. We can now write:

$$\frac{e\bar{\Phi}_s}{kT} = -\ln\left[(2\sqrt{\pi}\,\bar{R}\beta_n)^{-1}\left\{1 + \frac{eE_\infty}{kTV}\left(V(\underline{r}_s\cdot\underline{k}) + \underline{V}\cdot\underline{k} + (\underline{V}\cdot\underline{n})(\underline{n}\cdot\underline{k})\frac{\sqrt{\pi}}{2\beta_n}\right)\right\}\right].$$

The term $\nabla(\underline{r}_s \cdot \underline{k})$ arises from the integral of the undisturbed potential gradient from the origin of coordinates (the center of the satellite, say) to the surface point. This term is usually negligible, since typically $\nu(\underline{r}_s)/V \sim 0(10^{-1})$, except for very large satellites or very low trajectories. (Actually, this term is of interest only if we wish to compare potentials, say, at opposite ends of the body). Finally, if we assign unit vectors $\underline{i}$ and $\underline{p}$ to the free stream direction and the point on the body respectively, so that $\underline{V} = \underline{i}V$, $\underline{r}_s = \underline{p}\,r_s$, then:

$$\tilde{\Phi}_s = -\frac{kT}{e} \ln \left[\frac{1 + \frac{eE_\infty V}{kT\nu}\left(\underline{i}\cdot\underline{k} + \frac{\nu r_s}{V}\,\underline{p}\cdot\underline{k} + \frac{\sqrt{\pi}}{2S_\infty}\,\underline{n}\cdot\underline{k}\right)}{2\sqrt{\pi}\,\bar{R}\,S_\infty(\underline{i}\cdot\underline{n})} \right] \qquad (14)$$

where $S_\infty = (m_e V^2/2kT)^{1/2}$ is the "speed ratio" of the undisturbed plasma. It should be pointed out again that this result fails when $\underline{i}\cdot\underline{n} \approx 0$; otherwise it gives the dependence of the effect of the electric field $\underline{E}_\infty$ on the various angles involved. The dominant effect is normally that of the last term, since S_∞ is small, which illustrates that the effect is greatest when the electric field is normal to the surface.

The result given here is to be regarded as illustrative only; it does not apply, for example, at the back of the body, even for $\underline{i}\cdot\underline{n}$ not small, since the approximation $e^{\gamma}\,\mathrm{erf}\,\gamma_n \approx 1$ made above is valid only upstream of the body. At the downstream side $(e^{\gamma}\,\mathrm{erf}\,\gamma_n + 1) \to 0$ as $\gamma_n \to \infty$, so that the next term in the asymptotic expansion of $e^{\gamma}\,\mathrm{erf}\,\gamma_n$ would have to be retained, and the calculation modified accordingly.

3. The Potential for Conducting Bodies

The result of Equation (14) applies locally to the surface of a dielectric body. If the vehicle body is a conductor, we have to satisfy the condition in Equation (1). Equation (13) becomes, after the integrations are carried out:

$$\underline{n}\cdot\underline{j}_e\left[\frac{2}{e\,n_\infty(\underline{V}\cdot\underline{n})}\exp\left\{-\frac{e}{kT}\left(\tilde{\Phi}_s + \underline{E}_\infty\cdot\underline{r}_s\cdot\underline{k}\right)\right\}\right]$$

$$= -\left\{1 + \frac{e}{kT\nu}\left(\frac{\partial\tilde{\Phi}}{\partial r}\right)_s\cdot\underline{V}\right\}\left[\frac{1}{\sqrt{\pi}\,\beta_n}\,e^{-\beta_n^2} + \mathrm{erf}\,\beta_n + 1\right]$$

$$- \frac{eE_\infty}{kT\nu}\left[\frac{1}{\sqrt{\pi}\,\beta_n}\,e^{-\beta_n}(\underline{V}\cdot\underline{k}) + (\mathrm{erf}\,\beta_n + 1)\left\{\underline{V}\cdot\underline{k} + \frac{1}{2\beta_n^2}(\underline{V}\cdot\underline{n})(\underline{V}\cdot\underline{k})\right\}\right]$$

It is this expression, together with the corresponding expression for the ion current (11) which lead to our previous result (14). For a conductor these expressions must be integrated over the vehicle surface. Since we are not concerned here with any particular surface, there is no point in carrying matters further at this stage. We may note that this integration would be quite straight forward for simple surfaces such as spheres; for more complicated shapes the integration would have to be done numerically.

It should again be stressed that the surface potential obtained in the above manner must be regarded as an approximation. A more detailed calculation would have to include an account of the influence of the surface interactions on the motion of electrons in the Debye region. We shall return to this subject in Paragraph I.

H. THE NEAR FIELD- REGION B

1. The Approximate Potential Without Magnetic Field

In this section we shall deal with the induced electric field in regions B and B', which are outside the Debye region and in which the space charge density is small ($N_e/N_i - 1 << 1$). Neglecting the influence of the surface, the local electron density is given by the integral of Equation (7) over the whole of the velocity space. The Poisson equation becomes:

$$\nabla^2 \Phi = -4\pi e n_\infty \left[\frac{n_i(\underline{r})}{n_\infty} - \exp\left\{ \frac{e}{kT} (\Phi + E_\infty \underline{r} \cdot \underline{k}) \right\} \right].$$

The term $E_\infty(\underline{r} \cdot \underline{k})$ is the only modification required to the analysis of Alpert, Gurevich and Pitaevski of the problem without ambient field. Now, since $\nabla^2(E_\infty(\underline{r} \cdot \underline{k}) = 0$ and $(\Phi + E_\infty \underline{r} \cdot \underline{k}) \to 0$ as $\underline{r} \to \infty$ it is clear that the introduction of E_∞ into the problem affects only the boundary condition at the surface, which is now $(\Phi_s + E_\infty \underline{r}_s \cdot \underline{\kappa}) = 0$. In other words, apart from this condition, our solution for Φ is simply $-E_\infty(\underline{r} \cdot \underline{k})$ plus the solution which would have been obtained to the problem when $E_\infty = 0$. We shall see, moreover, that the effect of the surface condition on Φ is of second order; therefore to a first order, the induced electric field is unaffected by E_∞, and the total field is simply the sum of the original induced field plus the (new) ambient field. This being the case, we shall be able to make use of the results obtained previously by Alpert, et al, some of which are of direct interest to us here.

If we normalize the Poisson equation, we have

$$\nabla^2\left(-\frac{e\Phi}{kT}\right) = \left(\frac{d}{\delta_\infty}\right)^2\left[\frac{n_i(\underline{r})}{n_\infty} - \exp\left\{\frac{E_\infty\, \underline{r}\cdot\underline{k}}{kT} - \left(-\frac{e\Phi}{kT}\right)\right\}\right]$$

(where the Laplacian has been normalized with respect to d, the body dimension), and $d/\delta_\infty \gg 1$, as we have seen in Section C. The solution may therefore be written as an expansion in powers of $(\delta_\infty/d)^2$:

$$\frac{e\Phi}{kT} = -\frac{E_\infty\, \underline{r}\cdot\underline{k}}{kT} + \ln\left(\frac{n_\infty}{n_i(\underline{r})}\right) + O\left(\frac{\delta_\infty}{d}\right)^2 .$$

The terms $O(\delta_\infty/d)^2$, can be seen by iteration to be approximately:

$$\left(\frac{\delta_\infty}{d}\right)^2 \frac{\nabla^2 \ln\left(n_\infty/n_i(\underline{r})\right)}{\left(n_i(\underline{r})/n_\infty\right)} .$$

Thus the condition on Φ to be imposed on the surface enters the calculation only in terms of order $(\delta_\infty/d)^2$, and since we shall in any case not attempt to apply the present method near the body surface, the potential distribution will be taken to be simply:

$$\Phi = -E_\infty(\underline{r}\cdot\underline{k}) + \frac{kT}{e}\ln\left(\frac{n_\infty}{n_i(r)}\right), \qquad (15)$$

where $n_i(\underline{r})$ is the ion density calculated by the methods of kinetic theory, without reference to the magnetic and electric fields. Then, since we can always take the ion density to be the sum of the ambient density and the density of reflected ions: $(n_i = n_\infty + n_{i(r)}(\underline{r}))$, we have:

$$\underline{E} = \underline{E}_\infty - \frac{kT}{e}\frac{1}{n_i(\underline{r})}\nabla\left(n_\infty + n_{i,r}(\underline{r})\right). \qquad (16)$$

We shall now give several results for the ion distribution and evaluate the corresponding potential distribution. First, however, we shall consider methods for the evaluation of the function $n_i(\underline{r})$.

2. The Ion Density Distribution

Since the influence of the magnetic field is neglected, and the kinetic energy of ions is much greater than their thermal energy, we may assume that the particles move in straight lines. To find the density of reflected ions, we may use geometrical methods. We shall illustrate here how such a calculation may be carried out for the case of specular reflection for a body of arbitrary shape. It should be stressed that these remarks are intended to be an illustration only; the actual calculation may be quite complicated, depending on the shape of the body, and may have to be done numerically. Obviously, very simple geometries can be done analytically.

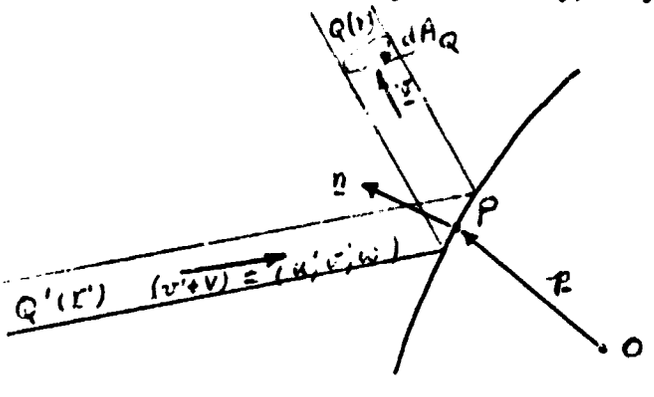

Let O be the center of coordinates and $\underline{p}$ the vector from O to a point P on the surface. $\underline{n}$ is the surface normal unit vector and dS is an element of surface at P. Associated with dS are two principal radii of curvature c_1 and c_2, say, and since the shape of the body is known, we may write:

$\underline{n}=\underline{n}(\underline{p})$; $c_1=c_1(\underline{p})$; $c_2=c_2(\underline{p})$

We consider the density at the target Q of particles originating at Q' and reflected specularly at P. Note that the density of particles at Q is:

$$n_i(r) = n_\infty + n_{i,r}{}^r(r)$$

where $\underline{r}$ is the position vector of Q; i.e., the density is simply the ambient density plus the density of reflected particles, $n_{i,r}(\underline{r})$. This applies only, of course, if Q is completely unshielded by the body.

Since we are dealing with specular reflections, the velocity of particles in PQ is given by:

$$\underline{v} = (\underline{v}'+\underline{V}) - 2(\underline{v}'+\underline{V})\cdot\underline{n}\,\underline{n}$$

The velocity in the Q'P direction is:

$$(\underline{v}'+\underline{V})\cdot(\underline{r}'-\underline{p})/|\underline{r}-\underline{p}| \cdot$$

If we denote this by u', and the two transverse components by v' and w', then:

$$d\Omega' = dv'\,dw'/u^2$$

is the solid angle of the approach cone to P. The element of area at Q, through which all particles incident at P and originating at Q' must pass, may be written:

$$dA_Q = dA_Q(\underline{r}, \underline{\rho}, dS, d\Omega')$$

It should be noted that dA_Q cannot, in general, be expressed in terms of a solid angle, since the envelope, of reflected trajectories need not converge at a point. (Consider, for example, the case of a cylindrical surface). Now, if f', say is the (uniform) distribution of incident particles, then the number of particles scattered toward Q, with velocities in the range v', dv', w', dw', is proportional to their density at P, which is $dv'\,dw' \int f'(u', v', w')\,du'$. The density at Q is therefore:

$$dv'\,dw' \int f'(u', v', w')\,du' \frac{dS}{dA_Q} \frac{\underline{r}\cdot\underline{\rho}}{|\underline{r}\cdot\underline{\rho}|}$$

But, $dv'\,dw' = u'^2\,d\Omega'$ and $d\Omega' = dS\,g(\underline{\rho}, \underline{r}')$, where g is a function of the geometry. We may therefore write the density at Q:

$$n_{i_r}(\underline{r}) = \int_{\text{Surface}} \int_{u>0} f'(u', v', w')\,du' \frac{\underline{r}\cdot\underline{\rho}}{|\underline{r}\cdot\underline{\rho}|} \left(\frac{dS}{dA_Q}\right) u'^2\, g(\underline{\rho}, \underline{r}')\,dS$$

where $u' = (\underline{v}' + \underline{V}) \cdot (\underline{r}' - \underline{\rho}) / |\underline{r}' - \underline{\rho}|$. The integration is over one velocity component and over the surface area of the body; care has to be taken that points on the body for which the vector $\underline{r} - \underline{\rho}$ cuts the surface are excluded from the integration.

As we have pointed out above, such an integration would have to be carried out by computing in all but the simplest cases. The result will be an expression for the ion density in terms of the vehicle velocity and the ion temperature (specifically the ratio $\frac{m_i V^2}{2kT_i}$). Since the effect of the thermal energy of ions is expected to be small, Alpert, Gurevich, Pitaevski have omitted the random motion altogether from these calculations, and have given a few expressions for

$n_{i,r}(r)$ for the case of a unidirectional stream of ions. In this case $n_{i,r}(r)$ is a function only of the geometry of the surface.

3. Effect of the Geomagnetic Field on the Induced Potential

In an unbounded region the distribution function of ions (or electrons for that matter) will not be influenced by the geomagnetic field provided this field is sensibly uniform over distances of the order of the body dimension. Since this is certainly the case upstream of the body, there is no need to modify our analysis (Section 4) below for this region.

Downstream of the body the situation is more complicated. This region is shaded so that ions with rectilinear or nearly rectilinear trajectories cannot penetrate. When a magnetic field is present and the ion trajectories become spirals, the penetration of this region is enhanced. This effect is obviously dependent on the orientation and the strength of the magnetic field, as well as on the ion velocity and temperature.

A general expression for the ion distribution function behind a body of circular cross-section is given by Alpert, Gurevich, Pitaevski. As far as the shading of the downstream region is concerned, it is sufficiently accurate to consider only the cross-section, rather than the three-dimensional shape, of the body. The integration of this distribution function requires computation in general, but for $\underline{H}$ parallel or perpendicular to $\underline{V}$ an analytical expression for $n_i(\underline{r})$ can be obtained. It can be shown that the effect of $\underline{H}$ is greatest (i.e., it mostly facilitates the penetration of ions) when $\underline{H}$ is parallel to $\underline{V}$.

It is readily seen that if the thermal motion of ions is altogether neglected then the ion density behind an obstacle must be periodic with period $2\pi V/\omega_i$ where ω_i is the ion Larmor frequency $eH/m_i c$. The effect of ion temperature is to reduce the amplitude or "smear out" this periodic distribution. We have attached Figure 4, taken from Alpert, et al, as an illustration. The latter effect depends on the value of $v_{i\ mean}/V_o$, while the periodic density distribution is important only over distances which are not small compared with the period. Finally, the body

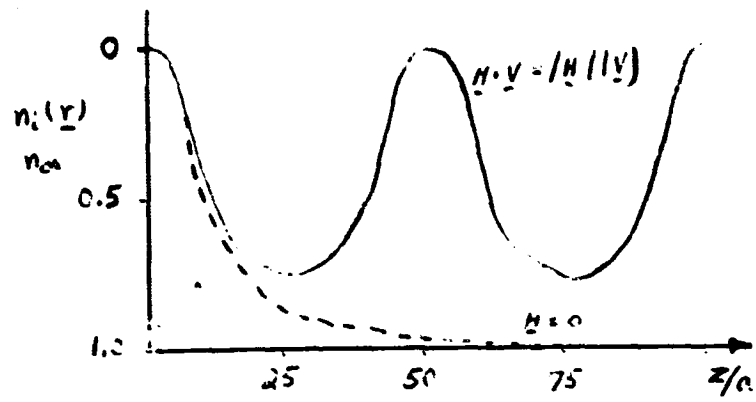

Figure 4: Ion Concentration on the Downstream Axis of a Sphere for $l_i/a = 1$, $(m_i V/ 2kT)^{1/2} = 8$

dimension must be of the order of the Larmor radius l_i or larger for ions to be shaded out over distances of the order of several periods. The significant parameters in determining the effect of the spiral motion of ions due to $\underline{H}$ are therefore $v_{i\,mean}/V$, d/l_i, and $z\omega_i/V$, where z is a downstream distance.

In the region of the ionosphere in which we are interested $\omega_i \approx 2\times10^2$/sec, $l_i \approx 5 \times 10^2$ cm, and $V \simeq 10^6$ cm/sec. Thus, for a typical satellite vehicle (see Section C):

$$v_{i\,mean}/V \sim O(10^{-1}) \; ; \; d_b/l_i \sim O(1) \; ; \; z\omega_i/V \sim O(10^{-1}),$$

whereas for the electric field meter

$$d_f/l_i \sim O(10^{-2}) \quad ; \quad z\omega_i/V \sim O(10^{-3}).$$

We conclude therefore that the effect of $\underline{H}$ might be important if we are interested in the electric fields induced by a vehicle, but negligible if the disturbance of ion density, and hence the induced potential, near the field meter is considered.

4. Electric Field Upstream of the Body

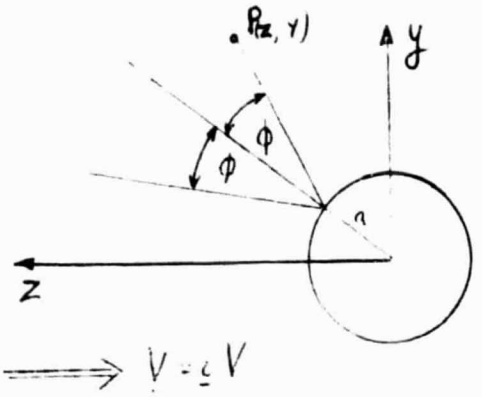

A simple example of the methods of Sections H 1 and H 2 is provided by the potential in the upstream region of a sphere. To avoid the complications involved in carrying out the integration of Equation (16) we again make the simplifying assumption that the ion thermal velocity can be neglected. All ions then move in the negative z direction, and only ions reflected specularly from point (a cos φ, a sin φ) can be scattered toward point (z, y).

It is easily shown that:

$$2z\cos\phi + 2y\sin\phi - y\csc\phi = a$$

The density of reflected ions can be shown to be:

$$n_{ir}(\underline{r}) = n_i(\underline{r}) - n_\infty = \frac{n_\infty R_i a^2}{y^2} \frac{\sin^2\phi\cos^2\phi}{1 - \frac{a}{y}\sin^3\phi}$$

If this is inserted into Equation (15) the electric field can be calculated at all points in the B region. As an example we take the point (z, o) on the upstream axis, for which the required expression is very simple. We find:

$$\Phi_{induced} = \frac{kT}{e} \ln\left\{1 + R_i\left(2\frac{z}{a} - 1\right)^{-2}\right\}$$

and

$$\underline{E}_{induced} = \underline{E} - \underline{E}_\infty = \underline{i}\,\frac{4kTR_i}{ea}\left(2\frac{z}{a} - 1\right)^{-1}\left\{\left(2\frac{z}{a} - 1\right)^2 + R_i\right\}^{-1}$$

The function $E_{induced}(z)$ is plotted in Figures 5a, b, for $R_i = 0.5$ and $T = 1000°K$.

ELECTRIC FIELDS IN REGIONS B AND B' - AN EXAMPLE

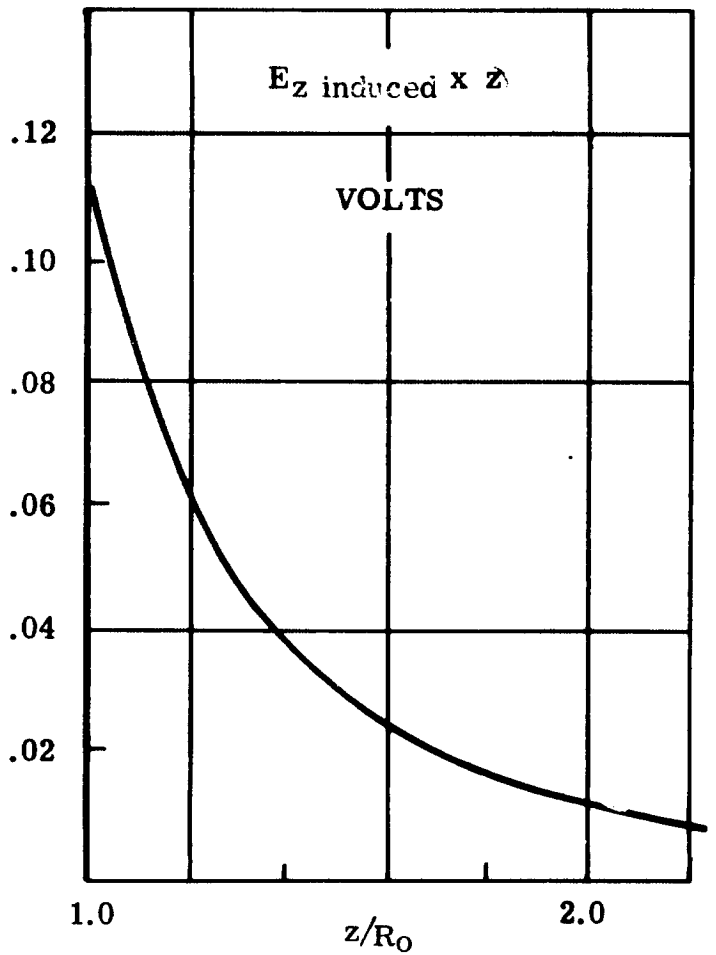

Figure 5a: Electric Field in Region B on $y = 0$, Upstream Stagnation Line

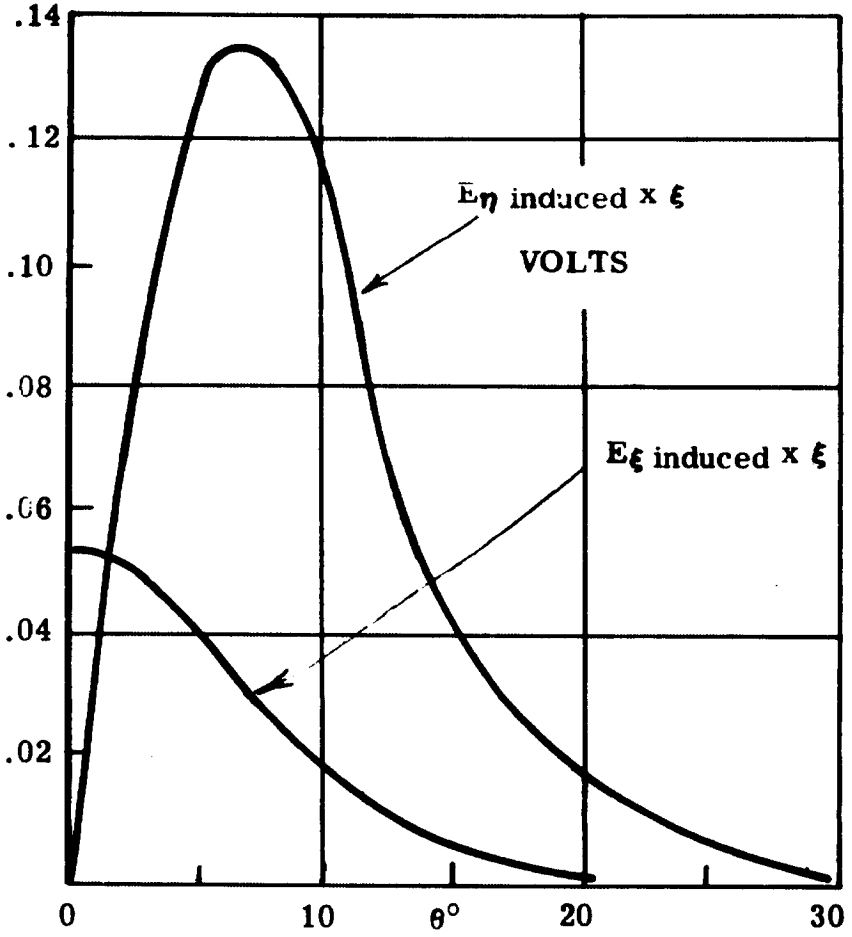

Figure 5b: Electric Fields in Region B' Parallel and Perpendicular to a Flat Plate vs Surface Inclination. For $T = 1000\ ^\circ K$, $\xi^2 = 34$ A $m_i S_\infty^2 / m_e = 34$.

It can be seen that the field decreases rapidly with upstream distances from the body. One body radius upstream of the stagnation point $E_{induced}$ is less than 0.01 volts/meter. The data of Figures 5a, b, should, of course, not be used for $z/a \sim 1$ since the above methods are inapplicable in the Debye region.

5. Electric Field Downstream of the Body

We shall present, in this section, a simple example of the electric fields to be expected downstream of a body in region B'. Although the approximate estimates derived below can be applied to any body, what we have in mind specifically is a component of the electric field meter itself, for example, the collector plate. We wish to estimate the induced electric field in the path of the electron beam when this is downstream of the plate.

In the region $|r| \gg 0 \ (d^2 V^2 \pi m_i / 8 kT)^{1/2}$, where $(\pi m_i/8 kT)^{1/2}$ is the thermal velocity of ions, the ion density, which is very low just behind the body, will have risen to approximately its ambient value. We can therefore write:

$$n_i(\underline{r}) = n_\infty + \delta n_i(\underline{r}),$$

where $\delta n_i(\underline{r})$ is the decrement of ion density due to shielding. The potential now becomes, from Equation (15), since $\delta n_i(\underline{r}) << n_\infty$

$$\Phi = -E_\infty \underline{r}\cdot\underline{k} + \frac{kT}{e}\frac{\delta n_i(\underline{r})}{n_\infty} + O\left(\frac{\delta_\infty}{d}\right)^2$$

The ions behave almost like a monoenergetic stream so that the density of reflected ions in the downstream region is very low and may be neglected. For an obstacle of cross-sectional area S perpendicular to $\underline{V}$ it can be shown that

$$\delta n_i(\underline{r}) = -\frac{n_\infty S m_i \underline{V}^2}{2\pi kT z^2} \exp\left\{-\frac{m_i \underline{V}^2}{2kT}\frac{x^2+y^2}{z^2}\right\}$$

where x, y, z are Cartesian coordinates, with z in the downstream direction. Thus,

$$\Phi = -E_\infty \underline{r}\cdot\underline{k} - \frac{S m_i \underline{V}^2}{2\pi e z^2} \exp\left\{-\frac{m_i \underline{V}^2}{2kT}\frac{x^2+y^2}{z^2}\right\}.$$

REPRODUCIBILITY OF THE ORIGINAL PAGE IS POOR

As an example we consider the case of a plate of area A, the normal to which makes an angle θ to the free stream direction. The electric fields may be calculated from Equations (1) and (2). If these are resolved into directions parallel (η) and perpendicular (ξ) to the plate, we obtain with $S = A \cos\theta$, and on $y = 0$,

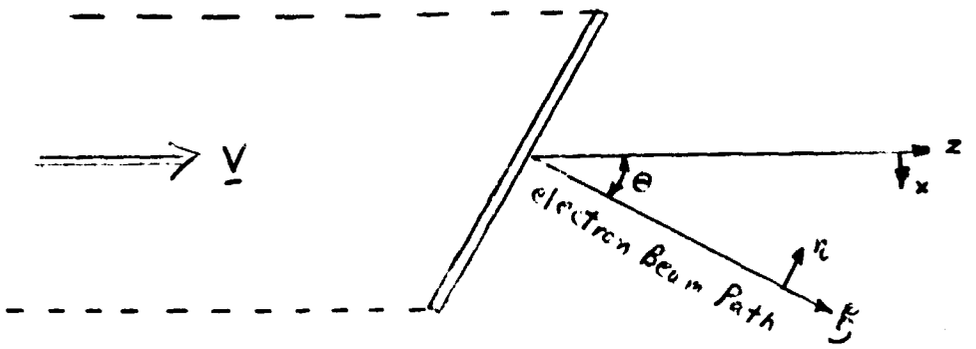

$$E_{\xi\,induced} = -\frac{2kTA}{\pi e \xi^3}\,\frac{m_i S_\infty^2}{m_e}\,\sec\theta\,\exp\left\{-\frac{m_i S_\infty^2}{m_e}\tan^2\theta\right\}$$

$$E_{\eta\,induced} = \frac{2kTA}{\pi e \xi^3}\,\frac{m_i S_\infty^2}{m_e}\,\sec\theta\left[\tan\theta\left(\frac{m_i S_\infty^2}{m_e}\sec^2\theta - 1\right)\right]\exp\left\{-\frac{m_i S_\infty^2}{m_e}\tan^2\theta\right\}$$

These results are illustrated in Figure 5b. If we regard the plate A as an electron beam collector plate, the field E_ξ would have no influence on the beam deflection. The field E_η is transverse to the beam, and is applicable at distances from the plate greater than the plate dimensions. The field is zero when the plate is normal to the free stream (by symmetry) and increases with plate deflection to a maximum value of about $0.14/\xi$ volts per meter, where ξ is in meters. For greater deflections the field decreases as the point at which it is

"REPRODUCIBILITY OF THE ORIGINAL PAGE IS POOR"

evaluated moves out of the wake of the plate.

I. THE PLASMA SHEATH

1. Conditions at Upstream Surfaces

We have shown previously that the surface potential is given approximately by $\Phi_s = kT_e e^{-1} \ln (2\sqrt{\pi}\bar{R}S_\infty)$ and that the Debye shielding distance is $\delta_\infty = (\epsilon_0 kT/e^2 n_{e\infty})^{1/2} = 69\,(T_e/n_{e\infty})^{1/2}$ meters near the front of the body, where T_e is in degrees K and $n_{e\infty}$ is in number per meter^3. The electric field in the Debye region is therefore of order $1.25\text{x}10^{-6}(T_e n_{e\infty})^{1/2} \ln (3.50\,\bar{R}S_\infty)$ volts per meter. We shall now show that this field must be nearly normal to the surface throughout an upstream Debye region.

Consider a spherical body, as illustrated in the figure in H-4. We have shown that in region B the induced potential is approximately

$$\Phi^{(\infty)} = -\frac{kT}{e} \ln\left(1 + \frac{n_{i,r}(\underline{r})}{n_\infty}\right)$$

where $n_{i,r}(\underline{r})$ is the local density of reflected ions, and is dependent upon the value of R_i the reflection coefficient. For a sphere we have shown that

$$\frac{n_{i,r}(\underline{r})}{n_\infty} = \frac{R_i a^2}{y^2} \frac{\sin^2\phi \cos^2\phi}{1 - \frac{a}{y}\sin^3\phi}$$

for specular reflection. The analysis of this section is carried out for specular reflection only; the corresponding calculations may easily be done for diffuse reflection, with similar results as far as the perpendicularity of the electric field is concerned, but we include only one case in this report. The tangential component E_{ll} of the electric field is given by:

$$\begin{aligned} E_{\parallel} &= \frac{n_{i,r}(\underline{r})}{n_{i,r}(\underline{r}) + n_\infty} E_{\parallel}' \\ &= -\frac{n_{i,r}(\underline{r})}{n_{i,r}(\underline{r}) + n_\infty}\left[\frac{kT}{e}\frac{1}{|\underline{r}|}\frac{n_\infty}{n_{i,r}(\underline{r})}\frac{\partial}{\partial\theta}\left(\frac{n_{i,r}(\underline{r})}{n_\infty}\right)\right] \end{aligned} \tag{17}$$

REPRODUCIBILITY OF THE ORIGINAL PAGE IS POOR

where

$$\left.\begin{aligned} x &= |\underline{r}| \cos\theta \;;\; y = |\underline{r}| \sin\theta \\ 2x\cos\phi &+ 2y\sin\phi - y\cos^2\phi = a \end{aligned}\right\} \tag{18}$$

from our analysis of Section H.2. Changing variables from $|\underline{r}|$, θ to y, φ, with

$$\frac{\partial}{\partial\theta} = \left(\frac{\partial y}{\partial\theta}\right)\frac{\partial}{\partial y} + \frac{\partial\phi}{\partial\theta}\,\frac{\partial}{\partial\phi}$$

we find, on substituting $n_{i,r}(\underline{r}) / n_\infty$ into Equation (17) that

$$\frac{E_{11}'\,|\underline{r}|\,c}{kT} = -\left\{\sin\phi\cos\phi\left(1-\frac{a}{y}\sin^3\phi\right)\right\}^{-1}\left[\frac{x}{y^2}\sin\phi\cos\phi\,(a\sin^2\phi - 2y)\right.$$
$$\left. + \left\{\frac{y\cos\phi - x\sin\phi + \frac{x}{2\sin\phi}}{y\cos\phi - x\sin\phi + \frac{y\cos\phi}{2\sin^2\phi}}\right\}\left\{2a(\cos^2\phi - \sin^2\phi) + \frac{a}{y}\sin^3\phi(1+\sin^2\phi)\right\}\right] \tag{19}$$

From this last equation and Equation(17) and (18) an expression for E_{11} in terms of y, φ, can be obtained. It is easily verified that $E_{11} = 0$ on $|\underline{r}| = a$, as it should be for a conducting body.

Consider now the point $|\underline{r}| = a + \delta_\infty$; $\theta = \varphi + \lambda$, as shown in Figure 3. Here $\delta_\infty << a$ and is intended to denote the distance to the edge of the Debye region. We can now write, for the point in question

$$y' = (a+\delta_\infty)\sin(\phi+\lambda) - a\sin\phi = y - y_s$$
$$\approx a\lambda\cos\phi + \delta_\infty\sin\phi$$

and

$$x' = (a+\delta_\infty)\cos(\phi+\lambda) - a\cos\phi = x - x_s$$
$$\approx -a\lambda\sin\phi + \delta_\infty\cos\phi$$

REPRODUCIBILITY OF THE ORIGINAL PAGE IS POOR

where small quantities of order $\lambda \delta_\infty$ have been neglected. Further since $y' = x' \tan 2\varphi$, we find after substitution into the above equations that $\lambda = (\delta_\infty / a) \tan \varphi$ and hence that:

$$y' = 2\delta_m \sin\phi \; ; \; x' = \delta_m \sec\phi \, (\cos^2\phi - \sin^2\phi) \qquad (20)$$

We now substitute $x = x_s + x'$, $y = y_s + y'$ into Equation (19) using Equation (20) and find after some algebra that

$$E_{11}' = \frac{4kT}{e\delta_m} \frac{\sin\phi}{\cos^3\phi} \left(\frac{\delta_\infty}{a}\right)^2 + O\left(\frac{\delta_\infty}{a}\right)^4$$

Now, in the conditions of interest to us, $|\underline{E}|$ in the Debye region is certainly of order $kT/e\,\delta_\infty$ or larger. And since from Equation (17) $E_{11} < 1/2\ E_{11}'$ we conclude that:

$$|E_{11}| / |\underline{E}| \sim O\left(\frac{\delta_\infty}{a}\right)^2$$

This completes our proof that the electric field in the Debye region remains normal to the surface throughout that region to terms of second order.

2. Calculation of the Electric Field in an Upstream Debye Region

We have shown that the region is thin and that conditions within it may be regarded as functions of the normal coordinate x only (see Figure 6). Although our simple demonstration of the previous section dealt with a spherical body, it is obvious that it would be equally applicable for any other body with a local radius of curvature a, provided only that $a >> \delta_\infty$, (i.e., we must deal with a "smooth" body away from all excrescences, holes, cuts, etc.).

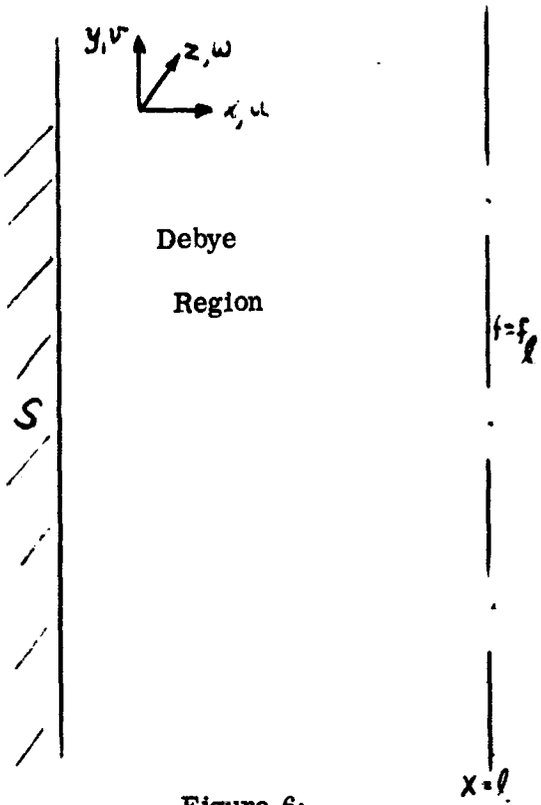

Figure 6:
Debye Region

Consider then, a flat surface at s (x=0) (Figure 6) and the "edge" of the Debye region at x = l. The energy of an electron is $1/2\ m_e (v^2 + w^2) + \epsilon$ where $\epsilon = 1/2\ m_e u^2 - e\Phi$. Here v, w are the transverse velocity components and u is in the x direction. Since conditions are independent of y and z in the Debye region, the Vlasov equation reduces to:

$$u \frac{\partial f}{\partial x} + \frac{e}{m_e} \frac{\partial \Phi}{\partial x} \frac{\partial f}{\partial u} = 0$$

with the solution

$$f = f(v, w, \epsilon)$$

i.e., v, w, and ϵ are constants of the motion of an electron. We may now divide the electrons in $0 < x < \ell$ into the following classes:

a) Incoming particles with insufficient energy to reach the surface;

$$u < 0\ ;\ \epsilon < -e\bar{\Phi}.$$

b) Incoming particles with energy sufficient to reach x = 0;

$$u < 0\ ;\ \epsilon > -e\bar{\Phi}.$$

c) Outgoing particles which have suffered specular reflection, with temperature characteristic of the plasma;

$$u > 0\ ;\ T = T_e$$

d) Receding particles diffusely reflected with temperatures characteristic of the surface;

$$u > 0\ ;\ T = T_s$$

e) Receding particles emitted from the surface with temperatures characteristic of the surface;

$$u > 0\ ;\ T = T_s$$

Similar categories could be established for ions, except that since the surface potential is usually negative, we should have to include "trapped particles," i.e., reflected or emitted particles with insufficient energy to pass to infinity. Also, the class (a) above would be empty, since all approaching ions must be attracted to the surface. However, in our problem we need concern ourselves only with electrons; as we have shown before, the kinetic energy of ions is too large for the effect of the potential to be significant. We may assume, therefore, that the ion distributions of region B persist right up to the surface, so that ion densities in the sheath are known.

We shall now make the following two additional assumptions:

a) Each class of electrons is separately subject to the Vlasov equation and its (partial) distribution function is given by

$$f_r = f_r(v, \omega, \ldots); \quad (r = a, b).$$

b) For the purposes of this illustration we may simplify matters by neglecting Classes (c), (d), and (e); that is, we assume complete absorption of electrons and no emission.

The distribution function at the edge of the Debye region is given by Equation (7) viz:

$$f(x=\ell) = n_\infty \left(\frac{m_e}{2\pi k T_e}\right)^{3/2} \exp\left\{\frac{e}{kT_e}(\Phi + E_\infty \underline{r} \cdot \underline{k})\right\} \exp\left\{-\frac{m_e}{2kT_e}(u^2+v^2+\omega^2)\right\}\left[1 - \frac{eE_\infty}{kT_e \nu}\underline{k}\cdot\underline{v}\right],$$

where we have neglected $\underline{V}$, since $|\underline{V}| \ll |\underline{v}_e|_{\text{mean}}$. Before proceeding to the next step, we must examine the term containing $(E_\infty \ \underline{k}\cdot\underline{v})$. The direction of the electric field E_∞, that is $\underline{k}$, may have arbitrary orientation with respect to the surface normal vector $\underline{n}$. The retention of this anisotropic term in the Debye region in the same form as that which we developed for the disturbed region A implies that the convective derivative (df / dt) is negligible in regions B and C, and that the distribution function therefore persists up to the surface (apart from truncations due to surface interactions). We shall not attempt a rigorous justification

REPRODUCIBILITY OF THE ORIGINAL PAGE IS POOR

of this assumption. But it can be seen to be reasonable when we consider that the electron mean free path is of the order of 10^3 cm, to 10^5 cm, which is certainly large compared to the vehicle dimension, and very large compared with the dimensions of components of the field meter.

The component of $E_\infty \underline{k} \cdot \underline{v}$ containing u is $E_\infty (\underline{k} \cdot \underline{n})$ u; the remaining components, with v and w will make no contribution when we come to integrate our distribution functions for the electron densities, (since $\int_{-\infty}^{\infty} e^{-\frac{1}{2}v^2} v\, dv = 0$). We shall therefore retain only this term. At x = i, then,

$$f(x=i) = n_\infty \left(\frac{m_e}{2\pi k T_e}\right)^{3/2} \exp\left\{\frac{e E_\infty \underline{i} \cdot \underline{k}}{k T_e}\right\} \exp\left\{-\frac{m_e}{2kT_e}(v^2+w^2)\right\} e^{-\epsilon/kT_e}$$
$$\left[1 - \frac{e E_\infty (\underline{k} \cdot \underline{n})}{k T_e \nu}\left\{\frac{2}{m_e}(\epsilon + e\bar{\Phi}_i)\right\}^{\frac{1}{2}}\right]. \quad (21)$$

Equation (21) is the distribution function f (v, w, ε) in the Debye region. Since all distribution functions for this one dimensional case are of Maxwellian form in the y and z directions, we need deal only with the functions F (ε):

$$F_{a,b}(\epsilon) = \int_{-\infty}^{\infty}\int_{-\infty}^{\infty} f_{a,b}\, dv\, du = C_{1,2}\, e^{-\epsilon/kT_e}\left[1 - \frac{e E_\infty (\underline{n} \cdot \underline{k})}{k T_e \nu}\left\{\frac{2}{m_e}(\epsilon + e\bar{\Phi}_i)\right\}^{\frac{1}{2}}\right],$$

where $C_{1,2}$ are constants. Now for particles of class (a) we must have $u < 0$; $\epsilon < -e\bar{\Phi}_s$ and $\epsilon > -e\bar{\Phi}$, the latter being the condition that the electrons have sufficient energy to penetrate to x. (It may be noted that complications would arise if the potential in the sheath were not monotonic; however, we do not expect this to be the case). We may now write:

$$F_a(\epsilon) = C_1\, H(-u)\, H(-\epsilon - e\bar{\Phi}_s)\, H(\epsilon + e\bar{\Phi})\, e^{-\epsilon/kT_e}\left[1 - \frac{e E_\infty (\underline{n} \cdot \underline{k})}{k T_e \nu}\left\{\frac{2}{m_e}(\epsilon + e\bar{\Phi}_i)\right\}^{\frac{1}{2}}\right],$$

where H $(u, \epsilon, \bar{\Phi})$ is the Heaviside unit function, and similarly

$$F_b(\epsilon) = C_2\, H(-u)\, H(\epsilon + e\bar{\Phi}_s)\, H(\epsilon + e\bar{\Phi})\, e^{-\epsilon/kT_e}\left[1 - \frac{e E_\infty (\underline{n} \cdot \underline{k})}{k T_e \nu}\left\{\frac{2}{m_e}(\epsilon + e\bar{\Phi}_i)\right\}^{\frac{1}{2}}\right].$$

REPRODUCIBILITY OF THE ORIGINAL PAGE IS POOR

We can now write down expressions for the density of particles of each class. After a change of the variable of interaction from u to ϵ and some rearrangement we have:

$$\frac{n_a(\Phi, \Phi_s, \Phi_\ell)}{C_1} = (2m_e)^{-1/2} \int_{-e\Phi_\ell}^{-e\Phi_s} e^{-\epsilon/kT_e} (\epsilon + e\Phi_\ell)^{-1/2} d\epsilon - \frac{eE_\infty (\underline{n}\cdot\underline{k})}{m_e kT_e \nu} \int_{-e\Phi_\ell}^{-e\Phi_s} e^{-\epsilon/kT_e} (\epsilon + e\Phi_\ell)^{-1/2} (\epsilon + e\Phi_\ell)^{1/2} d\epsilon \quad (22)$$

$$\frac{n_b(\Phi, \Phi_s, \Phi_\ell)}{C_2} = (2m_e)^{-1/2} \int_{-e\Phi_s}^{\infty} e^{-\epsilon/kT_e} (\epsilon + e\Phi_\ell)^{-1/2} d\epsilon - \frac{eE_\infty (\underline{n}\cdot\underline{k})}{m_e kT_e \nu} \int_{-e\Phi_s}^{\infty} e^{-\epsilon/kT_e} (\epsilon + e\Phi_\ell)^{-1/2} (\epsilon + e\Phi_\ell)^{1/2} d\epsilon \quad (23)$$

The term $\exp (e E_\infty \underline{r}_\ell \cdot \underline{k}/ kT_e)$ is due to the undisturbed ambient potential gradient (see Equation 21). The component perpendicular to the plate, that is, $(\underline{r}_\ell \cdot \underline{k})_{\perp} (E_\infty) = E_\infty \ell$ is negligible. The remaining components depend on the choice of center of coordinates and the point on the surface in question.

The quantities C_1, C_2 are related to the total density at the edge of the sheath of particles of each type

$$C_{1,2} = n_{e_{1,2}}(x=\ell) \left(\frac{m_e}{2\pi kT_e}\right)^{1/2} \exp\left(\frac{eE_\infty \underline{r}_\ell \cdot \underline{k}}{kT_e}\right),$$

where $n_{e\,a,b}\,(x = l)$ may be found from the distribution function at $x = l$. Thus,

$$n_{e_{a(x=\ell)}} = n_\infty \left(\frac{m_e}{2\pi kT_e}\right)^{1/2} \exp\left(\frac{eE_\infty \underline{r}_\ell \cdot \underline{k}}{kT_e}\right) \int_0^{e\Phi_s} e^{-\epsilon/kT_e} \left[1 - \frac{eE_\infty \underline{n}\cdot\underline{k}}{kT_e \nu} \left\{\frac{2}{m_e}(\epsilon + e\Phi_\ell)\right\}^{1/2}\right] \left\{2m_e(\epsilon + e\Phi_\ell)\right\}^{-1/2} d\epsilon \quad (24)$$

and $n_{eb}\,(x=l)$ is given by the same integral, but with limits $-e\Phi_s < \epsilon < \infty$. (It should be noted that the subscript 1 appears in the factor $(\epsilon + e\Phi_\ell)^{-1/2}$ in Equation (24), but not in Equations (22) and (23) since the former is to be evaluated at the edge of the sheath only). Since Classes (a) and (b) contain all incoming

REPRODUCIBILITY OF THE ORIGINAL PAGE IS POOR

electrons, we must have

$$n_{e a(x=\ell)} + n_{e b(x=\ell)} = n_\infty \exp\left\{\frac{e}{kT_e}\left(\bar{\Phi}_\ell + E_\infty \frac{\eta}{\ell}\cdot\underline{k}\right)\right\}\left[\frac{1}{2} + \frac{\sigma E_\infty (\underline{\eta}\cdot\underline{k})}{\nu (2\pi m_e kT_e)^{1/2}}\right] \qquad (25)$$

The term containing E_∞ on the right hand side of Equation (25) is the contribution of the anisctropy to the particle density in the velocity half-space $u < 0$.

It remains to evaluate the integrals in Equation (22) and (23). The first two integrals are simple, and turn out to be products of exponentials and error functions. The latter two integrals (from the anisotropic parts) appear, unfortunately, not to be expressible in terms of tabulated functions and should be computed. Since we have had no occasion to carry out such a computation, this section must remain incomplete. (The required integrals can be expressed as a one parameter family of functions).

The outline of the solution is however clear. We have to solve:

$$\frac{d^2\bar{\Phi}}{dx^2} = 4\pi e\left\{n_{e_a}(\bar{\Phi}, \bar{\underline{\Phi}}_s, \bar{\Phi}_\ell) + n_{e_b}(\bar{\Phi}, \bar{\underline{\Phi}}_s, \bar{\Phi}_\ell) - n_i(x)\right\}$$

where $n_i(x)$ is the known ion distribution obtained from kinematic considerations only, and n_{ea}, n_{eb} are given by Equations (22) and (23) in the functional form indicated. The potential $\bar{\Phi}_\ell$ is a known result of the analysis for region B. The Debye region solution $\bar{\Phi}(x)$ is therefore dependent on the choice of l for the edge of the Debye region. This, however, is arbitrary, and this fact constitutes one of the principal difficulties of this kind of analysis. It appears that some additional condition must be introduced, and although this question has received a good deal of attention in the literature, it is at present unclear what this condition should be.

3. The Downstream Debye Region

Downstream of the body ions are strongly shaded, and their density must decrease sharply as the surface of the body is approached. If the effect of the magnetic field is neglected it is rather easy to appreciate this physically and

calculate the ion density. As we have shown, field $\underline{H}$ has the effect of facilitating the penetration of ions into the region behind the obstruction, the effect being greatest when $\underline{H}$ is parallel to $\underline{V}$. Here again the significant parameters are $l_i/d_b \sim 0(1)$ (or $l_i/d_f \sim 0(10^2)$ and $z\omega_i/V$ where z, the downstream dimension should be interpreted now as δ_∞. Since $\delta_\infty \omega_i/V \sim 0(10^{-4})$ we conclude that the effect of $\underline{H}$ may be neglected. The ion density in the downstream Debye region can in fact be shown to be $0(n_\infty \delta_\infty^2/d_b^2)$ which is certainly very small, or in the case of field meter components, $0(n_\infty \delta_\infty^2/d_f^2)$ which is small enough, unless we are dealing with very small items.

It can also be seen that the electron density must be larger, but of the same order as the ion density, since electrons are rejected by the high negative potentials in this region. Now, the normalized Poisson Equation has the term $(d_b/\delta_\infty)^2 (n_i - n_e)/n_\infty$ on the right hand side (Equation 15) so that the charge density is the difference of two quantities both of the order of unity. The Laplacian therefore dominates the equation.

A suitable procedure for very low n_i, n_e would therefore be precisely the reverse of the analysis of Section H. There we found the potential, to a first order, by equating the electron and ion densities, the Laplacian making a negligible contribution. In the downstream Debye region, we obtain a first approximation to the potential from the Laplace equation, and treat the effect of charge density as a perturbation. Now,

$$\nabla^2\left(-\frac{e\Phi}{kT}\right) = \left(\frac{d_b}{\delta_\infty}\right)^2 \left\{ \frac{n_i(\underline{r})}{n_\infty} - \frac{1}{n_\infty} \int f_e \, d\underline{v} \right\}$$

$$\underline{v} \frac{\partial f_e}{\partial \underline{r}} + \frac{e}{m} \frac{\partial \Phi}{\partial \underline{r}} \frac{\partial f_e}{\partial \underline{v}} = 0$$

In this Poisson equation ∇^2 has again been normalized with respect to d_b; the right hand side is therefore O (1), whereas the Laplacian is $O(\Phi)$, that is $O(\ln(\delta_\infty/d_b))$. We are justified therefore in expanding as follows:

REPRODUCIBILITY OF THE ORIGINAL PAGE IS POOR

$$\bar{\Phi} = \Phi^{(0)} + \left(\frac{d_b}{\delta_m}\right)^2 \bar{\Phi}^{(1)} + O\left(\frac{d_b}{\delta_m}\right)^4$$

$$f = f^{(0)} + \left(\frac{d_b}{\delta_m}\right)^2 f^{(1)} + O\left(\frac{d_b}{\delta_m}\right)^4$$

On substitution into the above, we obtain:

$$\nabla^2 \bar{\Phi}^{(0)} = 0$$

$$\bar{v} \frac{\partial f^{(1)}}{\partial \bar{r}} + \frac{e}{m} \frac{\partial \bar{\Phi}^{(1)}}{\partial \bar{r}} \frac{\partial f^{(0)}}{\partial \bar{v}} = 0$$

$$\nabla^2 \bar{\Phi}^{(1)} = -\frac{kT}{e} \left\{ \frac{n_e(r)}{n_\infty} - \frac{1}{n_\infty} \int f^{(0)} d\bar{v} \right\}$$

$$\bar{v} \frac{\partial f^{(1)}}{\partial \bar{r}} + \frac{e}{m} \left\{ \frac{\partial \bar{\Phi}^{(0)}}{\partial \bar{r}} \frac{\partial f^{(1)}}{\partial \bar{v}} + \frac{\partial \bar{\Phi}^{(1)}}{\partial \bar{r}} \frac{\partial f^{(0)}}{\partial \bar{v}} \right\} = 0$$

The zeroth order potential is a solution to the Laplace equation with mixed boundary conditions, i.e., we know the surface potential and the electric field outside the Debye region. The solution to the zeroth order Vlasov equation is $f = f(\alpha_m)$, $m = 1, 2, \ldots 6$ where α_m's are constants of the motion of an electron in the field $\Phi^{(0)}$. If these constants can be found, we can also find the next approximation to the potential $\Phi^{(1)}$, which is the first order correction for the effect of space charge.

This, then, is a procedure which is suitable for the downstream region. Whether this method, when carried out numerically, would be simpler than a numerical solution of the Poisson and Vlasov equations, such as that of Parker, depends on the geometry and details of the problem. It would certainly reduce the numerical complexities if the geometry were such that $\bar{\Phi}^{(0)}$, the Laplace equation solution, could be written down immediately. If that were possible, the problem would be reduced from the solution of two simultaneous partial differential equations to the solution of the Vlasov equation only with a known potential.

Now, the zeroth order potential can be written down if the boundaries (at the surface and at the junction with region B') fall into a coordinate class for which the solution to Laplace's equation is given by one or other of the tabulated harmonic functions. Where the geometry is such that a two dimensional approximation is possible (end effects ignorable) then the theory of complex analytic functions may be used.

The next step, however, the solution of the Vlasov equation, or the determination of the constants of the motion, can rarely be carried out analytically. One would write down the Hamiltonian for the electron, and then seek a suitable canonical transformation (see, for example, Northrop).[15] In practice this is usually successful only in trivial cases, for which the constants of the motion are known in any case. It is for this reason, of course, that attempts at this problem, for electrostatic probes or electrodes, are always confined to one-dimensional or spherically symmetric cases. Since the potential distribution in our downstream Debye region will certainly not be spherically symmetric, it appears that in our case the function $\Phi^{(1)}$ could only be evaluated numerically.

Alpert, Gurevich and Pitaevski consider only the electrostatic potential $\Phi^{(0)}$ in their comments on the downstream problem, no doubt for the reasons given above. In the following section we shall also confine ourselves to $\Phi^{(0)}$, but not for the vehicle Debye region. It would be rather pointless to attempt to construct potentials for a body the shape of which is not yet known. Rather, we shall consider the electron beam field meter itself; the shape of the components of this instrument are simple plates. Furthermore, the results are of considerable importance in evaluating the response of the field meter.

4. Potential in the Downstream Region due to an Ambient Field

The potential distribution in the downstream Debye region has to satisfy several conditions. First, it must conform to the surface potential which is fixed by the condition that the total current into the surface is zero for equilibrium. Since the particle concentration in the downstream region is very low, it is a good

REPRODUCIBILITY OF THE ORIGINAL PAGE IS POOR

approximation to calculate the potential from the current flowing into the upstream part of the surface only. An approximate method for this purpose has been given in Section G-2. A more accurate estimation of the electron current would follow from the method of Section I-2, assuming that the required integrals there are computed. The second condition is that the potential match that is given by the expression in Equation 15 for the induced potential in Region B' at the junction of the latter with the Debye region. Finally, since, as we have shown in Section H-1, the potential in region B' is approximately the sum of the induced potential and the potential of the ambient field, we have to add a term which produces a uniform field outside the Debye region. We then have:

$$\bar{\Phi} = \bar{\Phi}_i + \bar{\Phi}_e$$

say, where Φ_i and Φ_e satisfy the conditions:

$$\nabla^2 \bar{\Phi}_i = 0 \; ; \; \bar{\Phi}_i(\underline{r}_s) = \bar{\Phi}_s \; ; \; \bar{\Phi}_{i \text{ at } B'}(\underline{r}) = -\frac{kT}{e}\left(\frac{n_i(\underline{r}) - n_\infty}{n_\infty}\right)$$

$$\nabla^2 \bar{\Phi}_e = 0 \; ; \; \bar{\Phi}_e(\underline{r}_s) = 0 \; ; \; \nabla \bar{\Phi}_e(\underline{r}) \underset{\underline{r} \to \infty}{=} -E_\infty \underline{k}.$$

We shall not attempt to solve the Laplace equation for the induced potential. The methods are well known, but would in practice have to be numerical, except for very simple surface shapes. One such example, for a sphere, has been given by Alpert, Gurevich and Pitaevski, and it is reproduced in Figure 7.

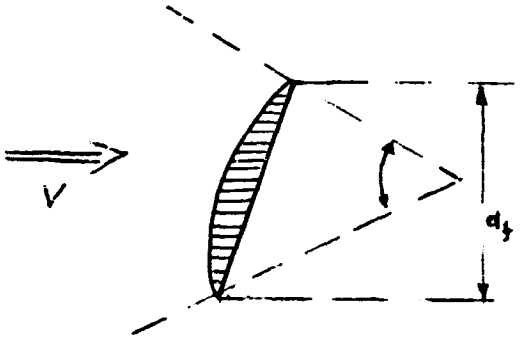

A rapid method of estimating the order of events in the downstream region is the following: The region of maximum rarification is that region bounded by the rear surface of the body and tangents to it making it an angle, $\tan^{-1}\left\{8kT/\pi m_i V^2\right\}^{1/2}$ (where we have used $(8kT/\pi m_i)^{1/2}$ as the mean thermal velocity) with the free stream direction. The downstream end of this region is therefore of order

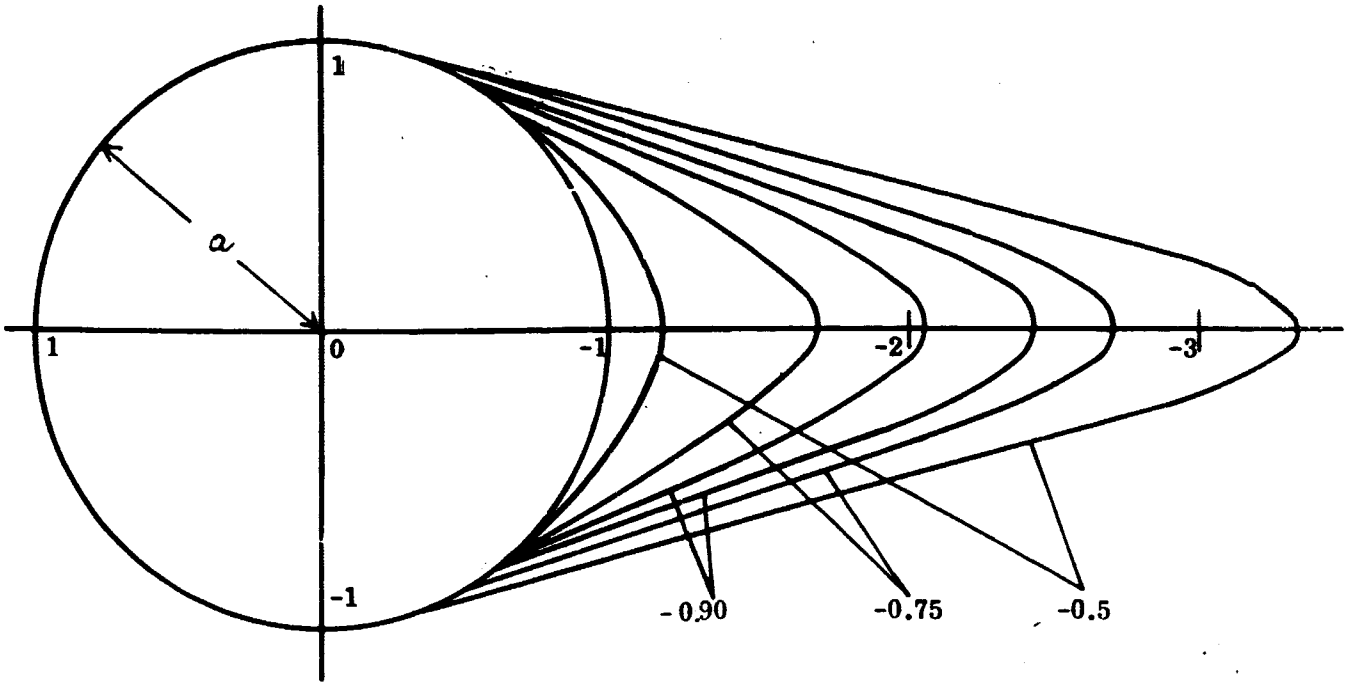

Figure 7 : Equipotentials Downstream of a Conducting Sphere for $e\Phi_s/kT = -0.50 \ln(\xi_\infty/a)$. Values indicated are in units of $-e\Phi/[kT \ln(\xi_\infty/a)]$. From Reference 7.

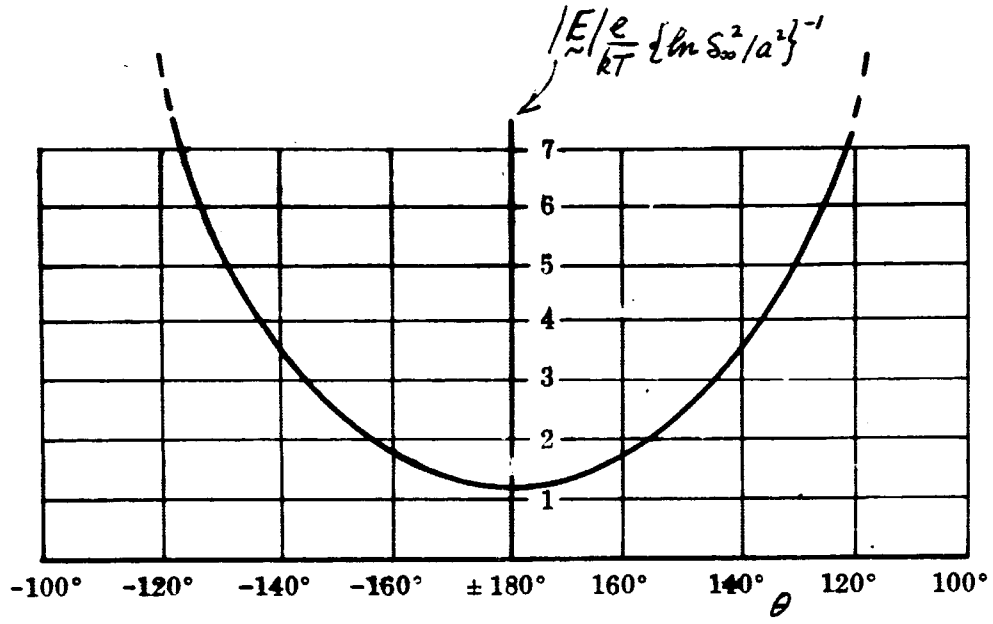

Figure 8: Field Intensity at the Surface of a Conducting Sphere vs Angle from Upstream Direction. From Reference 7.

REPRODUCIBILITY OF THE ORIGINAL PAGE IS POOR

$d_f V \{ \pi m_i/32\, kT \}^{1/2}$ behind the body. The ion density on the two tangents lines is of the order $4 n_\infty \delta_\infty^2/d_f^2$ and the potential is therefore approximately:

$$\bar{\Phi}_i = \frac{2kT}{e} \ln\left(\frac{2\delta_\infty}{d_f}\right)$$

The region upstream of this potential contour may be regarded as the downstream Debye region. The potential of the surface, however, is of the order kT/e and therefore (numerically) an order of magnitude or more smaller than the potential on the potential contour in question. Thus the electric field in the $\underline{V}$ direction is of the order:

$$\frac{3kT}{e d_f V}\left(\frac{2kT}{\pi m_i}\right)^{1/2} \ln\left|\frac{2\delta_\infty}{d_f}\right| \sim O\left[(V d_f)^{-1} \ln\frac{2\delta_\infty}{d_f}\right]$$

This field would apply on the axis, approximately. As can be seen in Figure 8 the field in the same direction near the edges of the body is greater. In the transverse direction the field is of the order.

$$4kT \ln(2\delta_\infty/d_f)/e d_f \sim O\left(d_f^{-1} \ln\frac{2\delta_\infty}{d_f}\right)$$

These orders of magnitude should be applied with caution. They certainly apply only when the normal to the rear surface is not at too great an angle to the freestream direction.

The potential field $\bar{\Phi}_e$ due to the external field represents a considerably simpler problem, and here the prospects for an analytical solution are good. We shall give a simple example for a two-dimensional case. This would be applicable to field meter components or vehicle components such as long bodies, antennas or rectangular collector plates of high aspect ratio.

We take Cartesian coordinates x, y, and write:

$$x = \frac{1}{2} a \cosh\mu \cos\theta \; ; \; y = \frac{1}{2} a \sinh\mu \sin\theta$$

so that μ, θ are elliptic coordinates. Consider the complex potential:

$$F(\mu+i\theta) = \bar{\Phi}_e + i\bar{\Psi}_e = -\tfrac{1}{2} E_\infty a \left[e^{\cdots} \cosh(\mu+i\theta) - e^{\cdots} \cosh(\mu_0+i\sigma)\right]$$

REPRODUCIBILITY OF THE ORIGINAL PAGE IS POOR

where Φ_e and Ψ_e are the potential function and the flow function, due to the ambient field, respectively. The former is:

$$\Phi_e(\mu,\theta) = \tfrac{1}{2} E_\infty a \left\{ \cos\gamma\cos\theta \left(e^{\mu_0-\mu}\cosh\mu_0 - \cosh\mu\right) + \sin\gamma\sin\theta\left(e^{\mu_0-\mu}\sinh\mu_0 - \sinh\mu\right)\right\}$$

In this coordinate system the lines μ = constant are ellipses. We see that:

$$\Phi_e \longrightarrow 0 \qquad \text{on } \mu = \mu_0$$

and

$$\Phi_e = -\tfrac{1}{2} E_\infty a \left\{ \cos\gamma\cos\theta\cosh\mu + \sin\gamma\sin\theta\sinh\mu \right\}$$
$$= -E\,(x\cos\gamma + y\sin\gamma)$$

The ellipse $\mu = \mu_0$ may therefore be regarded as body at zero potential. The field at infinity is E_∞ in a direction making an angle γ with the major axis.

If we let $\mu_0 \longrightarrow 0$ we have:

$$\Phi_e = -\tfrac{1}{2} E_\infty a \sinh\mu \cos(\theta - \gamma)$$

This is the potential around a flat plate of length 2a with a field E_∞ at infinity in the direction γ. The use of this coordinate system makes it possible, therefore, to deal with flat plates (such as collector plates) as well as bodies which can be represented approximately by elliptical cross-sections. Potential distribution around circular cross-sections can be represented approximately by selecting a larger value of μ_0.

For three dimensional problems we may here again make use of the various tabulated harmonic functions for suitable geometrical boundaries.

J. CONCLUSIONS

We have investigated various regions of interaction between the ionospheric plasma and surfaces moving at satellite velocities. In its most general form the problem involves the simultaneous solution of the Boltzmann and Poisson equations

plus surface conditions for the impingment of particles. To derive rapid methods of estimation for the induced electric fields we have divided the problem into:

1) The Far Field,

2) The Near Field, without surface conditions,

and

3) The Debye Regions, upstream and downstream of the body.

Since no specific shape or property of surface is given our work has been of an illustrative nature; the principle result being that we have assembled the methods which can be used for suitable calculations when the problem is more completely specified. However, the order of magnitude of the induced electric fields has been estimated for the various regimes of interaction, so that some reasonably adequate guidelines for the operation of the electron beam field meter and the interpretation of the data can be given.

The following are our principle conclusions:

1) We have given an electron distribution function valid in the far field and the near field. The effect of an ambient electric field due to ionospheric phenomena is to produce a small anisotropy in this distribution function.

2) The effect of induced and ambient electric fields on the motion of ions can be neglected. With the exception of certain circumstar , in which a magnetic field can facilitate the penetration of ions into the shaded region behind the obstacle, the effect of the geomagnetic field on the motion of ions can also be neglected (as far as our present interaction problem is concerned).

3) We have given a simple expression for the local potential of a dielectric surface and indicated how the potential for a conducting surface is to be calculated when the shape of the surface has been specified. Our expression is a function of the orientation of the velocity vector, surface normal vector, and ambient electric field vector.

4) The potential in the near field can be calculated, to a first order, from the condition of local charge neutrality. The problem therefore reduces to that of the kinematics and reflection of ions. We have put forward a method for the calculation of the density of ions reflected from the upstream surface.

5) Two illustrations of the potential distribution in the near field region have been given. The first applies to the regime upstream of a sphere. We have shown that the induced field on the axis is of the order of $0.1\ a^{-1}$ volts/meter (where a meters is the radius of the sphere) near the stagnation point (but outside the Debye region) and decays to approximately 10% of this value one body radius upstream of the stagnation point. The parameters in this example are typical of those expected in the E and F regions of the ionosphere. The details of such a calculation become more complicated for other blunt shapes, but the order of magnitude of the induced fields are expected to be about the same.

6) Our second example for the near field concerns the region downstream of an obstacle of arbitrary cross-sectional shape; a numerical example is given for an inclined flat plate typical of the electron beam gun housing or collector plate. This region is more than one body dimension downstream of the rear surface; upstream of it lies the Debye region which is here of the order of one body dimension in extent. In our example we have given expressions for the induced electric fields in the directions parallel and perpendicular to the electron beam path.

7) As regards the upstream Debye region, which is less than α 1 cm in depth, we have shown that the electric field in this regime remains perpendicular to the surface accurate to quantities of the second order. The problem of the upstream sheath can therefore be treated on a one dimensional basis. We have adapted a method due to previous authors to the case where the electron distribution function is anisotropic at the edge of the sheath. However, certain integrals arise which would have to be computed numerically and this has not been done.

8) Since ions are strongly shaded by the body, the downstream Debye region presents an extremely difficult problem, which we have not attempted. It can be shown however, that the solution to the Laplace equation is a good approximation to the potential in this region. The effect of space charge is of the second order. The boundary conditions are mixed, since we know the potential of the surface and the electric field at the junction of this Debye region and the downstream "near field". Here again, no specific problem has been posed and we have contented ourselves with an example of a region bounded by an inclined two dimensional flat plate and a uniform electric field at infinity.

9) As far as the operation of the electron beam field meter is concerned (assuming that this is placed sufficiently far from the influence of the carrier vehicle) we conclude that the effect of fields induced by the components of the instrument would be most severe when the beam path is nearly parallel to the direction of motion. In this case a large fraction of the beam path would lie in the wake of either the gun housing or collector plate, in which region transverse electric fields of the order of 10 to 100 volts/meter are to be expected. If the beam trajectory is of the order of 10 times the component dimension the angle between beam path and velocity vector should be no less than 20°. The effect of residual fields in the Debye region and the near wake can then be estimated when the geometry is specified.

PRECEDING PAGE BLANK NOT FILMED.

SECTION III
INSTRUMENT DESIGN AND PERFORMANCE

A. CONCEPTS

There are two major difficulties in measuring ionospheric electric fields by deflection of an electron beam. The first is that the deflection is very small. The second is that the earth magnetic field introduces a very large deflection. Figure 9 illustrates the sensitivities of the beam to both magnetic and electric fields. Note that for a 300 volt beam a magnetic field of 1 gamma produces as much deflection as an electric field of 11 millivolts/meter. Since the earth's field can be of the order of 40,000 gamma, a signal to noise ratio of 1/440,000 must be overcome in order to resolve one millivolt/meter.

Although it is conceivable that the magnetic field could be measured and the correction applied by subtraction, it is apparent from the foregoing that such an approach is not practical.

The means chosen to discriminate between the deflection due to magnetic versus electric fields is to modulate the electric field in a precise manner, by alternately creating and removing a Faraday shield around the beam. The magnetic field is unaffected by this, while the electric field is modulated in a square-wave fashion. By demodulating the output signal synchronously with the modulation, only the square-wave signal is accepted. In order to accurately measure deflections without requiring an extremely accurate mosiac target or other such device, the closed loop beam centering system is employed. A current collector target is divided into four segments as shown in Figure 10. The currents collected in two opposing segments are balanced against each other. The difference signal when amplified and applied as the voltage to an appropriate pair of deflection plates is then a direct measure of the field induced beam deflection. The component of this voltage which is synchronous with the chopper represents the electric field while the steady state voltage represents the magnetic field. It should also be noted that there is virtually no requirement on drift or d.c.

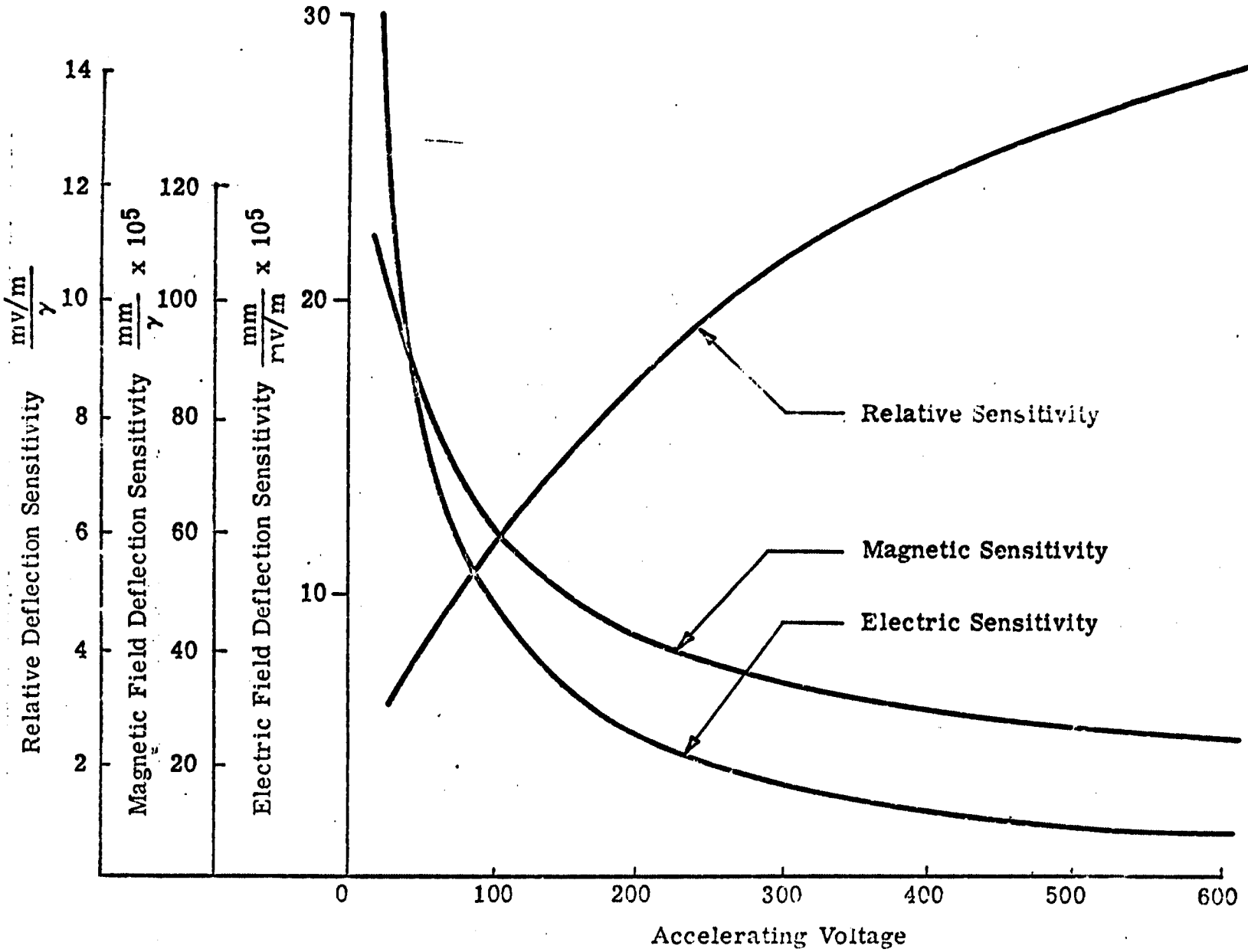

Figure 9 : Beam Sensitivities

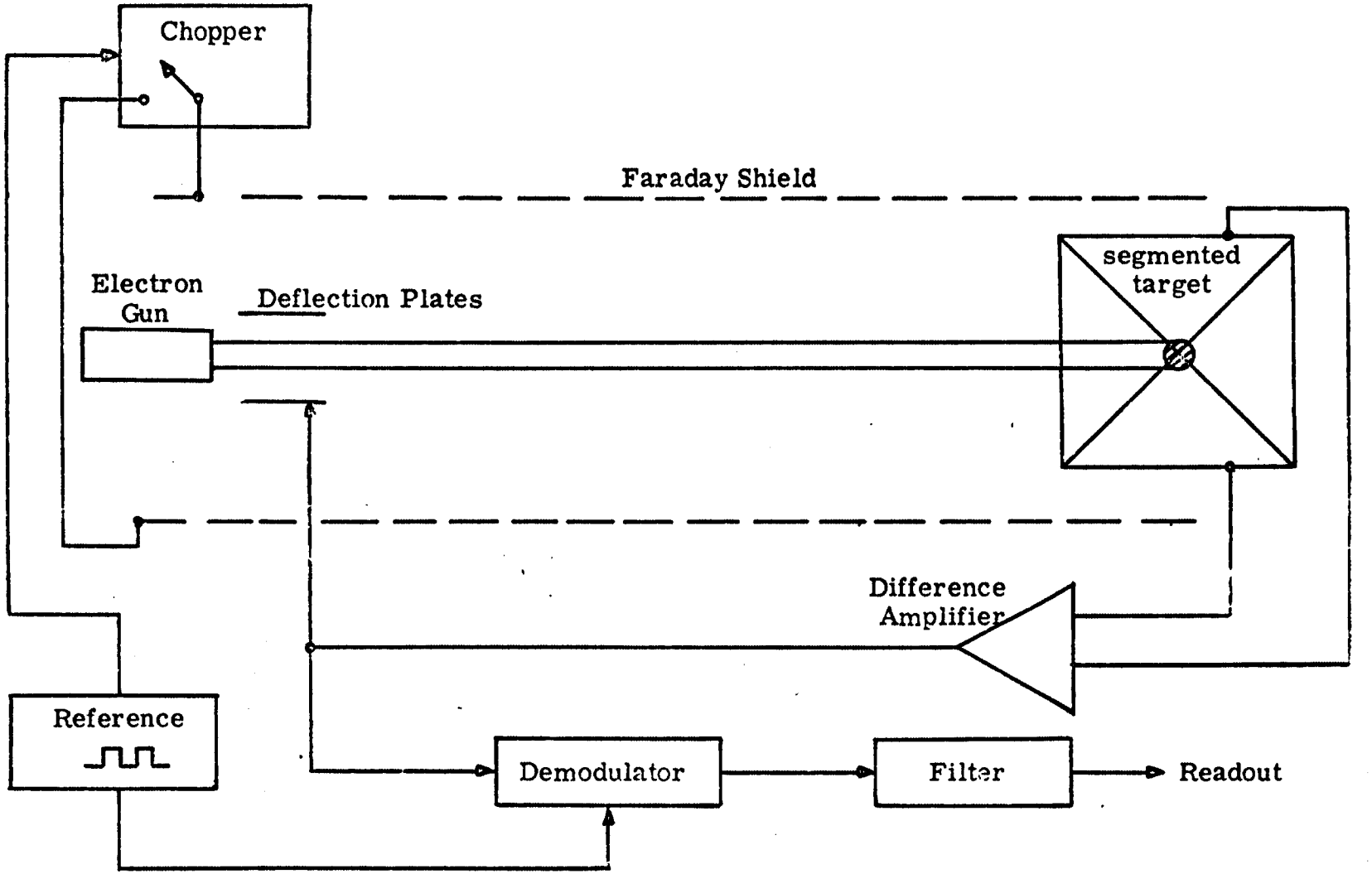

Figure 10: Electrostatic Field Meter (Single Axis Shown)

offset of the amplifiers in the loop, or on mechanical or thermal stability. Any misalignments in the gun-target arrangement will contribute to the d.c. deflection plate voltage and will not affect the electric field reading.

B. COMPONENT DESCRIPTION

Figure 11 is a functional block diagram of the meter showing some of the parameters of the loop. The conversion constants from electric and magnetic field to deflection are based on a 500 volt beam. A realistic design goal for the accuracy of this meter would be ± 1mv/m over a range of 10 mv/m to 100 mv/m and 1 or 2% accuracy over a dynamic range of 100 mv/m to 1000 volts/meter. The upper limit is determined by the ± 100 volts limitation of the readout equipment and power supplies. A schematic of the equipment as breadboarded to date is shown in Figure 12. Figure 13 shows the field meter breadboard model. The gun is visible toward the bottom. The differential current amplifiers A_1 for both axes are wrapped in the electrostatic shield above the target. A somewhat more detailed description of each component follows.

1. Electron Gun and Beam

The electron gun design chosen for the electric field meter is the electrostatic lens, hairpin filament type. This design provides a rugged, reliable gun which can provide an electron beam having a diameter of 1 mm or less, and focussed at distances up to 25 cm for accelerating voltages between 300 - 500 volts.

The electron gun being used in the laboratory experimental unit is the Superior Electronic Corporation, Type SE-2B, modified with a tungsten replaceable filament.

The beam current at the target is 1 microampere at a pressure of 10^{-5} torr. The filament is operated space charge limited drawing 3.6 amperes at 3 volts.

The control grid, biased positively, and the focus electrode are adjusted until the beam spot on the target plate has a maximum current density and is properly focussed. The cathode is negative 500 volts with respect to the grounded final accelerating anode. The filament is the cathode, and the acceleration potential is applied in a balanced method across the hairpin filament. Both a.c. and d.c. filament power has been used. Figure 14 illustrates the gun hookup.

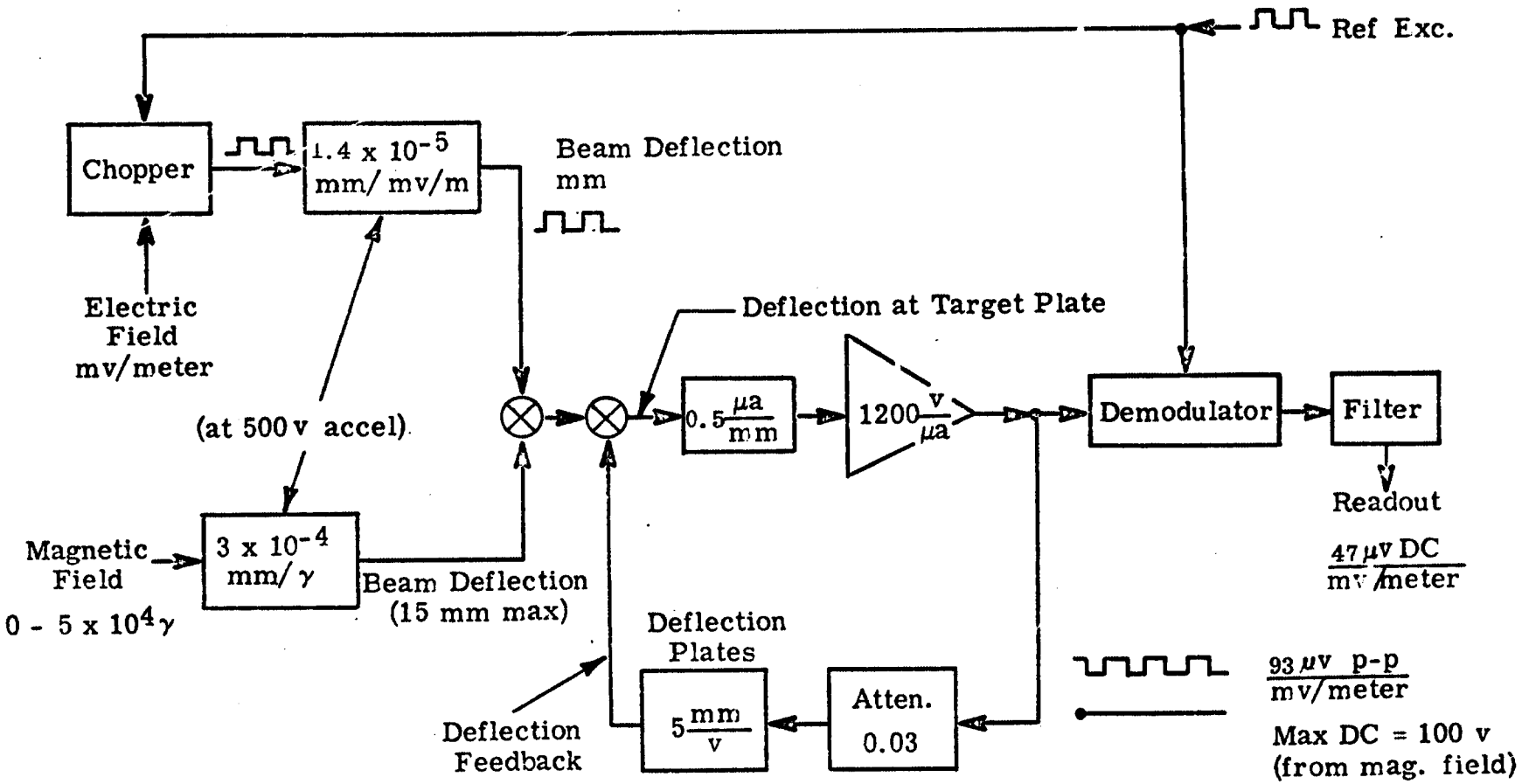

Figure 11: Electric Field Meter System - Block Diagram (Single Axis Shown)

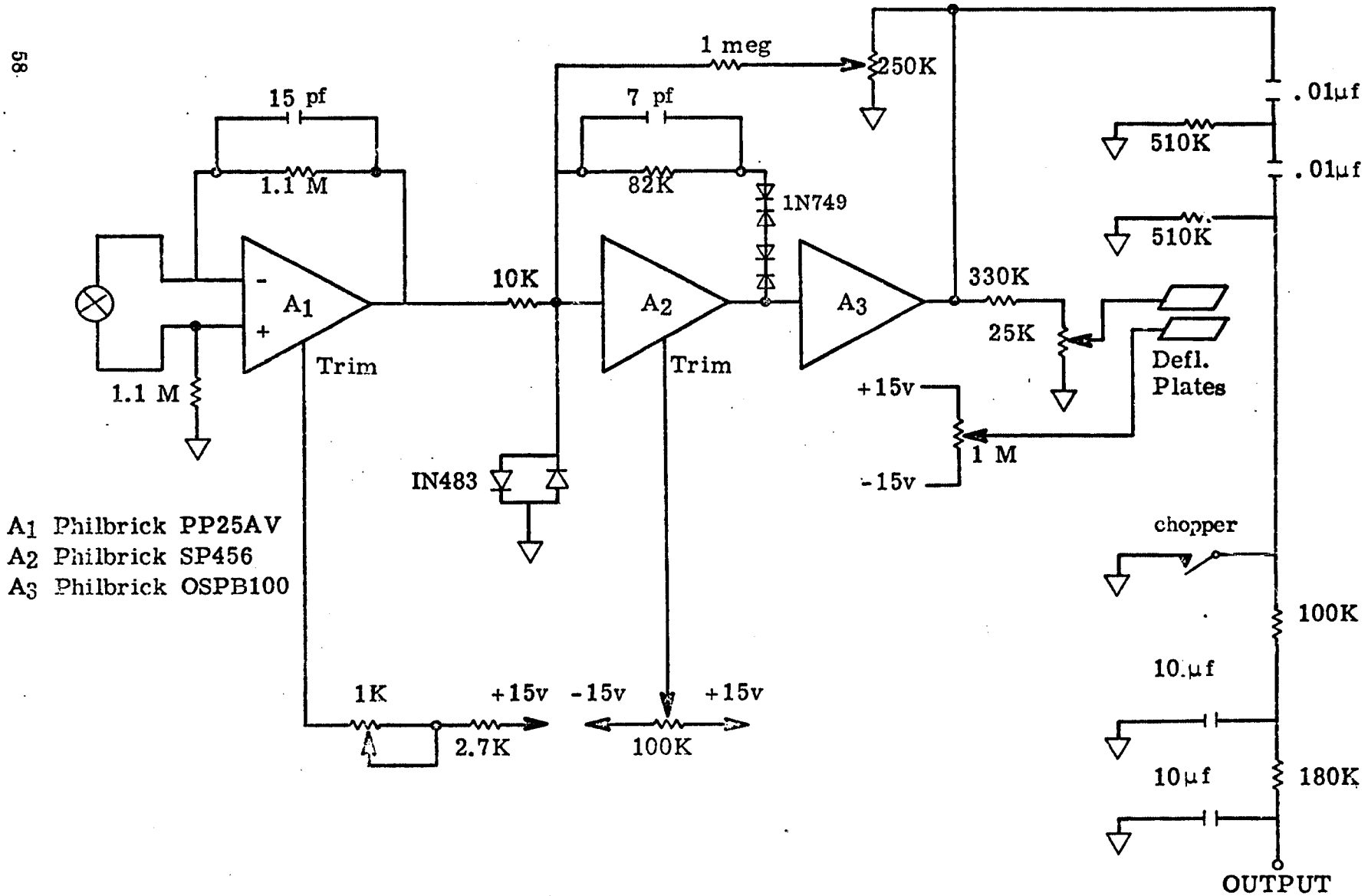

Figure 12: Laboratory Setup - Electric Field Meter (One Axis Shown)

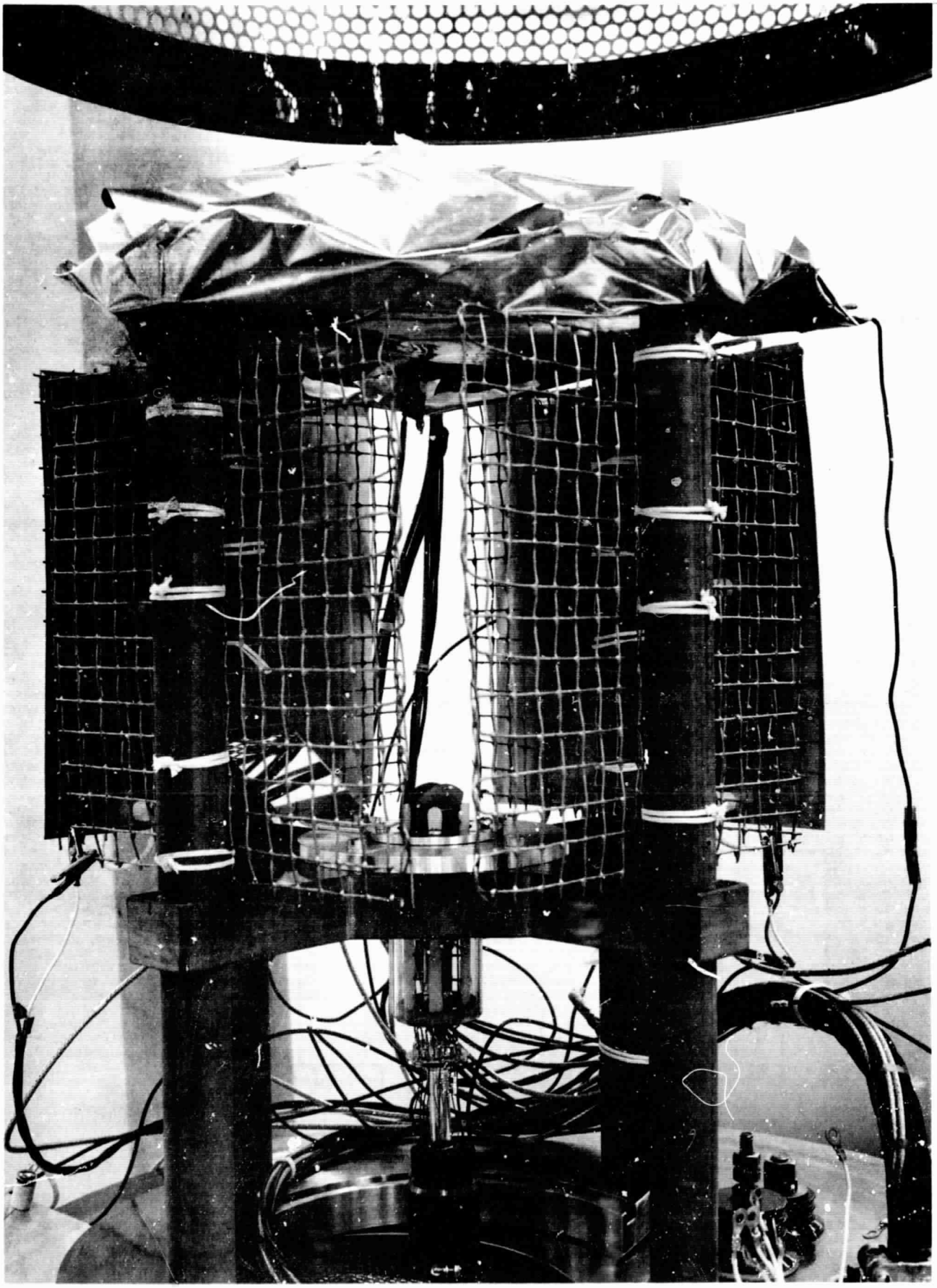

Figure 13: Field Meter Breadboard

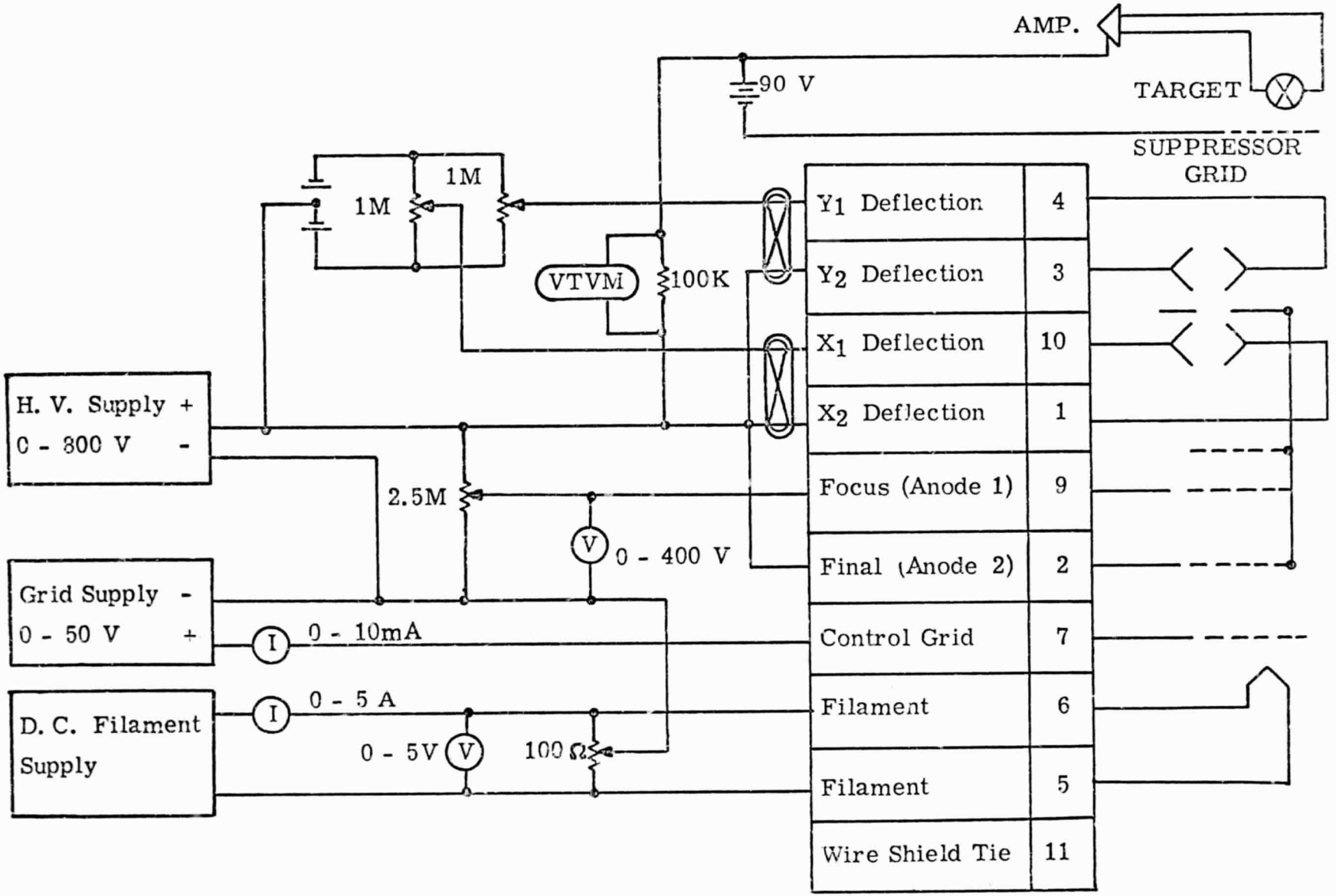

Figure 14: Gun Voltages

2. Target

The target presently used is made by depositing pure gold onto a flat glass surface. Leads are attached by means of silver filled conducting epoxy and lamp black is then deposited over the gold by holding the plate in a candle flame. The target is segmented into four isolated sections by scribing with a sharp stylus. A light dusting of optically active ZnS is applied all over the target expect for a 1/4 -inch diameter circle centered on the target center. This is for convenience in finding and focussing the beam. The purpose of the carbon is to protect the gold from the beam energy, as well as to give a somewhat lower secondary electron emission. One of the major problems was found to be secondary emission. A suppressor grid located 1/4-inch in front of the target plate and kept at a negative 90 volt potential with respect to the target was found to suppress secondary electrons sufficiently to allow the loop to operate. An open loop measurement on the breadboard showed that using the suppressor grid the target's conversion scale factor is 0.3 microamps per mm deflection Figure 15 shows the target and suppressor.

3. Deflection Centering Loop

a. Amplifiers

The first section consists of a current comparator circuit using an operational amplifier (A_1 in Figure 12). This circuit converts a current unbalance signal to a voltage with low source impedance. The scale factor for this conversion is equal to the value of the feedback and input resistance, 1.1 megohms, in this case. The amplifier and resistor are located directly behind the target plate to minimize pickup problems.

Operational amplifiers A_2 and A_3 provide a voltage gain of 1200 with a maximum linear output of ± 100 volts. Figure 16 gives the gain and phase characteristics which are shaped to permit stable closed loop operation.

b. Feedback Attenuator and Output Scale Factor

The scale factor of the output is proportional to the reciprocal of the attenuation in the feedback loop when sufficient forward gain is provided. The

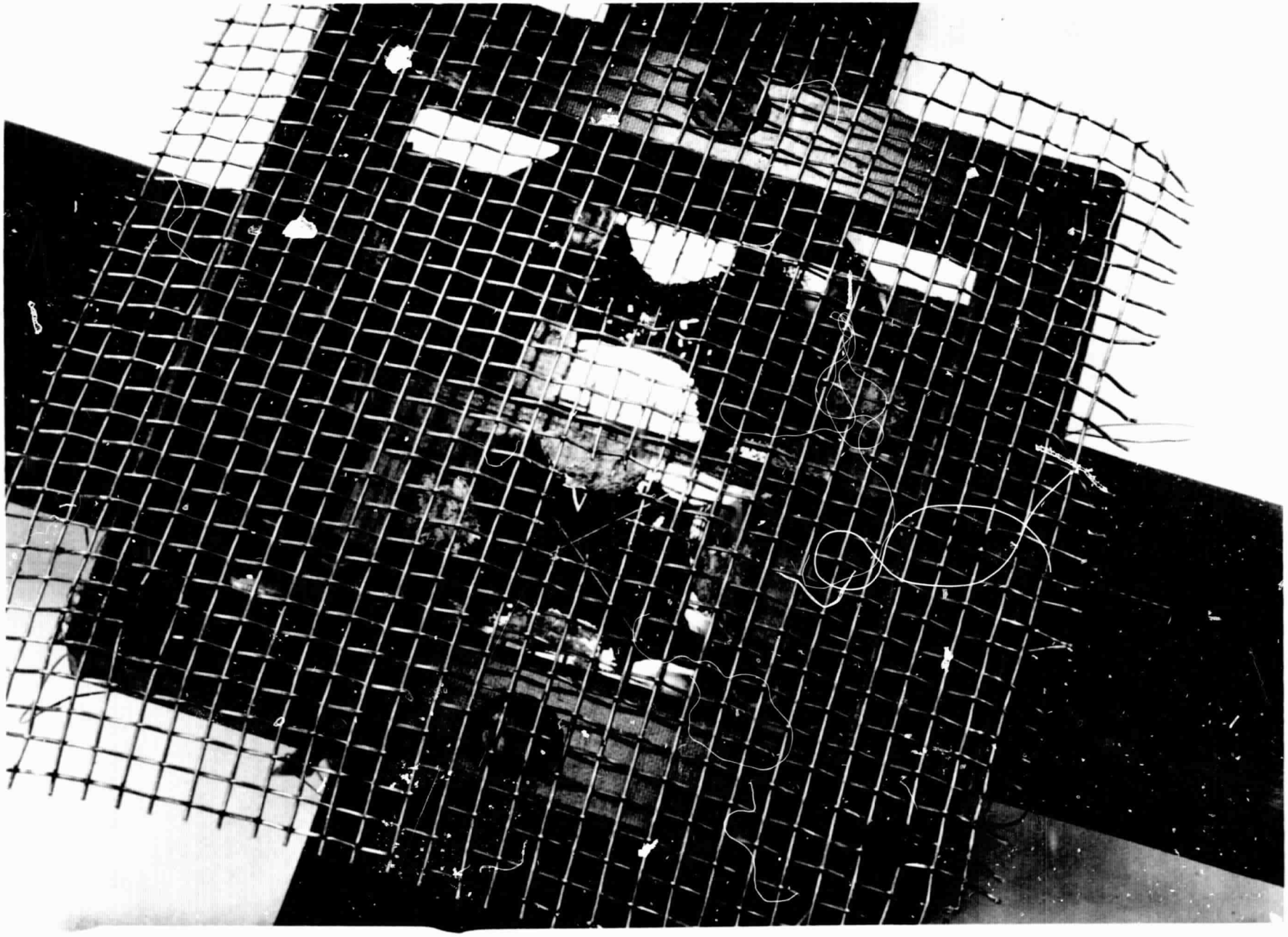

Figure 15: Target and Suppressor Grid

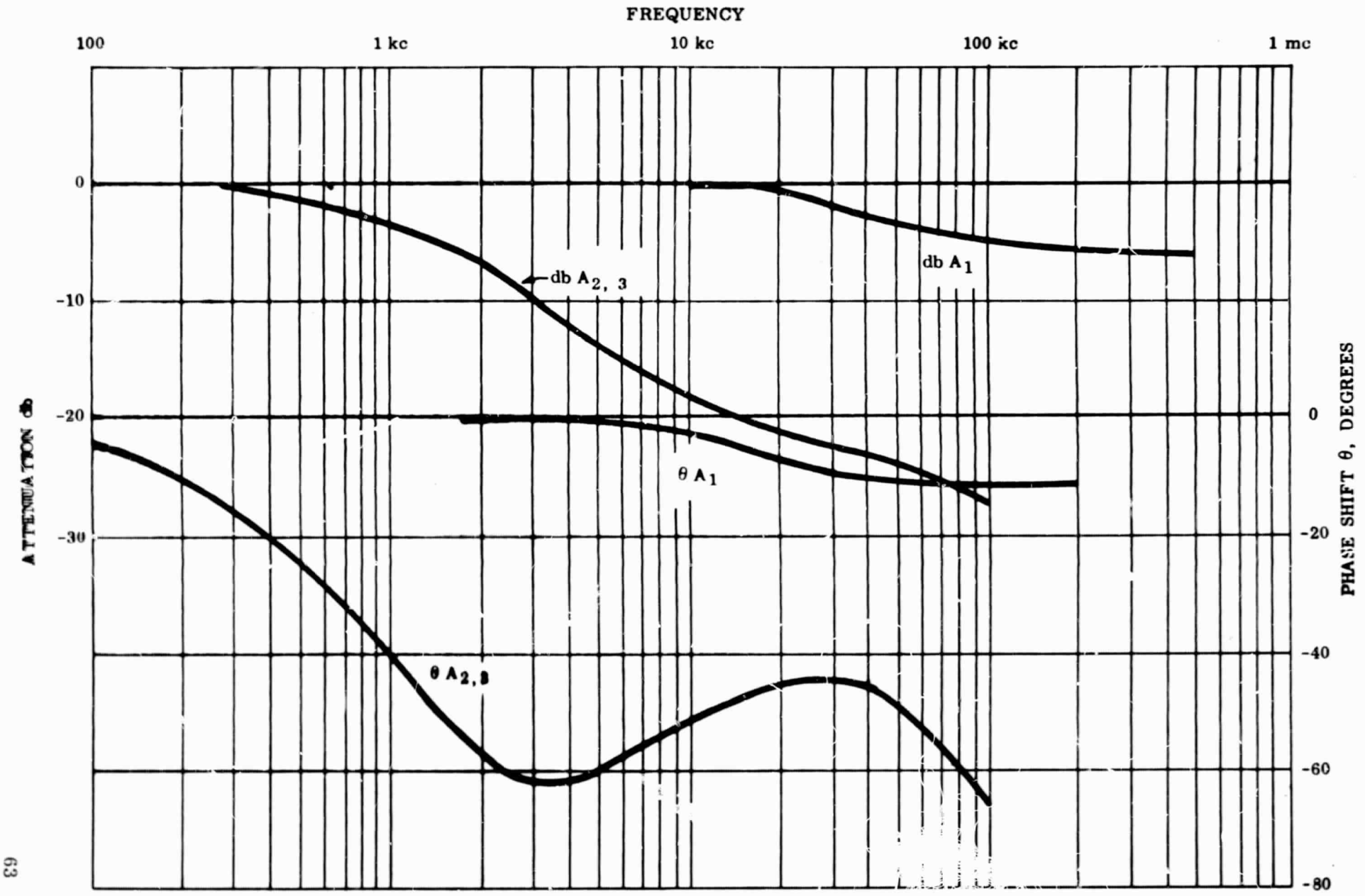

Figure 16: Amplifier Gain and Phase Characteristics

maximum scale factor is selected on the basis of the maximum d.c. output available to balance the maximum deflection due to magnetic fields. With a ± 100 volt limit on the d.c. output, the scale factor is ideally $47 \frac{\mu v \text{ d.c.}}{mv/m}$ at the output of the detector-filter.

c. Deflection Plates

The sensitivity of the deflection plates is approximately 2.4 mm/v for each plate. When both plates are driven in push-pull fashion the gain is 5 mm/v.

4. Faraday Cage

Modulation of an electric field in an ionized medium as conceived for the field meter has not yet been demonstrated in the laboratory. It is quite difficult to simulate the properties of the ionosphere and indeed it is questionable whether an adequate simulation is even feasible. For the breadboard tests to date a Faraday screen was constructed, consisting of a pair of 1/2-inch mesh screens on each axis. A voltage applied as a square wave across one axis produces a chopped field perpendicular to the beam. (See paragraph E 3)

5. Detector and Filter

The deflection plate voltage is coupled through a high pass filter to the chopper. The purpose of this is to suppress much of the flicker noise from the amplifiers. The demodulator is a capacitor coupled type with SPST switch. The chopper presently used is a standard Airpax series 600 which contains two synchronized poles in one package. The other pole is used for field modulation. The filter section consists of two RC sections. The high frequency response of the instrument is determined by this filter. In this case the cut off is set at 1/2 cps primarily because of the high level of background line frequency interference which must be filtered out at this point.

6. Readout

The readout used in the laboratory testing is a John H. Fluke differential a.c. - d.c. voltmeter, which is capable of resolving 0.1 mv d.c.

C. ENVIRONMENT

1. Vacuum System

The electric field meter is placed within an 18 inch diameter bell jar, which is 30 inches in height. The vacuum system is a 4 inch oil diffusion pump, Vactronic HVS4000 which is sustained through a mechanical pump, Welch 1397. A liquid nitrogen cold trap is in the line to the bell jar. Vacuum as low as 10^{-6} torr is maintained in the bell jar without the electron gun heated, and normal operation is a 5×10^{-6} torr with all systems of the meter operative. The pressure is measured by an ionized pressure gauge C.E.C. Model GIC-110, within the bell jar.

The experimental support structure was carefully designed to allow trapped gas to escape from screw threads and low outgassing material was used.

2. Spurious Field Interference

No attempt was made to isolate the meter from background power line interference. As a result the beam is subject to a.c. magnetic fields far in excess of anything that can be expected in a space application. The filter used in the laboratory has been selected to reduce this component of the output sufficiently so that the d.c. signal of interest can be read out. For a mission-designed instrument of course this filter will be redesigned. A side benefit of the pick up is that when it appears at the amplifier output (before demodulation and filtering) it gives a good visual indication that the beam is centered and focussed. Initial beam centering and fine focussing is greatly facilitated by this and it may be desirable in the future to provide a known a.c. field specifically for this purpose in calibration setups.

3. Mechanical Vibration and Isolation

It has not been found necessary to take any precautions against mechanical vibration beyond the initial step of isolating the roughing pump from the chamber. This was done by using a soft rubber tube which was solidly clamped to ground near its center.

D. LABORATORY TEST PROCEDURE

To operate the field meter the following steps are followed:

1) Check vacuum: Pressure should be less than 10^{-5} torr.

2) Bring filament voltage slowly up until filament current is 3 amperes. Wait for pressure to rise and fall again. Bring filament current to 3.6 amperes.

3) Turn on gun voltages, amplifier power, and bias supplies.

4) If a beam has been previously centered and adjustments have not been disturbed the beam is now operative. If initial adjustments are being made the following steps are followed:

   a) Disconnect deflection plates from amplifier output (both axes). Ground deflection plates. Set initial voltages

      Acceleration voltage = 500 v
      Focus voltage = 120 v
      Control grid voltage = +21 v
      Suppressor grid voltage = - 90 v

   b) Sweep X and Y deflection voltages systematically until spot is located.

   c) Bring spot to a place on target where it can be seen clearly.

   d) Trim focus and grid voltages to give well focussed spot, approximately 1 mm in diameter.

   e) Bring spot to center of target.

   f) Observe output of A_3 for both X and Y axes. Adjust X and Y focussing, control grid, and centering controls to get maximum output from each axis without saturation. Close loop by re-connecting deflection plates to A_3 outputs. The loop is now operating, and the field may be applied.

E. LABORATORY PERFORMANCE

1. Setup

Figure 17 shows the setup used for measuring the input-output characteristics of the meter.

2. Loop Output Characteristics

The scale factor of the meter components were adjusted to agree with the Block Diagram of Figure 11 and an input versus output run was made for the X axis. Figure 18 shows the result. Because of various losses in the detection and filtering the scale factor approximates $17 \frac{\mu v}{mv/meter}$ instead of the ideal which is $47 \frac{\mu v}{mv/meter}$.

3. Mesh Screening Tests

Tests were made to determine the shielding effectiveness of screens of various mesh size. The design of the Faraday screen is dictated by two considerations. It is required to provide effective electrostatic shielding but it is also necessary that the screen interact with the local plasma as little as possible. The design approach is to use an open mesh of fine wire. In order to determine the minimum spacing required to give effective shielding, a series of tests of shielding effectiveness were made. Shield boxes (10" x 10" x 12") simulating the Faraday cage were constructed of various materials from 1-1/8" hexagonal mesh to solid aluminum foil. Probes consisting of 2 aluminum foil plates 2" x 4" separated by 1-3/4" were placed in the shield boxes. The entire assembly was placed between large aluminum sheets (2-1/2' x 2-1/2') which were connected across a 1 kc voltage source. It was found that the 1/2" x 1/2" mesh provided 99% shielding effectiveness. The wire size is immaterial with respect to shielding effectiveness and therefore can be made as fine as structural considerations will allow. It is expected that wire approximating No. 35 strung on struts of slightly larger cross section will be suitable. At a distance of 5 inches, the plasma disturbance caused by the wire is expected to be insignificant, as the plasma wake effect becomes negligible at 100 body radii (about 0.3 inch).

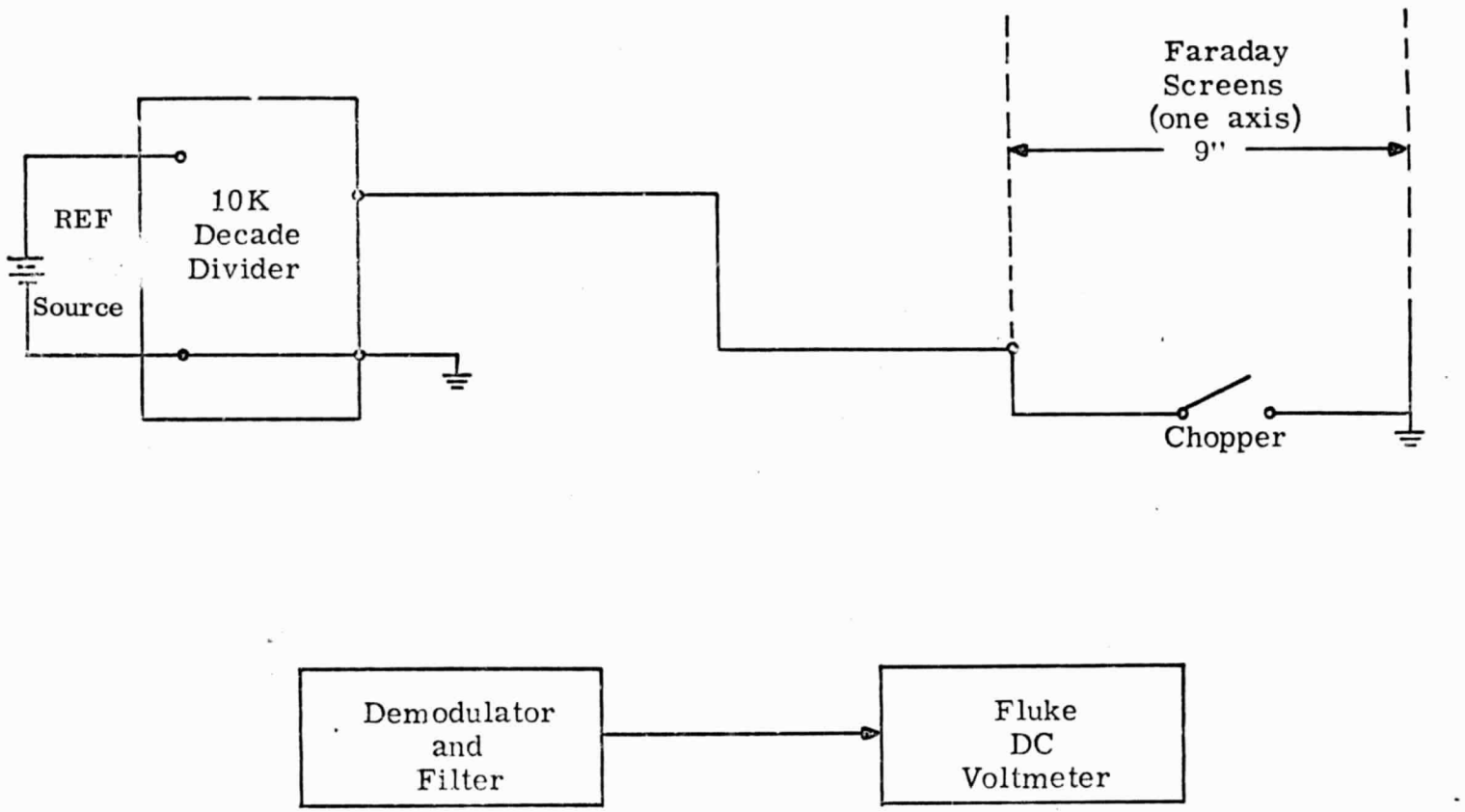

Figure 17 : Scale Factor Measurement

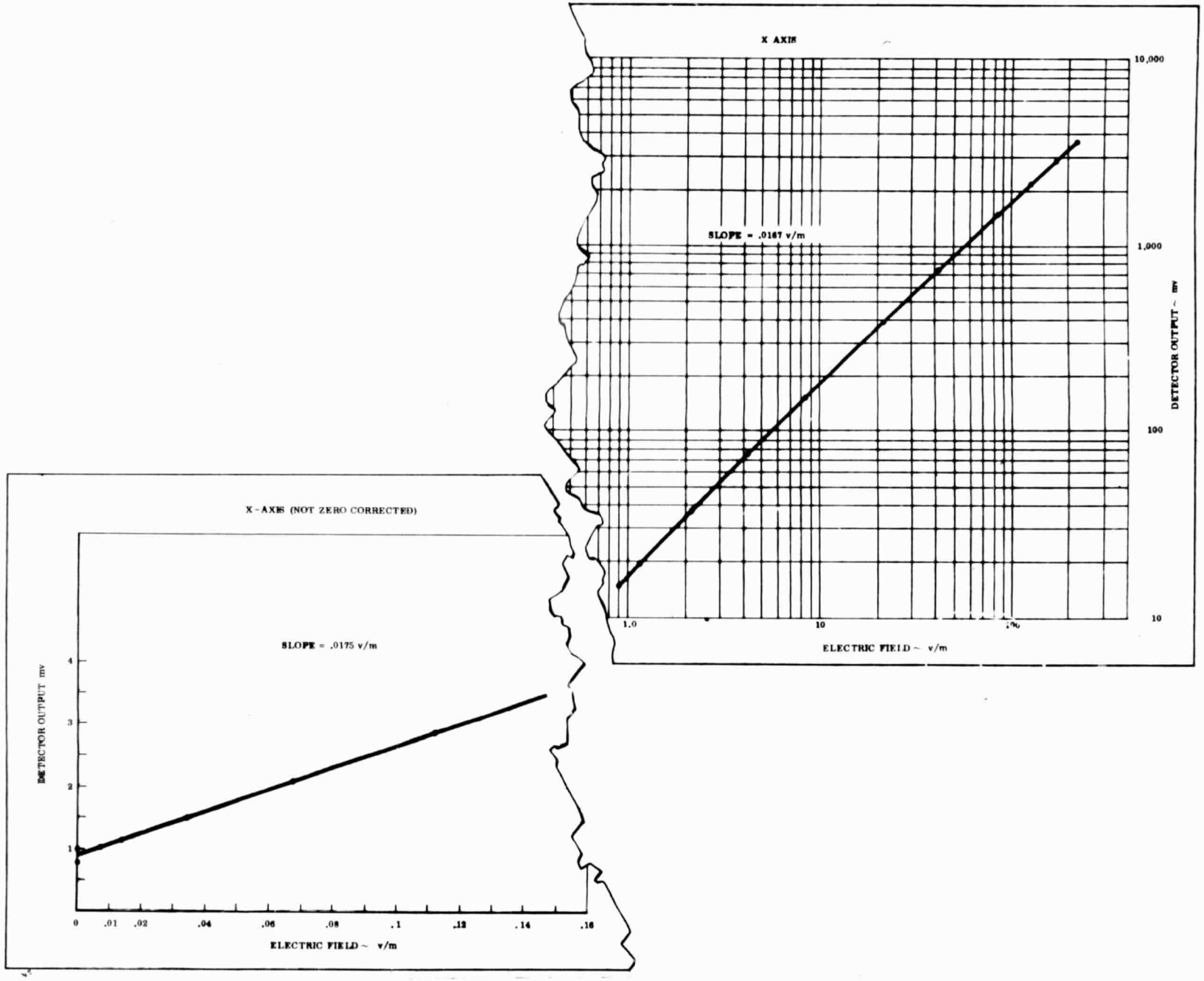

Figure 18: Electric Field Meter Response - X Axis

PRECEDING PAGE BLANK NOT FILMED.

SECTION IV
MISSION CONSIDERATIONS

A. MISSION CATEGORIES

The potential missions for which an electron beam deflection electric field meter would provide the required information can be divided in two categories:

1) Engineering or Housekeeping
2) Scientific or Survey

These measurement missions were briefly mentioned in the introduction of this report and are divided as follows:

1. Category I - Engineering or Housekeeping

   a) Electric fields associated with charge particulate contaminant clouds caused by the efflux of materials from a spacecraft. These clouds present a potential hazard to optical and electromagnetic experiments and observations required in performing the mission of the flight.[20]

   b) Electric fields which are associated with the plasma sheath which surrounds the spacecraft. These electric fields are associated with the charge separation which occurs within the sheath, and correlate with experiments modifying the sheath as well as the sheath's influence upon experiments.[21 thru 23]

   c) Large charged bodies moving within the magnetosphere experience reaction force. Part of this force is caused by the charged body moving through the ambient electric fields that exist within the ionosphere. This force can produce drag and moments on the charged bodies.[24-36]

   d) In the lunar space environment, the ambient electron density and particle density are extremely low. Thus, during the rendezvous and docking of the Lunar Excursion Module with the orbiting

spacecraft, electric fields may exist. The electric field survey of the space between these vehicles would provide confidence that no hazardous situation exists.[37]

2. Category II - Scientific or Survey:

a) There is evidence both theoretical and measured that electric fields exist within the ionosphere. The variation of these fields are attributed to or are the cause of various phenomena observed within the ionosphere and magnetosphere. A survey of this field as extensive as the surveys of the magnetic field will provide the required information to better understand the earth's environment. Surveys taken on long duration missions covering different altitudes, light conditions, seasons, and solar wind conditions will provide the basis for improved models of magnetosphere-solar wind interactions, auroral display, red arc occurrence, and equatorial jet phenomena. Space weather predictions will also be aided, as well as providing another means of observing nuclear explosions in space.

b) Specific sounding rocket measurements within or above auroral displays will provide correlation of the electric field measurements performed by various electrostatic potential probes and barium vapor cloud experiments.

B. MISSION CONCEPTS

The intrinsic values of the electron beam electric field meter are:

- Wide dynamic range (five orders of magnitude),
- Sensitive to weak fields (10 millivolts/meter field measured with a sensitivity of ± 1 millivolt/meter),
- Non-interaction sensing element (less than 1 microampere electron beam).

These attributes permit the meter to be versatile, capable of performing the various missions previously mentioned.

With the exception of the sounding rocket experiments, all other missions could be performed sequentially on a multipurpose spacecraft such as the AAP workshop. The use of extensible boom and multiple meters will permit the performance of the various experiments by the placement of the meters at the appropriate positions to measure the associated electric fields.

1. Category I - Engineering or Housekeeping Missions:

a. Charged Contaminant Cloud Electric Fields

One of the most serious problems that faces optical missions is the generation of particulate clouds. The probability that these obscuring clouds are charged due to photoemission or the efflux process is reasonably strong. Thus the measurement of electric fields between the spacecraft and the clouds in the vicinity of optical ports provide an indication of the formation of these charged clouds. The correlation of the electric field measurements and the consequences of various avoidance and removal techniques that will be developed to alleviate the contaminant problem provide a means to develop and evaluate these techniques.

The electric field that will prevail between the spacecraft and the cloud is dependent upon the relative difference of their charges, their respective geometries, the distance between them and the conductivity of the media between them. An estimate of the range of electric field from 10 millivolts/meter to 100 volts/meter includes a wide variety of combinations of these parameters. The possible distance over which the fields exist from just outside the plasma sheath to within 5 body radii from the spacecraft provides a measuring range that includes most of the possible cloud-spacecraft geometries. Beyond this range, the cloud should diffuse sufficiently so as not to represent an optical problem.

b. Sheath Interaction Electric Fields

The analysis presented in Section II of this report discusses the electric fields associated with the plasma sheath surrounding the spacecraft. Fields across this sheath vary from 1 volt/meter to 1000 volt/meter depending upon the altitude of the vehicle within the ionosphere, the degree of photoemission, and the position of the station at which the field measurement is being made relative to the

velocity direction. The measurement of unperturbed sheath fields is necessary to provide a basis to determine the additional fields due to charge contaminant cloud formation.

In addition the plasma sheath is disturbed by the efflux of charged particles from the surface and the performance of electromagnetic experiments aboard the spacecraft. Finally, the plasma sheath can interfere with experiments being conducted aboard.

The measurement of the electric fields on the surface and in the near vicinity of the spacecraft provides data of the environmental field and its variation. Correlation of these variations with the data obtained by the other experiments aboard provides a better understanding of the phenomena they are observing.

c. Forces and Moments Due to Ionospheric Electric Fields

The observed decay rates of vehicles orbiting with the ionosphere do not correlate well with density measurements. Residuals in the mean motion have been equated to unknown variations in the atmospheric density via the relatively well-quantified aerodynamic forces. A charged body moving through an ambient electric field experiences an electrodynamic force. This force can contribute to orbit decay and, when taken into account as a perturbative influence, can lead to a reassessment of the inferred spatial and temporal variations in ionospheric density. For example at an altitude of 1300 km the aerodynamic force on a 1 meter radius sphere is about 10^{-9} newtons, while the electrodynamic force is of the same order of intensity.

Thus a mission designed to measure the electrodynamic force will provide the first complete set of data from which electrodynamic drag may be directly inferred. Future space programs will benefit by providing a more complete specification of the force and moment environment.

The electrodynamic force requires the measurement of the ambient electric field (E_∞) and the surface electric field (E_S). When the distortion from

spherical symmetry of the plasma sheath is considered, the reaction force experienced by a spherical body is:

$$\bar{F} = -2\pi \epsilon r^2 (\bar{E}_S \cdot \bar{n})\bar{E}_\infty \text{ Newtons}$$

where:

- r is the body radius in meters
- E_S is the surface electric field in volts/meter
- n is the outward directed surface normal
- E_∞ is the ambient ionospheric electric field in volts/meter
- ϵ is the electric permittivity of the media in farads/meter

The performance of this mission requires a surface electric field meter and an ambient electric field meter. The ambient electric field approximately exists beyond a distance of 5 body radii from the spacecraft. The decay of the spacecraft electric field depends upon the ionospheric parameters and the geometry of the spacecraft. In Section II of the report the decay of the electric field is discussed. This choice of 5 body radii from mission flown between 200 km and 2000 km altitude, assures degradation of spacecraft fields sufficiently below ambient field levels.

The range of electric field values are:

Surface Electric Field:	from 1 volt/meter up to 1000 volts/meter
Ambient Ionospheric Electric Fields:	from 10^{-2} volts/meter up to 1 volt/meter

The precision with which the electrodynamic force is determined depends upon the number of surface field measuring stations that are used. Each measurement results in a local reaction force; if sufficient measurements are made around the spacecraft, the integrated force acting upon the spacecraft can then be determined.

d. Electric Fields During Rendezvous in a Lunar Environment

The differential charge build-up of an excursion module on the lunar surface for periods up to two weeks in the sun, as compared to the orbiting spacecraft which is alternately in the dark and light present a potential hazard during

rendezvous. Since the environment is of extremely low density, charges do not redistribute rapidly. Thus excessive charge located on the excursion module may exist during rendezvous. An electric field monitor examining the space between the two vehicles can warn of a potentially dangerous field which exists. Shorting rods can then be applied to neutralize the charge difference permitting the docking maneuver to proceed. The wide dynamic range of the meter permits the observation of the build-up of the electric field over large distances, thus allowing sufficient time to take corrective action.

2. Category II - Scientific or Survey Missions:

a. Ambient Electric Field Survey Within the Ionosphere

The electric field ambient within the ionosphere has been measured to vary from less than 10 millivolts/meter to slightly greater than 100 millivolts/meter. The electric field is maximum perpendicular to the magnetic field lines due to the tensor conductivity of the ionosphere, and is generally directed toward the equator.

The weak electric fields, the ionization of the environment, and the apparent electric field due to the motion of the instrument through the magnetosphere have made measurements of these fields extremely difficult.

The design of the electron beam electric field meter considered the sensitivity and plasma wake requirements as previously discussed, while the apparent electric field is considered in the following sections with regard to the demands placed upon the spacecraft attitude resolution requirements.

b. Sounding Rocket Exploration of Auroral Electric Fields

Many experimenters have flown near vertical sounding rocket flights in the auroral display regime with a variety of electric field measurement devices. The choice of the vertical flight is the near cancellation of the apparent $(\bar{v} \times \bar{B})$ field due to the motion through the magnetosphere. There is general correlation of the range of intensity and direction of the electric field during an auroral display.

The electron beam field meter would provide measurements which could be compared with those of many instruments and techniques that have been used to examine the electric fields.

C. METER CONSTRAINTS

The use of the electron beam electric field meter within the ionosphere is restricted by various environmental considerations. These constraints include the following:

- Orientation of the meter to the flow field
- Location of electron beam relative to physical structures
- Meter measures two orthogonal field components
- Outgassing, secondary emission and photoemission influence on the electron beam parameters
- EMI and RFI caused by the device or within the environment.

Thus a mission definition phase includes these constraints in the development of a mission program.

1. Orientation of the Meter to the Flow Field:

In Section II of this technical report the analysis of the influence of the flow field and plasma sheath upon the electric field being measured is discussed. The significant aspect of this study was that the orientation of the meter must be such that the electron beam is in a plane perpendicular to the flow field. An allowable variation of $\pm 30°$ from this position is computed, thereby reducing the attitude control requirement of the spacecraft to easily attainable limits.

This orientation assures that the wakes of the components of the meter do not intersect the beam, thereby maintaining the ambient electric field intensity along most of the path of the beam.

2. Location of the Electron Beam Relative to Physical Structures:

The electron beam field meter should be located at least 5 body radii from the spacecraft for ambient field measurements to assure that the electric fields associated with the plasma sheath about the craft do not distort the ambient field. However, when plasma sheath field measurements are being made the device is located as close as possible to the surface of the spacecraft.

The Faraday cage which surrounds the electron beam is located 10 cm from the electron beam. The wire composing the cage is 0.05 mm in radius. Thus the beam is located in excess of 1000 wire radii away from the cage. Negligible field distortion will result due to the introduction of the Faraday cage, providing that the orientation of the device to the flow field is maintained.

3. Meter Measure Two Orthogonal Components of the Electric Field:

Since the forces produced by electric field components along the electron beam do not produce beam deflection, the device responds to only two of the three components of the electric field vector.

Thus to measure all three components of the electric field, two possibilities exist:

(a) Use two meters, orthogonal to each other, and located in the plane perpendicular to the flow field.

(b) Rotate the vehicle, using one meter which lies in the plane perpendicular to the flow field.

The use of the two meters permits redundancy in the measurement of the electric field component parallel to the flow field, thus permitting correlation of readings.

4. Outgassing, Secondary Emission and Photoemission Effects:

During the mission various phenomena will change the ambient properties of the ionosphere. Three of these are:

- Outgassing
- Secondary Emission
- Photoemission for surfaces.

Each of these must be considered to assure proper design of the meter and interpretation of the measurement.

a. Outgassing

The efflux of waste material and gases will raise the ambient pressure in the vicinity of the vehicle. An electron beam traversing a region of increased pressure will experience additional collisions. These collisions will cause an attenuation of the beam electron density by scattering. Since the number of ion pairs produced is directly related to the beam current, the use of a one microampere or less beam assures that the number of ion pairs produced is not excessive for reasonable pressure rises. It would be advantageous to raise the acceleration potential of the electron gun, as this would also reduce the ions produced; however, as the beam voltage rises, the beam is less sensitive to the electric field. A parametric study indicated that an operation voltage between 300 - 500 volts would optimize the device.

(1) Electron Beam Interaction with the Environment

The electron beam collides with gas particles along its path, two results of these collisions are the reduction of beam current at the target and the production of ions and electrons.

(a) Beam Current Reduction Due to Collisions

The electron beam must traverse up to 20 cm path length through the environment. The reduction in beam current can be estimated as a function of gas pressure, beam voltage, and path length.

If we assume that ion focusing and space charge spread are negligible, then the spatial rate of change of beam current along its path is given by

$$\frac{dI}{dz} = -\mu\rho I$$

or

$$\ln \frac{I'}{I_o} = -\mu \rho z.$$

The logarithmic decrement of beam current (μ) is given by [38]

$$\mu = \frac{7.4 \times 10^9}{V} \text{ cm}^2/\text{gm}$$

for diatomic gases such as O_2, N_2. Where V is beam voltage in volts.

For the range of voltage of interest for the meter, μ is

V(volts	300	400	500	600	700
μ (cm^2/gm)	2.48×10^7	1.86×10^7	1.48×10^7	1.24×10^7	1.06×10^7

The gas density as a function of pressure at 300°K is

pressure(mm of Hg)	10^{-4}	10^{-5}	10^{-6}
ρ (gm/cc)	2×10^{-10}	2×10^{-11}	2×10^{-12}

The percentage of beam current that reaches the target located 20 cm from the electron source is shown in Table I.

Table I. Reduction in Beam Current Due to Scattering

Pressure (mm) / (volts) Voltage	10^{-4}	10^{-5}	10^{-6}
300	80.0%	97.7%	99.7%
400	84.0%	98.3%	99.8%
500	87.1%	98.6%	99.9%
600	89.1%	98.8%	99.9%
700	91.2%	99.1%	100 %

The temperature of 300°K would represent outgassing particles from a manned spacecraft. The space ambient temperatures would rise up to 1400°K, this would further reduce the mass density corresponding to the local pressure. Thus using 300°K provides the most severe beam attenuation for a given pressure. Since it is doubtful that the ambient pressure would rise 2 or more orders of magnitude, beam reduction due to scattering does not appear to be a problem.

(b) Environment Modifications Due to Electron Beam and Gas Interaction

The electron beam will collide with the outgassing particles and produce ions along its path length. The number of ions produced by the beam in a diatomic gas was found empirically to be [39]

$$N = \frac{3.75 \times 10^{23} I p}{V} \quad \text{ions/cm-sec.}$$

where

I is the beam current in amperes

p is the ambient pressure in mm of Hg

V is the beam voltage in volts.

The ion production rate per cm of path length, assuming an ambient pressure of 10^{-5} mm of Hg per microampere of beam current is

Beam Voltage (volts)	300	400	500	600	700
N(#/cm-sec	1.25×10^{10}	9.3×10^{9}	7.5×10^{9}	6.25×10^{9}	5.3×10^{9}

These ion-electron pairs are produced along the electron beam, and are scattered to fill the volume. If we neglect loss rates such as recombination and attachments, the electron density in an arbitrary volume around the beam can be estimated, providing we know the dispersion rate.

The electrons produced upon the ionizing collision will have their velocities reduced by the coulombic forces of the surrounding ions. These ions will slow the electrons down to approximately the ion thermal velocity. The ions produced by the beam will see a negative potential well in the center of the beam and will drift into the beam, this will partially neutralize the space charge spread of the beam.

The electron density in the vicinity of the beam is

$$n = \frac{NL}{\sigma v_e} \text{ electrons/cc}$$

where

- L is the path length (cm)
- σ is the area of the arbitrary cylinder (cm^2)
- v_e is the velocity of the scattered electrons (3×10^4 cm/sec)

The current density of these scattered electrons across a surface is given by:

$$J = ne\, v_e = \frac{eN}{2\pi r}$$

where

- r is the radial distance from the beam to the surface
- e is the electronic charge

Table II shows these relationships as a function of pressure for a 600 volt electron beam having 1 microampere of current, 1 millimeter in diameter and 20 cm long.

Photoemission current densities in the order of 10^{-9} amp/cm are reported by Whipple[40] on Nike-Apache rockets at an altitude of 160 km. Since N, n, and J are linearly dependent on the beam current, Table II can be used for any beam current. Using a one microampere electron beam, the environment is not significantly altered for rise in neutral particle densities up to 3×10^{11} particles/cc and beam location as close as 1 cm to the vehicle surface. Higher current beams must be located sufficiently far from surfaces, so that the ions they produce are dispersed.

REPRODUCIBILITY OF THE ORIGINAL PAGE IS POOR;

Table II: Electron Beam Influence Upon the Environment

Neutral Environment			N #ion/cm-sec.	n e/cc			J amperes/cm^2		
n_o $\frac{\#}{cc}$	Alt. Equiv. n_e ambient	Pressure at 300°K mm of Hg		r = 1 cm	r = 10 cm	r = 100 cm	r = 1 cm	r = 10 cm	r = 100 cm
3×10^{11}		10^{-5}	6.25×10^{9}	5×10^{4}	5×10^{3}	5×10^{2}	10^{-10}	10^{-11}	10^{-12}
3×10^{10}	200 km 10^{5} e/cc	10^{-6}	6.25×10^{8}	5×10^{3}	5×10^{2}	5×10^{1}	10^{-11}	10^{-12}	10^{-13}
3×10^{9}	300 km 10^{6} e/cc	10^{-7}	6.25×10^{7}	5×10^{2}	5×10^{1}	5	10^{-12}	10^{-13}	10^{-14}
3×10^{8}	400 km 5×10^{5} e/cc	10^{-8}	6.25×10^{6}	5×10^{1}	5	5×10^{-1}	10^{-13}	10^{-14}	10^{-15}
3×10^{7}	600 km 10^{5} e/cc	10^{-9}	6.25×10^{5}	5	5×10^{-1}	5×10^{-2}	10^{-14}	10^{-15}	10^{-16}

b. Secondary Emission

The electron beam striking the collecting plate creates secondary emission of electrons, which would cause the ambient electron density to rise if they were allowed to escape. In addition, the secondary electrons effectively reduce the current being used to drive the nulling loop.[41]

Thus, a screen mesh located close to the target with a repelling voltage of 90 volts, assures that most of the secondaries return to the target. Thus, the ambient electron density is not appreciably changed and sufficient current is available to drive the loop.

c. Photoemission and Charge Particle Fluxes

Various mechanisms exist in the ionosphere for the production of charged particle fluxes. Thus in the design of the instrument it was necessary to allow for the change of the ambient flux density which is distributed uniformly across the surface of the segmented collector plate. The technique of measuring the differential current caused by the deflection of a less than 1 mm diameter electron beam which is continually nulled to the center of the target plate, permits fluxes of greater than 10 microamperes to occur without saturating the differential amplifier. Whipple[40] reports that characteristic photoemission current density is about a nano-ampere per square centimeter. A target plate of one square cm would have a negligible current rise due to incident flux, permitting the differential amplifier to operate normally.

d. EMI and RFI

There are two aspects of EMI and RFI; (1) that which is produced by the device, (2) that which is produced by the environment which limits the usefulness of the device.

(1) EMI and RFI of the Device

Considering each component separately, it is possible to establish the devices EM or RF produced environment.

(a) Electron Gun

The electron gun has a directly heated filament which for the laboratory model is pure tungsten. It uses D.C. current of 3.6 amperes and voltage of 3 volts. The filament lead wires are twisted, thus magnetic fields are cancelled.

The accelerating potential is 500 volts D.C. and the focussing screen potential is 120 volts D.C. The electrostatic shielding of the gun structure eliminates static electric field from the environment.

The electron beam is less than one microampere and travels 18 cm to the target. The magnetic field produced is approximately:

$$B = \mu_o I/2\pi r \quad \text{weber/m}^2$$

where

$r = 5 \times 10^{-4}$ meters

$I = 10^{-6}$ amperes

$\mu_o = 4\pi \times 10^{-7}$ henry/meter

Thus, the magnetic field produced by the beam at its surface is approximately 10^{-10} webers/meter^2.

The chopper is electromechanical and thus has a small noise EMI spectrum about its 400 cps rate. This power spectrum will be insignificant after encasing within the read-out chassis.

(2) EMI and RFI of the Environment

Since the device is designed to measure electric fields both static and slowly varying, externally produced electric or magnetic fields would disturb its readings. However, since the measurements are highly filtered around the chopping frequency, rapidly varying fields will be discriminated against. Magnetic fields of any nature are discriminated against by the operation of the Faraday cage.

Elimination of the disturbance of static or slowly varying electric field is obtained by either physical separation or orientation of the device with respect to the source. A constant background electric field can be normalized out of the measurements.

D. ATTITUDE RESOLUTION REQUIREMENTS

Since the electric field meter is located aboard a spacecraft moving relative to the magnetosphere the electric field ($\bar{E}'$) measured by the meter exists only in the reference frame moving with it.[42] It is therefore necessary to transform this field to a frame fixed relative to the earth, since this is the ambient electric field ($\bar{E}$) within the ionosphere. Where $\bar{E} = \bar{E}' - \bar{V}_s \times \bar{B}$.

In order to accomplish this transformation it is necessary that the following be measured:

- Vector ambient magnetic field relative to the spacecraft,
- Velocity of the spacecraft relative to the earth,
- Attitude of the spacecraft relative to the frame of reference fixed to the earth.

1. Requirements for Resolution of Attitude Measurements:

The velocity vector of an orbiting vehicle can be determined to better than one part in 10^5 by ground tracking. However, it is necessary to know the attitude of the vehicle relative to the inertial frame to use this velocity measurement in computing the ($\bar{v}_s \times \bar{B}$) field acting on the vehicle. The local magnetic fields are measured by on-board three axis magnetometers. The velocity vector can be related to the satellite reference frame using the attitude measurements. In this frame the electric field measurement is made.

We can examine the requirement upon the attitude measuring system for a given error in the determination of the ($\bar{v}_s \times \bar{B}$) field. This component of the measured electric field consists of the following terms:

$$\bar{e} + \Delta\bar{e} = (\bar{v}_s \times \bar{B}) + (\bar{v}_s \times \Delta\bar{B}) + (\Delta\bar{v}_s \times \bar{B}) + (\Delta\bar{v}_s \times \Delta\bar{B})$$

where

$\Delta\bar{B}$ is the error in the measurement of B

$\Delta\bar{v}_s$ is the error in the velocity due to the error in measurement of the vehicle attitude.

The error terms can be examined separately, and the last term on the right hand side can be neglected because of smallness. Thus the error is:

$$\Delta\bar{e} = (\bar{v}_s \times \Delta\bar{B}) + (\Delta\bar{v}_s \times \bar{B})$$

The maximum error occurs when $\Delta\bar{B}$ is perpendicular to $\bar{v}_s$ and $\Delta\bar{v}_s$ is perpendicular to $\bar{B}$ simultaneously. From this the $|\Delta v|$ error can be related to the other terms as:

$$|\Delta v_s| = \frac{|\Delta e| - |v_s \Delta B|}{|B|} \text{ meters/second}$$

and the attitude measurement error permissible is:

$$\Delta\alpha = \frac{|\Delta v|}{|v|} \text{ milliradian.}$$

Table III lists the required attitude accuracy in radians of arc for orbital velocity of 7.5×10^3 meter/second upon assumed errors in measuring the magnetic field and desired accuracy of determining the $(\bar{v}_s \times \bar{B})$ field. This is based on the maximum error, thus the accuracy of $(\bar{v}_s \times \bar{B})$ will be better most of the time. The maximum magnetic field is assumed to be 0.4 gauss (4×10^{-5} webers/m^2).

This table shows the most severe requirements on the attitude measuring system. It shows the range from the most precise measurement of about 0.1 milliradian (roughly to within 20 seconds of arc) to a rather crude measurement of 25 milliradians (roughly 1.5 degrees of arc). Therefore system sensitivity can be estimated based upon the accuracy of the magnetometer measurements, resolution of the attitude measurement, and the acceptable error in the $(\bar{v}_s \times \bar{B})$ determination.

Table III - Required Attitude Resoltuion (Milliradians)

Δe (millivolts/meter) \ ΔB (milligauss)	0.5	1	2.5	5
0.4	0.88	--	---	---
0.8	1.4	0.17	---	---
2.0	5.4	4.2	0.8	---
4.0	12.0	10.8	7.5	0.8
8.0	26.0	24.0	21.0	14.0

2. Component of Electric Field Parallel to the Magnetic Field:

It is possible to determine the component of the electric field which is parallel to the magnetic field without knowledge of the spacecraft attitude in an inertial frame of reference. The two aspects of this technique which reduce its value are:

(a) Since the conductivity of the ionosphere is anisotropic, the electric field sustained parallel to the magnetic field is in the order of 100 times less than the electric field perpendicular to the magnetic field.

(b) Knowledge of the parallel and perpendicular components of the electric field do not completely define the field orientation.

However, for completeness the following analysis is included:

$$\bar{M} = \bar{E} + \bar{v} \times \bar{B} \qquad (26)$$

where

M is the electric field as measured by the instrument (V/m)

E is the ambient electric field (V/m)

B is the local magnetic field (web/m^2)

v is the vehicle velocity (meters/sec)

The apparent electric field due to the electron velocity relative to the magnetic field is eliminated by the Faraday cage technique used with this instrument described in Section III of this report.

Now if the scalar product is taken with the magnetic field and the measured electric field we have:

$$\bar{B} \cdot \bar{M} = \bar{B} \cdot \bar{E} + \bar{B} \cdot (\bar{v} \times \bar{B}) \tag{27}$$

since, $\bar{B} \cdot (\bar{v} \times \bar{B}) = 0,$

$$\bar{B} \cdot \bar{M} = \bar{E} \cdot \bar{B}$$

Thus, $$E_{\parallel} = \frac{\bar{E} \cdot \bar{B}}{|B|} = \frac{\bar{M} \cdot \bar{B}}{|B|} \tag{28}$$

where $E_{\parallel}$ is the electric field component parallel to the magnetic field.
In terms of the three directional field components $M_1 M_2 M_3$ (measured in a satellite fixed coordinate system) and of the three field components $B_1 B_2 B_3$ measured by magnetometers directed along the same vehicle axes, one obtains for Equation (28):

$$E_{11} = \frac{M_1 B_1 + M_2 B_2 + M_3 B_3}{(B_1^2 + B_2^2 + B_3^2)^{1/2}} \tag{29}$$

Thus, E_{11} can be measured without recourse to measurement of velocity V or of vehicle attitude angles.

An error analysis of Equation (29) has been made. Table IV gives typical results of the accuracy of E_{11} (in millivolts/meter) based upon assumed errors in individual measurements M and magnetic field measurement errors. Thus, if each component of M is measurable to 1 mv/meter the parallel field E_{11} may be calculated to the same accuracy if magnetic components are known to 0.5 milligauss (50 gamma) or better.

Table IV. Error in E_{11} (millivolts/meter)

error in individual components of M, millivolts/meter	Error in B (milligauss)	0.5	1	2.5	5.0
	0.4	0.53	0.81	1.81	3.56
	0.8	0.87	1.07	1.94	3.62
	2.0	2.0	2.12	2.67	4.06
	4.0	4.0	4.06	4.36	5.34
	8.0	8.0	8.03	8.2	8.75

3. Magnetic Field Measurement Requirements:

Whenever the error due to the vehicle motion is excessive with respect to the electric field being measured, it is necessary not only to know the vehicle velocity and attitude, but also the magnetic field.

Thus, a three axis fluxgate magnetometer is a necessary associative meter to fully reduce the data collected by any electric field meter on an orbiting spacecraft moving relative to the magnetosphere.

The fluxgate magnetometer responds to all magnetic fields. Internal magnetic fields generated aboard the spacecraft decay as the inverse cube of the ratio of the distance to the meter and the radius of the spacecraft. Thus a magnetometer located 5 body radii from the spacecraft, permits internal magnetic fields which leak out to be as large as 0.5 gauss without jeopardization of the measurement of the ambient magnetic field for orbits between 200 and 2000 km altitude.

A three axis fluxgate magnetometer can be calibrated to have a precision of 1 milligauss for magnetic fields as large as 0.5 gauss. Its physical size is a cylindrical sensor of 50 cu. inches and an auxiliary power and read-out package of 75 cu. inches. Its total mass is 3 pounds.

4. Attitude Resolution Requirements for Specific Missions:

Since the magnitude of the electric field varies with each mission, the degree to which the attitude must be known also varies.

Assuming that the magnetic field components are each measured to an accuracy of 1 milligauss, the velocity of the vehicle relative to the earth is measured to better than one part in 10^5, and the orbit lies between 200 - 2000 km; it is then possible to assess the required attitude resolution requirements for the mission.

a. Category I - Engineering or Housekeeping

(1) Charged Contaminant Cloud Electric Fields

Since the range for this field is extremely wide (10^{-2} to 10^{2} volts/meter) which reflects our lack of knowledge of the phenomena, the range of attitude resolution is likewise wide.

To maintain an error less than 10% of the expected field value, the attitude resolution necessary to measure the minimum field expected is 40 seconds of arc, while the attitude resolution requirement for the largest field is in excess of 90° with errors less than 1% expected.

This range of attitude requirements from 40 seconds to over 90° indicates that with improved knowledge of the phenomena better predictions of attitude resolution accuracy will be obtained. These may well prove to present no problems to typical manned spacecraft systems.

(2) Sheath Interaction Electric Field

Since these fields are typically reasonably strong (from 10^{0} to 10^{2} volt/meter), the attitude resolution requirements are essentially non-existent. They range from 1.5° to over 90° of arc for less than 1% error in measurement.

(3) Forces and Moments Due to Ionospheric Electric Fields

For this mission two electric fields must be measured; the surface and the ambient electric field. Attitude resolution for surface field measurements were given in (2) above, while the range of ambient electric field values (from 10^{-2} to 10^{0} volts/meter) requires high precision of attitude resolution.

For ambient electric field attitude resolution requirement is for 40 seconds of arc for an error of 10% for the minimum field and 1% or better for the maximum field.

(4) Lunar Environment

Since the magnetic field in the lunar environment is significantly smaller than near earth, and since the range of electric fields (10^{-1} - 10^{3} volts/meter) indicate relatively strong fields, it is doubted that the ($\bar{v} \times \bar{B}$) contribution will represent a significant problem.

b. Category II - Scientific or Survey Missions

(1) Ambient Electric Field

The attitude requirement of 40 seconds of arc was discussed previously. This would assure an error less than 10% at the minimum field value and less than 1% at the maximum field value.

(2) Sounding Rockets

The use of the near vertical trajectory in the polar regions minimizes the ($\bar{v} \times \bar{B}$) problem when measuring the ambient electric field. The two reasons are:

- The vertical trajectory nearly cancels the ($\bar{v} \times \bar{B}$) contributions to the measurements of the ascending and descending legs.
- The magnitude of the ($\bar{v} \times \bar{B}$) contribution is small due to the low velocity and small angle between these vectors.

5. R.M.S. Error Analysis

In order to establish a reference frame on the vehicle, we shall consider the plane in which the vehicle velocity vector and the local magnetic field vector lie as the xy plane and the orthogonal direction to this plane as the z axis.

The magnitude of the vehicle velocity will be determined by ground radars. Accuracies better than one part in 10^5 can be obtained for orbiting vehicle velocities. Thus the length of this velocity vector can be assumed as known, while the errors in determining the attitude of the vehicle relative to an inertial frame create an error circle at the end of the velocity vector (assuming that all error angles are equally probable).

The magnetic field measurement has an error assumed to be equal in all directions, thus an error sphere is generated at the end of the magnetic field vector.

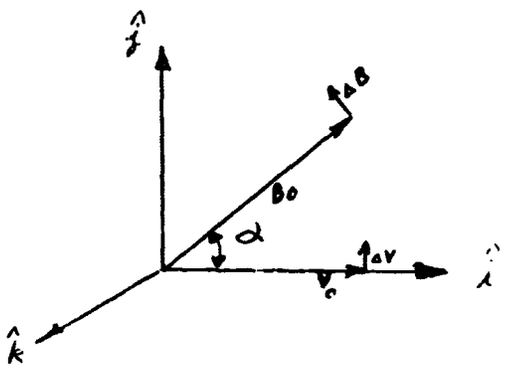

The direction error of the velocity vector is $\epsilon = |\Delta v| / |v_o|$ and the magnetic field error is $\delta = |\Delta B| / |B_o|$. Thus vectorially we have

$$\Delta\bar{v} = (\epsilon v_o)(\hat{j}\cos\beta + \hat{k}\sin\beta)$$

where β is the angle between the y axis and the $\Delta\bar{v}$ in the yz plane.

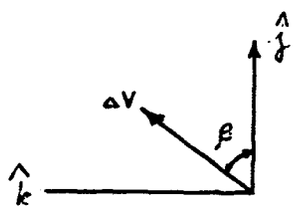

and

$$\Delta\bar{B} = (\delta B_o)\left[(\hat{i}\cos\varphi + \hat{j}\sin\varphi)\cos\theta + \hat{k}\sin\theta\right]$$

where φ is the angle between the x axis and the projection of the $\Delta\bar{B}$ on the xy plane and θ is the angle between its projection and the vector.

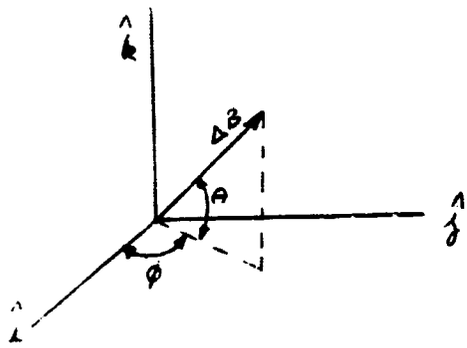

The expansion of the measured $(\bar{v} \times \bar{B})$ is then

$$\bar{v} \times \bar{B} = \bar{v}_o \times \bar{B}_o + (\Delta\bar{v} \times \bar{B}_o) + (\bar{v}_o \times \Delta\bar{B}_o) + (\Delta\bar{v}_o \times \Delta\bar{B}_o)$$

Neglecting the last term on the right hand side, we can determine the error in the measurement as;

$$\bar{\Sigma} = (\Delta\bar{v} \times \bar{B}_o) + (\bar{v}_o \times \Delta\bar{B}_o) = \epsilon v_o B_o \left[\hat{i}(-\sin\alpha \sin\beta) + \hat{j}(\cos\alpha \sin\beta) + \hat{k}(-\cos\alpha \cos\beta) \right]$$

$$+ (\delta v_o B_o) \left[\hat{j}(-\sin\theta) + \hat{k}(\sin\varphi \cos\theta) \right]$$

The square of the error is

$$\Sigma^2 = (\epsilon^2 v_o^2 B_o^2) \left[\sin^2\alpha \sin^2\beta + \cos^2\alpha \sin^2\beta + \cos^2\alpha \cos^2\beta \right]$$

$$+ (\delta^2 v_o^2 B_o^2) \left[\sin^2\theta + \sin^2\varphi \cos^2\theta \right]$$

This can be reduced to:

$$\frac{\Sigma^2}{v_o^2 B_o^2} = \epsilon^2 \left[(\cos^2\alpha + \sin^2\alpha \sin^2\beta) \right] + \delta^2 (\sin^2\theta + \sin^2\varphi \cos^2\theta)$$

By integrating over the angles, the average square (error) can be determined.

$$\langle \Sigma^2 \rangle = \frac{1}{4\pi^3} \int_0^{2\pi} \int_0^{2\pi} \int_{-\pi/2}^{\pi/2} \left[\epsilon^2 (\cos^2\alpha + \sin^2\alpha \sin^2\beta) \right.$$

$$\left. + \delta^2 (\sin^2\theta + \sin^2\varphi \cos^2\theta) \right] d\theta d\varphi d\beta$$

$$\langle \Sigma^2 \rangle = \epsilon^2(\cos^2\alpha + \frac{\sin^2\alpha}{2}) + \delta^2(3/4)$$

The r.ms error is then:

For $\alpha = 0°$ $\quad \Delta = \sqrt{\epsilon^2 + \frac{3}{4}\delta^2}$ (maximum error)

and

For $\alpha = 90°$ $\quad \Delta = \sqrt{\frac{\epsilon^2}{2} + \frac{3}{4}\delta^2}$ (minimum error)

The three axis fluxgate magnetometer is capable of an accuracy of 10^{-3} gauss. Assuming the maximum field is 0.5 guass; then δ is:

$$\delta = \frac{\Delta B}{|B|} = \frac{10^{-3}}{5 \times 10^{-1}} = 2 \times 10^{-3}$$

$$\delta^2 = 4 \times 10^{-6}$$

The attitude resolution requirement for a given maximum r.m.s. error then can be computed as:

$$\epsilon^2 = \Delta^2 - \frac{3}{4}\delta^2$$

Since accuracy of 1 millivolt/meter or better for an electric field due to $\bar{v}x\bar{B}$ of approximately 500 millivolts/meter; the r.m.s. error allowable should be less than 2×10^{-3}.

The attitude resolution for the maximum error to be 2×10^{-3} is:

$$\epsilon^2 = 10^{-6}$$

or

$$\epsilon = 10^{-3}$$

$$\epsilon = \frac{|\Delta v|}{v_o} \simeq \text{error angle (for small angles).}$$

This analysis indicated the attitude resolution on an r.m.s. error basis in 10^{-3} radians or about 4 minutes of arc.

6. Summary of $(\bar{v} \times \bar{B})$ Problem:

The discussion presented in this section was intended to point out a problem inherent with all electric field meters located aboard a spacecraft moving relative to the magnetosphere. The extent of the problem depends upon:

- The range of electric field values to be measured,
- The trajectory of the vehicle,
- The velocity of the vehicle,
- The precision to which the measurement must be made.

The accuracy of 40 seconds of arc indicated as the most severe requirement, is actually a greater restraint than will normally be required. This resolution requirement was derived for the case where the error in the velocity measurement was perpendicular to the error in the magnetic field measurement. This situation is extremely rare, and a minimum resolution requirement would more realistically lie between 1 and 2 minutes of arc, and the r.m.s. error analysis is less restrictive.

E. MISSION CONFIGURATIONS

Although there are many possible configurations we will consider two which encompass most of the missions:

- Multipurpose Mission aboard AAP workshop
- Sounding Rocket Ballistic Mission.

1. Multipurpose Mission

The choice of the AAP workshop as the spacecraft was based upon the following:

- Orbits exist between 200 - 2000 km.
- Attitude Resolution capabilities are excellent.
- Possibility of Astronaut operation of device.
- Surface extent sufficient for meaningful surface field measurements.
- Payload capacity.

- Optical charged cloud problem will probably exist.
- Many electromagnetic experiments will be performed modifying or being modified by the plasma sheath.
- Correlation of ambient electric field changes before, during and after solar flares.
- Extensive duration missions, providing an excellent survey of the electric field under many conditions. In addition, electrodynamical drag and moments will have sufficient time to accumulate to be significant.

a. Concept of Mission

Since there are many possible objectives for the electric field measurements, and many common attributes; the concept of a few meters at appropriate and variable locations which sequentially are used for different measurements has been adopted.

The minimum number of meters and their locations are as follows:

- One - surface electric field meter, electron beam oriented perpendicular to flow, located downstream from most EM experiments.
- Two - electric field meters mounted on extensible booms variable distance from surface to 5 body radii, electron beam oriented perpendicular to flow and orthogonal to each other.
- One - three axis fluxgate magnetometer mounted on boom 5 body radii in length.

The sequencing of measurements will permit time sharing of the limited number of meters available. Normal operation will have a duration of two minutes, and the frequency will be four time an orbit.

Mission	Meters Required	Expected Measured Values
Category I		
a. Charged cloud fields	A, B, C	10^{-2} to 10^{2} volts/meter
b. Plasma sheath fields	A	10^{0} to 10^{3} volts/meter
c. Forces and moments	A, B, C	10^{-2} to 10^{3} volts/meter
	(magnetic field (C))	(10^{-2} to 5 x 10^{-1} gauss)
Category II		
a. Survey	B, C	10^{-2} to 10^{0} volts/meter

where: meter A is the surface electric field meter,
meter B is the extensible boom mounted electric field meters,
meter C is the boom mounted magnetometer.

Each meter will normally operate 8 minutes per orbit. The life expectancy of the filament is over 500 hours; thus roughly 4,000 orbits or about 8 months operation can be expected from each meter. This will be reduced if the meters are placed in continuous operation mode to observe a charged cloud formation or dissipation; or to observe events for longer than two minutes during a solar flare.

The output of the meters will be a d.c. voltage (0 - 5 volts) suitable for either telemetry or recording or both. Each electric field meter requires 4 data read-out channels and 20 housekeeping channels; the magnetic field meter requires 4 data and 10 housekeeping channels. This is a preliminary estimate requiring about 90 channels when all meters are operative. During the experiment definition phase, redundancy will be eliminated and time sharing of channels will be considered, based upon the number of channels available for telemetry. Since the data can be read out after the measurement, the number of channels can be reduced to fit any specific flight mission plan. Standard IRIG telemetry sampling rates will be used and time standard will be the spacecraft clock.

b. Physical and Electrical Configuration

The spacecraft being considered is the AAP workshop whose body radius is about 3 meters and length about 15 meters. Thus the 5 body radii extensible boom has a maximum length of 15 meters. This boom will support either an electric field meter sensing head having a mass of one pound (this unit was shown in Figure 1) or a magnetometer head, also weighing one pound in cylindrical shape - 3 inches in diameter and 6 inches long. A design study to be conducted during the experiment definition phase will finalize the extensible control mechanism, the stresses allowable for the boom, and its load carrying capacity. A cable harness will connect the sensing heads of the meters to their respective housekeeping packages located within the spacecraft. The electric field housekeeping unit will have a mass of 2 pounds, cylindrical shape of 6 inch diameter, 6 inch length. The magnetometer housekeeping unit has a mass of 2 pounds, and cylindrical shape of 3 inches diameter and 10 inches in length. The total cable mass for each extensible harness is estimated at 5 pounds and the booms' mass is estimated at 10 pounds. The boom storage container will be a cylinder of 1 foot diameter and 0.8 feet wide. The booms will extend up to 15 meters in length and be 2 inches in diameter. The total payload mass is estimated as follows:

Unit	Quantity	Total Mass pounds (kg)	pounds (kg)
Electric Field Sensing Heads	3	3 (1.361)	3 (1.36)
Magnetometer Sensing Head	1	1 (0.454)	1 (0.454)
Electric Field Housekeeping Package	3 (if simultaneous)	6 (2.71)	-
	1 (if sequential)	-	2 (0.905)
Magnetometer Housekeeping Package	1	2 (0.905)	2 (0.905)
Extensible Boom Package	2 (if two E meters on same boom)		20 (9.05)
	3	30 (13.6)	-
Cable Harness	3	15 (6.6)	15 (6.6)
	max.	57 (25.8)	min. 43 (19.4)

( ) System International Units (kg)

Therefore a total payload weight between 43 to 57 pounds is extimated for the experiment.

The electrical power is assumed to be available from the spacecraft prime power, and only signal conditioning is included in the mass estimate. The housekeeping units will draw the power from the meter operations, and the boom extension package will draw the power during erecting and length variation procedure. The power drain is estimated as:

Unit	Quantity	Stand-by	Average	Maximum(watts)
Electric Field Meter	3	6	36	45
Magnetometer	1	1	1	2
Boom	3	0	1.5	3
Total power requirements:		7	38.5	50 watts

This power estimate is based upon a tungsten filament, which is being used in the laboratory breadboard. The total power requirement can be reduced by as much as 10 watts per electric field meter if oxide coated filaments are used. This would reduce the payload requirements to:

Power Requirements	Stand-by	Average	Maximum (watts)
Payload total	2	8.5	20

In summary the flight package including 3 electric field meters, 1 magnetometer, 2 or 3 booms with housekeeping and harnesses is estimated to have a mass of 43 to 57 pounds and an electrical requirement of 2 watts standby, 8.5 watts to 20 watts for operation. The conceptual sketch of the multi-purpose mission is shown in Figure 19.

2. Sounding Rocket Ballistic Mission

These flights provide a means of measuring the ambient electric fields during solar flares or auroral displays. Two ballistic launches of sounding rockets would be desirable. Since the magnetic field flux tubes terminate in the polar regions, a launch site such as Fort Churchill would be preferred. One launch will be accomplished during a quiet solar period and the other during active solar periods. A near vertical launch would permit the near cancellation of the $(\bar{v}_s \times \bar{B})$

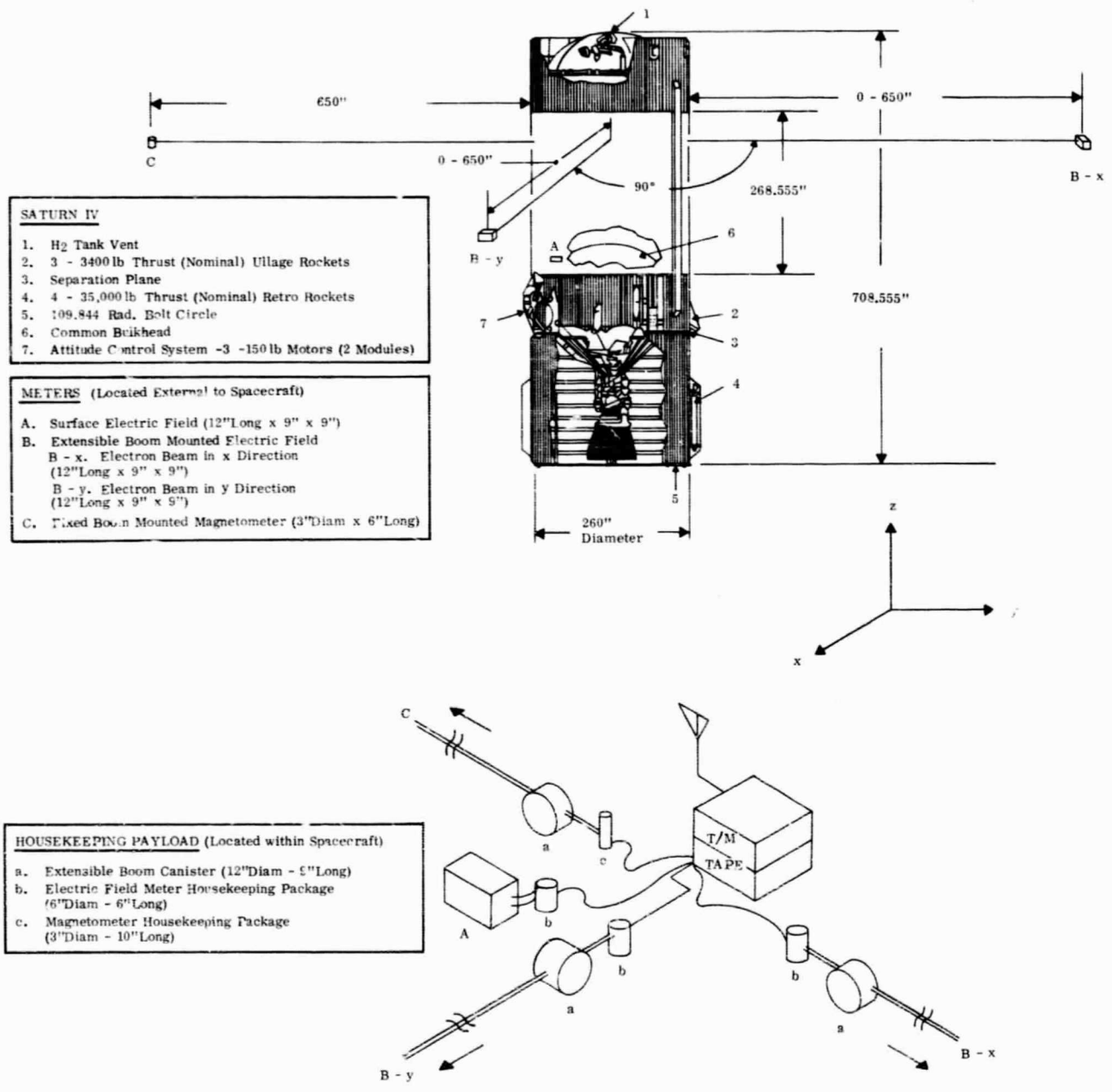

Figure 19: AAP Workshop Conceptual Configuration

electric field, thus the vehicle attitude and velocity need be known to moderate accuracy. The ambient vector electric and magnetic field, and the plasma to vehicle potential differences will be measured. The apogee will be in the order of 2000 km, and data will be telemetered to ground stations negating the need for recovery. The vehicle would be spin stabilized, thus only one electric field meter is required for the three components of the electric field.

The meter, aligned as shown in Figure 20 , will present minimum plasma sheath interference due to the component parts of the meter. The ambient electric field meter will be mounted on a folded boom which would extend at an altitude of 100 - 200 km and remain extended to re-entry. A symmetrical boom would house the three axis magnetometer. All systems would operate continuously from time of boom extension to re-entry. Data will be processed within the housekeeping payload and telemetered from the vehicle. Ground radars will track the payload throughout the flight.

a. Ballastic Flight Considerations

A near vertical launch in the polar region would reduce the magnitude of the $(\bar{v}_s \times \bar{B})$ field which perturbs the electron beam electric field measurement. In addition the symmetry of the ascent and descent of the payload permits approximate cancellation of the perturbing field from the data. However, to assure knowledge of the magnetic field vector during the flight it is recommended that a three axis fluxgate magnetometer, capable of resolving each magnetic field component to an accuracy of 1 milligauss, be mounted on a symmetrical folded boom to the electric field meter. The boom length would be about 5 feet depending upon the structural constraints of the payload. This distance assures the decay of the vehicle plasma sheath electric field to less than 1 millivolt/meter at the meter providing the meter is not in the vehicle wake, and requires the internal magnetic field of the vehicle to be less than one gauss for 1/2 foot radius housekeeping payload. The internal magnetic field is minimized by choice of materials, and placement of current carrying wires.

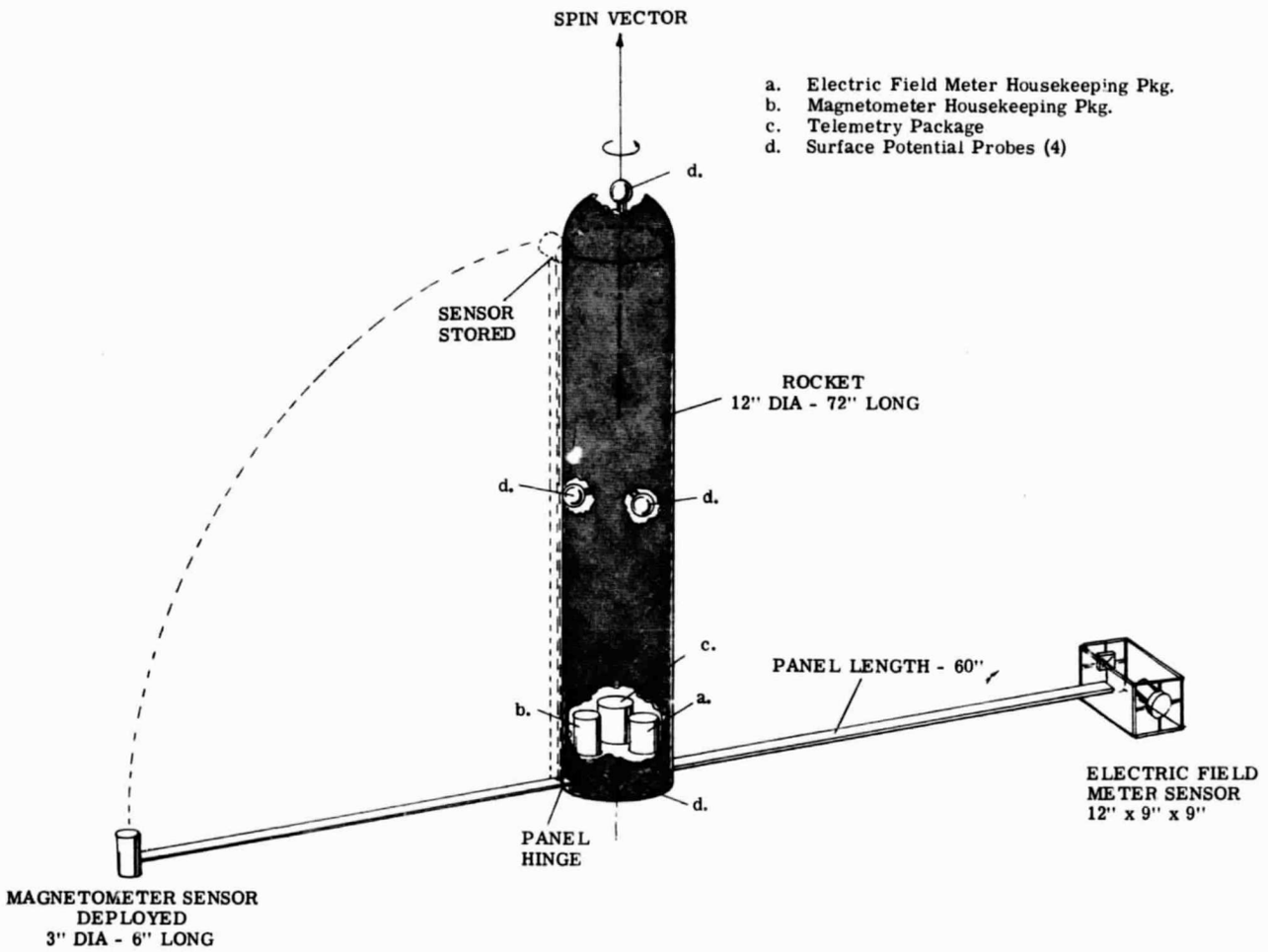

Figure 20: Sounding Rocket Conceptual Configuration

Spin stabilization is recommended as the simplest method to maintain attitude during the flight. However, the spin rate chosen must represent a compromise between the electron beam Faraday cage chopping rate, the number of E field samples per measurement integration, the time variation of the nutation of the payload, and the number of degrees rotation smear per measurement. For example, a spin rate of 10 r.p.m. would permit 30 samples at a 400 cps chopping rate and a vehicle rotation of 5 degrees during integration

Since the most important data is the ambient electric field vector relative to the magnetic field vector, precise knowledge of vehicle attitude at the time of measurement is not required. The modulation of the telemetered data due to vehicle nutation would provide sufficient attitude information for data reduction.

The electron beam for the ambient electric field meter will be fired in a direction perpendicular to the velocity vector. Providing that nutation angle is less than 30°, this orientation will assure that the beam is not in the wake of the components of the meter. If we let the velocity lie along the z axis, then the beam is in the x-y plane. Thus during rotation the components E_z and E_x and then E_z and E_y are alternately measured every 90° of rotation. By sampling every 5° it is possible to reconstruct the electric field vector during the measurement. The altitude change during each 5° measurement is about 1000 feet, decreasing as it nears the apogee. Electrostatic surface potentiometers will be placed at various locations on the payload to monitor the surface field changes. Due to the probable size of the housekeeping payload for the ballistic flight, it is doubtful that a surface field meter would be appropriate for this test.

b. Physical and Electrical Configurations

For this mission one electric field meter and one magnetometer with associated housekeeping packages, as well as two five foot booms with two cable harnesses and prime power batteries is required.

The mass estimate is:

Electric Field Sensor Head	1 pound	(0.4536 kg)
Electric Field Housekeeping Package	2 pounds	(0.906)
Magnetometer Sensor Head	1 pound	(0.4536)
Magnetometer Housekeeping Package	2 pounds	(0.906)
Harnesses (two)	2 pounds	(0.906)
Boom (two)	6 pounds	(2.72)
Batteries and mounts	10 pounds	(4.536)
Telemetry Transmitter	6 pounds	(2.72)
Total Payload Weight:	30 pounds	(13.6)

( ) System International Units (kg)

The electric power requirement is 12 watts for 30 minutes or 6 watt-hours.

F. IN-FLIGHT ELECTRIC FIELD METER OPERATION

After boom extension, the filament is allowed 1/2 minute warm-up prior to the application of the gun voltages. The amplifiers are normally in stand-by operation maintaining temperature and voltage stability. The electromechanical chopper is activated when filaments are being warmed-up. When the electron gun is fully operational, the Faraday cage is shorted (zero electric field), the electron beam is centered by the nulling voltages on the two axis deflection plates. The zero electric field voltage is recorded along with spacecraft time and attitude data. The sequencing of the chopped field calibration is started. The synchronous detector provides a d.c. voltage proportional to the electric field which is chopped by the intermittent application of the Faraday cage. The calibration of electric field versus output voltage will be initially performed on the ground. In flight calibration is accomplished by applying stepped known voltages at the chopping rate to the Faraday cage plates when they are not shorted together and recording the nulling voltages. After calibration, the normal operative mode occurs; the external electric field to be measured is chopped by the action of the Faraday cage and the d.c. output voltage of the two axis are stored for telemetry or recovery. The form of the output will be a 0 - 5 volt signal which can be used in standard telemetry.

A typical operation procedure is given below:

Typical Operation Procedure

1. Stand-by condition, amplifiers warm and stable,
2. Boom extension
3. Filament warm-up (1/2 minute); electromechanical chopper operative,
4. Gun voltages applied,
5. Faraday cage shorted (zero field calibration) d.c. output voltage of demodulator-filter is tored.
6. Faraday cage opened (electric field calibration), chopped voltages applied to two axis Faraday plates in turn, d.c. output and applied input voltages are stored for calibration to update ground calibration.
7. Normal chopped mode, Faraday cage is alternately created and removed, the d.c. output voltage of the demodulator-filter is stored.

In addition to the d.c. output voltage, the time of measurement, the attitude of the vehicle and the vector magnetic field are required to interpret the electric field measurements. These data must be telemetered with each reading.

REFERENCES

1. O'Brien, Brian, J., "The Magnetosphere and Auroras," Astronautics and Aeronautics, July, 1967, pp. 16-26.

2. Wildman, P.J.C , "A Device for Measuring Electric Fields in the Presence of Ionization," Jour. of Atom. and Terr. Physics, V. 127, No. 3, 417 (1965).

3. Kavadas, A., and Johnson, D.W., "Electron Densities and Electric Fields in the Aurora," Space Research IV, North Holland Publishing Co., 1964, p. 365.

4. Haerendel, G., Report of an electric field measurement using neutral gas and ionized barium clouds presented at the ESRO Conference in Stockholm, Sweden, 1965.

5. Fahleson, U., "Theory for Electric Field Measurements in the Magnetosphere with Electric Probes," Royal Inst. of Tech., Sweden, Report 66-02, Feb., 1966.

6. Shriver, E.L., "Investigation of the Deflection of an Electron Beam as a Means of Measuring Electric Field Strength," MSFC, NASA TX-53435, April, 1966.

7. Ya. L. Alpert, A.V. Gurevich and L.P. Pitaevski, "Space Physics with Artificial Satellites," Consultants Bureau, New York, (1965).

8. Kum-Min Chen in, "Interactions of Space Vehicles with an Ionized Atmosphere," edited by S.F. Singer, p. 465, Pergamon Press, (1965).

9. V.S. Chou, L. Talbot, and D.R. Willis, Phys. Fluids, Vol. 9, No. 11, p. 2150, (1966).

10. A.H. Davis and I. Harris, in "Rarefied Gas Dynamics," Proceedings of the Second International Symposium, Academic Press, (1961).

11. Pung Nien Hu and Sigi Ziering, Phys. Fluids, Vol. 9, No. 11, p. 2168, (1966).

12. R. Jastrow and C.A. Pearse, J. Geophys. Res., Vol. 62, p. 413, (1957).

13. R.E. Kiel and W.A. Gustafson, Phys. Fluids, Vol. 8, No. 8, p. 1531 (1966).

14. L. Kraus and K.M. Watson, Phys. Fluids, Vol. 1, p. 480, (1958).

15. T.G. Northrop, "The Adiabatic Motion of Charged Particles," Interscience Publishers, New York, (1963).

16. Lee W. Parker, NASA Contractor Report, NASA CR-618, October, 1966, also CR-401, March, 1966.

17. E. Wasserstrom, C.H. Su and R.F.Probstein, Phys. Fluids, Vol. 8, No. 1, p. 56, (1965).

18. G.L. Gdalevich and I.M. Imyanitov, in NASA Technical Translation, NASA, TT F-389, p. 367, (1966).

19. P.L. Bhotnager, E.P. Gross and M. Krook, Phys. Rev., Vol. 94, No. 3, p. 511, (1954).

20. McPherson, D.G., "ATM Contamination Study," NASA CR-61173, May, 1967.

21. F.T.F. Osborne, F.H.C. Smith, R.E. Barrington and Mather, W.E., "Plasma Induced Interference in Satellite v.l.f. Receivers," Canadian Jour. of Physics, Vol. 45, (1967), p. 47-56.

22. F.W. Crawford, R.S. Harp and Manter, T.D., "Pulsed Transmission and Ringing Phenomenon in a Warm Magnetoplasma," IEEE International Antennae and Propagation Symposium, 1966, Palo Alto, California.

23. F.W. Crawford and R. S. Harp, J. Geophys.Res., Vol. 70, p. 587, (1965).

24. Cook, G.E., "On the Accuracy of Measured Values of Upper-Atmosphere Density," J.G.R., Vol. 70, No. 13, (July, 1965).

25. Bryant, R., "Densities Obtained from Drag on the Explorer 17 Satellite," J.G.R., Vol. 69, (1964).

26. Newton, G.P., R. Horowitz, and W. Priester, "Atmospheric Density and Temperature Variations from Explorer 7 Satellite and Further Comparison with Satellite Drag," Planet. Space Sci., Vol 13, pp 599-616, (1965).

27. Friedman, M.P., "A Critical Survey of Upper Atmosphere Density Measurements by Means of Ionization Gauges," Smithsonian Inst. Astrophysical Observatory, Report No. 217, (July, 1966).

28. Nigam, R.C., "Effect of Atmospheric Oblateness on the Acceleration of Satellite," J.G.R., Vol. 69, No. 7, pp. 1361, (1964).

29. Drell, S.D., H.M. Foley and M.A. Ruderman, "Drag and Propulsion of Large Satellites in the Ionosphere," J.G.R., Vol. 70, No. 13, p. 313, (1965).

30. Grovers, G.V., "Atmospheric Densities Obtained from Satellite Orbits," Proc. of the First International Symposium on Rocket and Satellite Meteorology, p. 422-436, John Wiley & Sons, Inc., New York (1963).

31. Axford, W.I., and C.O. Hines, "A Unifying Theory of High Latitude Geophysical Phenomena and Geomagnetic Storms," Can. J. Phys., Vol. 39, p. 1433, (1961).

32. Megill, L.R., and N.P. Carleton, "Excitation by Local Electric Fields in the Aurora and Airglow," J. of Geoph. Res., Vol. 69, p. 101 (January, 1964).

33. Bostrom, R., "A Model of the Auroral Electrojets," J.Geophys. Res., Vol. 69, p. 4983-4999, (1964).

34. Atkinson, G., "Polar Magnetic Substroms," J. of Geophys. Res., Vol. 72, p. 1491, (March, 1967).

35. Manual on Rockets and Satellites, Berkner, L.V., Editor, Vol. VI, p.164-168, Pergamon Press, (1958).

36. Gurevich, A.V., and A.M. Moskalenko, "Braking of Bodies Moving in a Rarefield Plasma," Space Research, NASA TT F-389, p.322-341, (May, 1966).

37. M. Petschek, "Surface Electric Field Measurements," NASA SP-88, NASA Summer Conference on Lunar Exploration and Science, Falmouth, Mass., (1965).

38. Markevitch, B.W., and F.C. Hurlbut, "The Study of Electron Beam Attenuation in Air," University of California Report TR HE 150-142, (February, 1957).

39. Spangenberg, K.R., Vacuum Tubes, McGraw Hill, New York, (1948).

40. Whipple, Jr., E.C., "The Equilibrium Electric Potential of a Body in the Upper Atmosphere and in Interplanetary Space," NASA TM X-55368, Goddard Space Flight Center, (June 6, 1965).

41. Massey and Burhop, Electronic and Ionic Impact Phenomena, Clarendon Press, (1956).

42. F.T.F.Osborne and M.A. Kasha, "The v x B Interaction of a Satellite with its Environment," Canadian Jour. of Physics, Vol. 45, p. 263-277, (1967).

PRECEDING PAGE BLANK NOT FILMED.

APPENDIX I

FARADAY CAGE OPERATION IN THE IONOSPHERE

The proper operation of the Faraday Cage by electrically shorting and opening several sections of the cage necessitates certain requirements which may be stated as follows:

1) The electrically unconnected segments of the cage must not distort the ambient electric field at the location of the electron beam.

2) The electrically conducting plasma must not provide circuit closing equivalent to that in (3).

3) The electrically connected segments of the cage must provide a field free region at the location of the electron beam.

4) The external plasma must provide sufficient charge to the cage segments so that on disconnect, the charge distribution present before connection is restored. This must be accomplished within the allotted time.

We may investigate requirements (1) and (2) by considering the following problem. There are a number of conductors of finite extent immersed in a conducting medium of different conductivity. Far from the finite conductors and extending to infinity, there is a uniform electric field. Find the field everywhere in space.

Since the fields are stationary, we may assume them to be given by the negative gradient of a scalar potential Ψ. The following boundary conditions exist at the interface between the finite conductors and the infinite medium. First, the potential is continuous, or:

$$\Psi_i = \Psi_o \tag{1}$$

where the subscript i designates the interior of the finite conductors and o the exterior infinite medium. Since the normal component of the current density is continuous (this follows from the divergenceless character of the current density in steady state)

$$\sigma_i \frac{\partial \Psi_i}{\partial n} = \sigma_o \frac{\partial \Psi_o}{\partial n} \tag{2}$$

where σ is the electrical conductivity and $\partial \Psi / \partial n$ is the normal derivative. In both regions Laplace's equation is obeyed since:

$$\nabla \cdot j = \nabla \cdot \sigma \underline{E} = - \nabla \cdot (\sigma \nabla \Psi) = 0 \tag{3}$$

and in particular if σ is uniform.

$$\nabla^2 \Psi = 0 \tag{4}$$

It may be noted that for a dielectric immersed in a dielectric medium, Laplace's equation is also satisfied and the boundary conditions are:

$$\Psi_i = \Psi_o \tag{5}$$

$$\epsilon_i \frac{\partial \Psi_i}{\partial n} = \epsilon_o \frac{\partial \Psi_o}{\partial n} \tag{6}$$

where ϵ_i and ϵ_o are the interior and exterior dielectric constants. Hence, if we have the solution of a problem involving conductivities, then we also have the solution for dielectric constants.

In the problem which concerns us, the conductivity of the Faraday cage exceeds, by many orders of magnitude, the conductivity of the plasma in which it is immersed.

In such circumstances further simplification becomes possible. Consider the boundary conditions:

$$\frac{\sigma_o}{\sigma_i} \quad \frac{\partial \Psi_o}{\partial n} = \frac{\partial \Psi_i}{\partial n} \tag{7}$$

Let σ_o / σ_i become very small while $\partial \Psi_o / \partial n$ remains bounded. Then, $\partial \Psi_i / \partial n$ becomes small and vanishes in the limit. Thus the boundary conditions reduce to:

$$\Psi_i = \Psi_o \tag{8}$$

$$\frac{\partial \Psi_i}{\partial n} = 0 \tag{9}$$

If it is assumed that Ψ_i is constant or zero everywhere inside the conductor then the above boundary conditions are satisfied with:

$$\Psi_o = 0 \tag{10}$$

on the boundary. Thus the problem will reduce to the problem of the potential exterior to conductors immersed in a vacuum. It may further be noted that the requirement that $\partial \Psi_o / \partial n$ remain bounded is satisfied provided the conductor has no sharp points or edges at which the field may become very large.

We shall illustrate the above discussion with the problem of a conducting elliptic cylinder immersed in a conducting medium. In the limit of zero eccentricity the elliptic cross section will reduce to a line. We use the notation of Reference 1. The elliptic cylinder coordinates are defined by the following equations:

$$\begin{aligned} &x = 1/2\ a\ \cosh \mu \cos \theta\ ; \quad y = 1/2\ a \sinh \mu \sin \theta \\ &h_\mu = h_\theta = 1/2\ a \sqrt{\sinh^2 \mu + \sin^2 \theta} = 1/2\ a \sqrt{\cosh^2 \mu - \cos^2 \theta} \\ &r = \sqrt{(x + 1/2\ a)^2 + y^2} \end{aligned} \tag{11}$$

where the curves μ = constant are ellipses and the θ curves are hyperbolas, all with foci at $x = \pm 1/2\ a$. The scale factors are designated by h_μ and h_θ. The symbol r is the magnitude of the radius vector. The following diagram illustrates the coordinates:

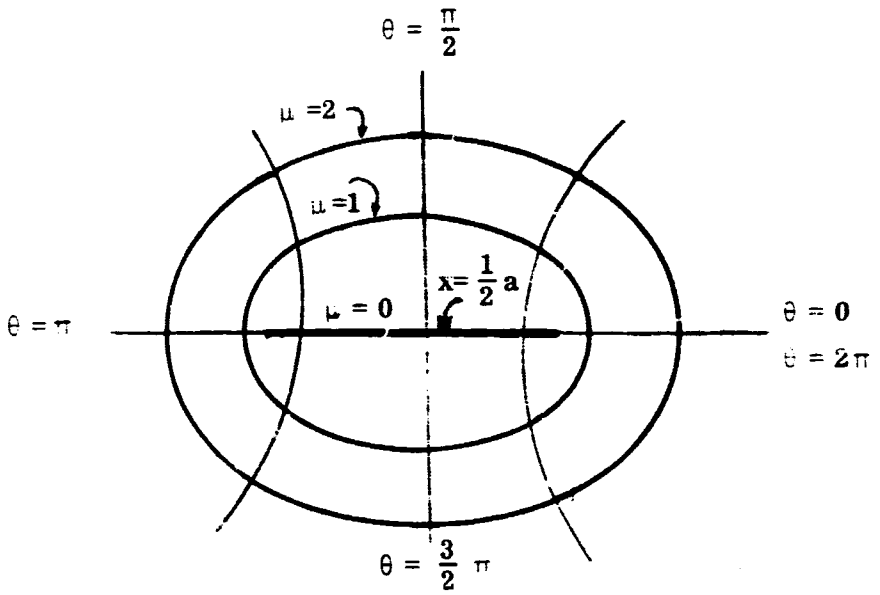

Let us assume that the cross section of the conducting elliptic cylinder is oriented so that its boundary coincides with one of the coordinate ellipses. Assume that the uniform field of magnitude E is oriented so that its direction forms an angle γ with the x axis. The potential for this field is given by:

$$\begin{aligned} \Psi_u &= -E\ (x \cos\gamma + y \sin\gamma) \\ &= -1/2\ E\ a\ (\cosh\mu \cos\theta \cos\gamma + \sinh\mu \sin\theta \sin\gamma) \end{aligned} \tag{12}$$

The problem is reduced to finding those fields, both internal and external to the elliptic cylinder, which on being added to the uniform field satisfies the boundary conditions. The Laplace equation in these coordinates has the elementary solutions u, θ, $e^{\mu} \cos\theta$, $\cosh(n\mu)\sin(n\theta)$, etc. Exterior to the cylinder, the added field must go to zero at infinity. Inside there is only the requirement that the fields remain finite. Hence the total interior potential is given by:

$$\Psi_i = \Psi_u + A \cos h\, u \cos \theta + B \sin h\, u \sin \theta \qquad (13)$$

The total exterior potential is given by:

$$\Psi_o = \Psi_u + C\, e^{-\mu} \cos \theta + D\, e^{-\mu} \sin \theta \qquad (14)$$

Making use of the orthogonality of the trigonometric functions and the boundary conditions of Equations (1) and (2) we may solve for the coefficients A, B, C, D.

The results are finally, for $\mu < \mu_o$

$$\Psi = \frac{1}{2} E a\, e^{\mu_o} \left[\frac{\cos h\, \mu \cos \theta \cos \gamma}{\cos h\, \mu_o + \frac{\sigma_i}{\sigma_o} \sin h\, \mu_o} + \frac{\sin h\, u \sin \theta \sin \gamma}{\frac{\sigma_i}{\sigma_o} \cos h\, \mu_o + \sin h\, \mu_o} \right] \qquad (15)$$

and for $\mu > \mu_o$

$$\Psi = - E (x \cos \gamma + y \sin \gamma) + \frac{1}{4} E a \left(\frac{\sigma_i}{\sigma_o} - 1\right) e^{\mu_o} \sin h\, (2 \mu_o)\, e^{-\mu} \left[\frac{\cos \theta \cos \gamma}{\cos h\, \mu_o + \frac{\sigma_i}{\sigma_o} \sin h\, \mu_o} + \frac{\sin \theta \sin \gamma}{\sin h\, \mu_o + \frac{\sigma_i}{\sigma_o} \cos h\, \mu_o} \right] \qquad (16)$$

It can be seen that by making the identification in Equations (15) and (16)

$$\sigma_i \rightarrow \epsilon$$

$$\sigma_o \rightarrow 1$$

we obtain the result of Equation (10.1.27) of Reference (1) for a dielectric cylinder, of dielectric constant ϵ, immersed in vacuum with dielectric constant unity.

Consider Equation (16) for μ_o small. Now,

$a \sinh \mu_o$ is the minor axis and

$a \cosh \mu_o$ is the major axis of the ellipse

$$\tanh \mu_o = \frac{\text{minor axis}}{\text{major axis}}$$

For $\mu_o << 1$, $\tanh \mu_o \simeq \mu_o$, and

$$\mu_o \simeq \frac{\text{minor axis}}{\text{major axis}}$$

Let us consider the field distortion (the added field) of Equation (16) for the case of $\sigma_i / \sigma_o \gg 1$. Let Ψ_d be the potential for the distorted field.

$$\Psi_d \simeq \frac{1}{2} E a \mu_o e^{-\mu} \left[\frac{\cos\theta \cos\gamma}{1/\frac{\sigma_i}{\sigma_o} + \mu_o} + \frac{\sin\theta \sin\gamma}{\mu_o / \frac{\sigma_i}{\sigma_o} + 1} \right]$$

We make the assumption that $1/\frac{\sigma_i}{\sigma_o} << \mu_o$ although $\mu_o << 1$.

Then, $\Psi_d \simeq \frac{E}{2} a e^{-\mu} \cos\theta \cos\gamma$

Let us now consider the field at a point equidistant from the ends of the major axis and outside the ellipse as in the diagram below.

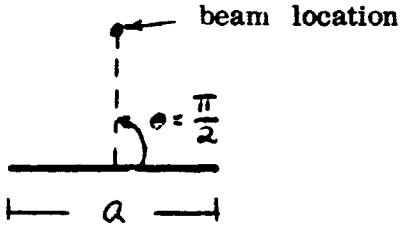

This is the orientation of the electron beam relative to one of the sides of the Faraday cage. The distorted field component perpendicular to the major axis, $E_{\perp}$, is given by:

$$E_{\perp} = -\frac{1}{h_{\mu}} \frac{\partial \Psi}{\partial \mu}$$

The component parallel to the strip is:

$$E_{\parallel} = \frac{1}{h_{\theta}} \frac{\partial \Psi}{\partial \theta}$$

Now,

$$\frac{\partial \Psi_d}{\partial \mu} \simeq -\frac{E}{2} a e^{-\mu} \cos\theta \cos\gamma$$

$$\simeq 0, \text{ for } \theta = \frac{\pi}{2}$$

or

$$E_{\perp} \simeq 0, \text{ for } \theta = \frac{\pi}{2}$$

$$E_{\parallel} \simeq \frac{E e^{-\mu} \sin\theta \cos\gamma}{\sqrt{\cosh^2 \mu - \cos^2 \theta}}$$

$$\simeq \frac{E e^{-\mu} \cos\gamma}{\cosh \mu}, \text{ for } \theta = \frac{\pi}{2}$$

Thus at this point, the distorted field is parallel to the plate.

A measure of the distortion may be taken to be:

$$\frac{E_{\parallel}}{E} = \cos\gamma \ (1 - \tanh \mu)$$

Maximum distortion occurs for $\gamma = 0$, where the fractional distortion is:

$$D = 1 - \tanh \mu$$

Since,

$$y = \frac{1}{2}\, a \sin h\, \mu \sin \theta,$$

then for: $\theta = \pi/2$, $\sin h\, \mu = \frac{2y}{a}$

For the present case,

$$y = 4\frac{1}{2}''$$

$$a = 8''$$

Therefore, $\sin h\, \mu = 1.125.$

Finally, $D \approx .25$

If we now consider the effect of two plates symmetrically located with respect to the beam, we find that the beam is at $\theta = \pi/2$ for one plate and $\theta = 3\pi/2$ for the second plate.

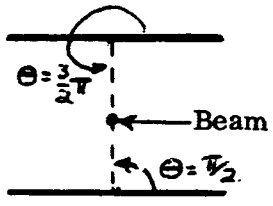

Considered separately the distortion fields due to the presence of the plates cancel at the beam location. However, this result can only be considered a first approximation to the problem of two conducting plates, since each plate is in a field which is the result of the external field and the presence of the other plate. We may however conclude from the relatively small conductivity of the plasma that the fields are those in a vacuum, hardly disturbed by the current flow in the plasma.

The requirement (3) that the Faraday cage provide adequate shielding when electrically closed has been tested experimentally and been found satisfactory.

The requirement (4) is easily satisfied throughout the ionosphere. The electrical closure of the cage segments permits a flow of charge and a redistribution such as to provide zero field within the cage. The disconnect which follows does not automatically provide redistribution of the charge to its original position. In a hard vacuum, then, disconnect would not accomplish anything. The field would still remain zero within the cage. However, in the ionosphere charge transport will take place in such a manner as to restore the original fields. An estimate of the time τ required to achieve this can be made as follows:

The surface charge density ρ_s on a metallic surface which terminates a field E is:

$$\rho_s = \epsilon_o E$$

where ϵ_o is the electrical susceptibility of a vacuum. The current density j in the plasma which flows as a result of the field E is given by:

$$j = \sigma E$$

where σ is the plasma conductivity. The time τ, then is:

$$\tau = \frac{\rho_s}{j} = \frac{\epsilon_o}{\sigma}$$

The value of ϵ_o is about $10^{-9}/36\pi$. The value of σ may be calculated from the formula:

$$\sigma = \frac{n_e e^2}{m \nu_{e,\, n+i}}$$

where n_e is the electron density, e is the electronic charge, m is the electronic mass and $\nu_{e,\, n+i}$ is the collision frequency of electrons with neutrals and ions. Values of n_e and $\nu_{e,\, n+i}$ may be obtained from Table II of Reference (2). Typically calculated values of σ are about 10 mhos per meter. Consequently τ is much shorter than the period corresponding to the 400 H frequency of opening and closing the Faraday cage.

REFERENCES

1. P. M. Morse and H. Feshbach, "Methods of Theoretical Physics," Chapter 10, p 1195-1200, McGraw-Hill, New York (1953).

2. Ya. L. Al'pert, A. V. Gurevich, and L. P. Pitaevskii, Soviety Phys. Uspekhi 6, 13 (1963).